ABSTRACT

CYCLIC ELECTRON TRANSFER PATHWAYS IN *SYNECHOCOCCUS* SP. PCC 7002 CYANOBACTERIA DURING PHOTOSYNTHESIS AT HIGH LIGHT INTENSITY

By Anuradha Marathe

With current global warming, there is growing interest in coupling carbon dioxide (CO_2) capture to chemical synthesis via photosynthesis. Cyanobacteria convert up to 10% of the sun's energy into biomass compared to 1% by energy crops and 5% by eukaryotic algae. Cyanobacteria and microalgae can thus potentially produce biofuels in an economical and environmentally sustainable manner at rates sufficient to replace a substantial fraction of fossil fuels. To employ cyanobacteria for biofuels, a detailed knowledge of photosynthetic electron pathways is required. Linear electron flow from photosystem II (PSII) via the plastoquinone (PQ) pool, cytochrome (Cyt) *bf* complex, and photosystem I (PSI) generates ATP and NADPH. Cyclic electron flow around PSI and the Cyt *bf* complex generates ATP only, provides the 'extra' ATP for efficient CO_2 fixation, and is implicated in defenses against photodamage. Cyclic electron flow mediated by the NAD(P)H dehydrogenase (NDH-1) complex is the major, known cyclic pathway in cyanobacteria. In plant chloroplasts, a PSI – Cyt *bf* supercomplex catalyzes cyclic flow. Such a supercomplex has not been identified in cyanobacteria and the contributions of linear and cyclic electron flow under different environmental conditions remain poorly understood. In this thesis, the fast-growing, high-light tolerant, marine cyanobacterium, *Synechococcus* sp. PCC 7002 and two mutants, NdhF (lacking the NDH-1 complex) and PetB-R214H (impaired electron flow in the Cyt *bf* complex) were investigated with respect to cyclic electron transfer pathways under optimal and high, full-sunlight conditions. PSI and Cyt *bf* kinetics were studied with pump-probe, kinetics spectrophotometer (Biologic JT-10) that can monitor light-induced redox changes in the photosynthetic apparatus of living cells. The NDH-I route accounted for most of the cyclic flow (~10% of the total) under optimal light as observed previously. At high light intensity, PSI content decreased but cyclic electron flow increased dramatically in both the wild type and NdhF mutant. Most interestingly, in the NdhF mutant at high light intensity, cyclic electron flow accounted for 50% or more of total electron flow. These data suggest that this efficient cyclic electron flow is catalyzed by the formation of a PSI – Cyt *bf* supercomplex required for adaptation and growth of *Synechococcus* sp. PCC 7002 cyanobacteria at extreme, high-light intensities.

CYCLIC ELECTRON TRANSFER PATHWAYS IN *SYNECHOCOCCUS* SP. PCC 7002 CYANOBACTERIA DURING PHOTOSYNTHESIS AT HIGH LIGHT INTENSITY

by

Anuradha Marathe

A Thesis Submitted
In Partial Fulfillment of the Requirements
For the Degree of

Master of Science-Biology

Microbiology

at

The University of Wisconsin Oshkosh
Oshkosh WI 54901-8621

January 2012

COMMITTEE APPROVAL

T Colin Keller Advisor

1/20/2012 Date Approved

Member

1/18/12 Date Approved

Member

1/18/12 Date Approved

PROVOST
AND VICE CHANCELLOR

1/20/12
Date Approved

FORMAT APPROVAL

Maria Mondoff

1/18/12
Date Approved

ACKNOWLEDGMENTS

I would like to offer my sincere appreciation to Dr. Toivo Kallas, my advisor, for his guidance throughout the duration of this thesis project. I would also like to thank the members of my thesis committee, Dr. Colleen McDermott and Dr. Lisa Dorn, for their time and advice. Finally, I wish to thank my parents, Anant and Meenakshi Marathe, for their continuing support of all my endeavors.

TABLE OF CONTENTS

Pages

LIST OF TABLES..... v

LIST OF FIGURES..... vi

CHAPTER I- INTRODUCTION..... 1

1.0 Photosynthesis and Importance of Cyanobacteria..... 1
2.0 Cyanobacterial Photosynthetic Apparatus..... 2
3.0 Linear Electron Flow..... 5
4.0 Need for an 'Extra' ATP 9
5.0 Cyclic Electron Flow..... 10
6.0 Proposed Pathways of Cyclic Electron Flow..... 14
7.0 Role of Cyclic Electron Flow in Protection of Photosynthetic Apparatus.. 16
8.0 State Transitions..... 18
9.0 Cyclic Electron Flow Under Environmental Stress Conditions..... 20
10.0 Tolerance of High Light Intensity..... 22
11.0 Model Organism for this Thesis……..... 24
12.0 Synechococcus sp. PCC 7002 wild type and Strains……..... 25
13.0 Present Study: Spectroscopic Experiments..... 26
14.0 Photosystem I – cytochrome *bf* supercomplexes..... 29
15.0 Objectives of the Thesis Research..... 31
16.0 Expected Outcomes..... 31

CHAPTER II – CYCLIC ELECTRON FLOW UNDER HIGH LIGHT INTENSITY

1.0. Introduction..... 33
2.0. Materials and Methods..... 39
3.0. Results..... 44
4.0. Discussion..... 78
5.0. Conclusion..... 89

APPENDIX..... 91

REFERENCES..... 113

.

LIST OF TABLES

		Pages
Table 1.	Cyanobacterial strains, media requirements and antibiotics	41
Table 2.	P700 reduction kinetics +/- DCMU in *Synechococcus* wild type, NdhF and PetB-R214H mutants grown under optimal and high light	49
Table 3.	Cyclic electron flow as a percentage of total electron flow in *Synechococcus* wild type, NdhF and PetB-R214H mutants grown under optimal and high light	50
Table 4.	P700 reduction kinetics +/- DCMU and DBMIB in *Synechococcus* wild type, NdhF and PetB-R214H mutants grown under optimal and high light	58
Table 5.	P700 reduction kinetics +/- DCMU, KCN, and MV in *Synechococcus* wild type, NdhF and PetB-R214H mutants grown under optimal and high light	60
Table 6.	P700 reduction kinetics after pre-illumination of *Synechococcus* wild type and NdhF mutant grown under optimal and high light	67
Table 7.	Cyt *bf* kinetics +/- DCMU and DBMIB in *Synechococcus* wild type, NdhF and PetB-R214H mutants grown under optimal and high light	74
Table 8.	P700 reduction kinetics +/- DBMIB and 4-1HQ of *Synechococcus* wild type, NdhF and PetB-R214H mutants grown under optimal and high light	77

LIST OF FIGURES

		Pages
Figure 1:	The photosynthetic apparatus of cyanobacterial thylakoid membrane.....	4
Figure 2:	Linear electron flow in the cyanobacterial thylakoid membrane.....	7
Figure 3:	Cyclic electron flow in the cyanobacterial thylakoid membrane.....	14
Figure 4**:**	Growth of wild type *Synechococcus* sp. PCC 7002 under high light intensity.....	24
Figure 5:	Scanning electron micrograph showing rod-shaped *Synechococcus* PCC 7002 cells.....	26
Figure 6:	P700 kinetics in the *Synechococcus* wild type and NdhF strains grown under optimal light.....	46
Figure 7:	P700 kinetics in the *Synechococcus* wild type and PetB-R214H mutant grown under optimal light.....	48
Figure 8:	P700 kinetics in the *Synechococcus* wild type grown under optimal and high light.....	52
Figure 9:	P700 kinetics in the *Synechococcus* NdhF mutant grown under optimal and high light.....	54
Figure 10:	P700 kinetics in the *Synechococcus* PetB-R214H mutant grown under optimal and high light.....	56
Figure 11:	P700 reduction kinetics in the *Synechococcus* wild type, NdhF and PetB-R214H strains grown under optimal and high light.....	62
Figure 12:	P700 kinetics with far-red illumination in the *Synechococcus* wild type, NdhF and PetB-R214H strains grown under optimal and high light.....	65
Figure 13.	Cyt *bf* kinetics in the *Synechococcus* wild type grown under optimal and high light.....	69

LIST OF FIGURES (Continued) pages

Figure 14. Cyt *bf* kinetics in the *Synechococcus* NdhF mutant grown under optimal and high light..... 70

Figure 15: Cyt *bf* kinetics in the *Synechococcus* PetB-R214H mutant grown under optimal and high light..... 71

.

CHAPTER I

INTRODUCTION

1.0 Photosynthesis and importance of cyanobacteria

The majority of life on earth depends on the oxygen and carbon polymers produced by photosynthetic organisms. Photosynthesis is the biological process converting the electromagnetic energy emitted by the sun (in the form of sunlight) into biochemical energy and thus acting as the direct or indirect energy source for nearly all life on earth. Photosynthetic organisms such as plants, cyanobacteria and algae convert carbon dioxide into organic compounds and evolve oxygen through photosynthesis. These photosynthetic organisms, or photoautotrophs, play an important role as the primary producers of food in every ecosystem.

The earth's primitive atmosphere contained no molecular oxygen (O_2). As oxygenic photosynthetic organisms (i.e. the cyanobacteria) evolved over two billion years ago (Carr et al. 2006), they increased the level of atmospheric oxygen in the primitive atmosphere through photosynthesis. Among photosynthetic organisms, cyanobacteria are the most ubiquitous and genetically diverse group, which drastically changed the Earth by oxygenating the atmosphere. They obtain their name from the bluish green color (cyan = blue). This bluish green color is because of the bluish green pigment called phycocyanin. Cyanobacteria account for approximately 25% of the global photosynthetic activity and some of them are also involved in nitrogen fixation (Olson 2006). Cyanobacteria are prokaryotic photoautotrophs and are mostly unicellular. Many

cyanobacteria grow in colonies or filaments often surrounded by a mucilaginous or gelatinous sheath. Some Cyanobacteria also form motile filaments, called hormogonia. These hormogonia are formed during asexual reproduction and they travel away from the main biomass to bud and form new colonies elsewhere. Many cyanobacteria also display circadian rhythms which were once thought to be an attribute exclusive to eukaryotic cells. In addition to oxygenating the atmosphere, Cyanobacteria played another important role in evolution. Several lines of evidence indicate that modern day plant chloroplasts evolved from endosymbiotic cyanobacterial ancestors (McFadden 2001).

2.0 Cyanobacterial Photosynthetic Apparatus

To perform photosynthesis, cyanobacteria possess a highly organized system of internal thylakoid membranes encompassing components of respiratory as well as photosynthetic electron transport (Albertsson 2001). The light harvesting antenna proteins or phycobilisomes are also attached to the thylakoid membranes. Energy from sunlight is captured by these phycobilisomes and funneled through the chlorophylls to the two reaction centers of photosynthesis (Blankenship 2002). The reaction center chlorophyll emits an electron upon excitation and this starts the series of electron transfer through the photosynthetic apparatus. Figure 1 shows a detailed representation of the photosynthetic apparatus located within the thylakoid membrane. Photosystem II, Photosystem I and Cytochrome *bf* complexes are the major complexes in this photosynthetic apparatus (DeRuyter and Fromme 2008). Both the photosystems I and II (hereafter PSI and PSII) have phycobilisomes attached to them (Whitmarsh and

Govindjee 1995). Light captured by these phycobilisomes excites the reaction center chlorophylls inside the photosystems and causes a flow of electrons between the photosystems through the plastoquinone-plastoquinol pool (hereafter PQ pool) and cytochrome *bf* (hereafter Cyt *bf*) complex (Ort and Yocum 1996).

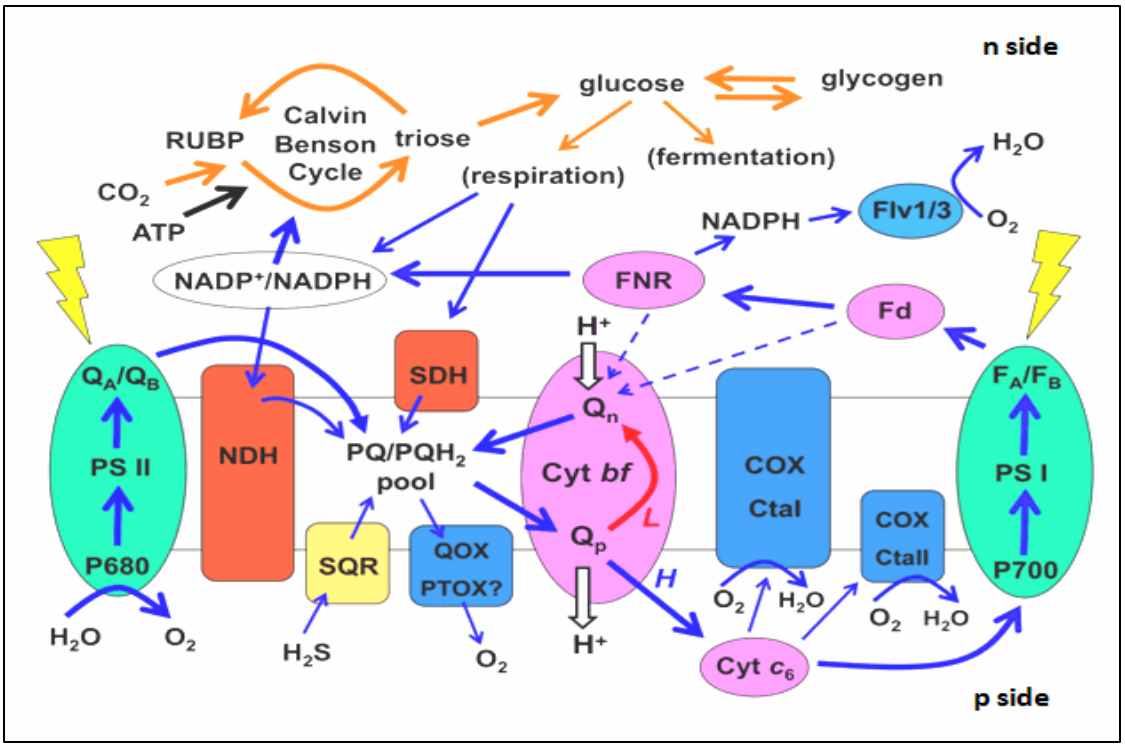

Figure 1. The photosynthetic apparatus of cyanobacterial thylakoid membranes. PS II and PS I: photosystem II and photosystem I; P680: reaction center of photosystem II; Q_A and Q_B: plastoquinone A and plastoquinone B; PQ pool: plastoquinone / plastoquinol pool; Cyt *bf*: cytochrome *bf* complex; Q_p: Q_o or plastoquinol oxidation site; Q_n: Q_i or plastoquinone reduction site; Cyt c_6: cytochrome c_6; P700: reaction center of photosystem I; Fd: ferredoxin; FNR: Ferredoxin-NADPH oxidoreductase; NDH: NADPH Dehydrogenase complex; SDH: Sucinate Dehydrogenase complex; COX: Cytochrome *c* oxidase encoded by CtaI and CtaII genes; QOX: Quinone oxidoreductase; PTOX: Plastid Terminal oxidoreductase; (?): question mark indicates that there is no evidence for PTOX in *Synechococcus* 7002; Flv1/3: Flavoproteins Flv1 and Flv3. p side: positive side of thylakoid membrane where protons are deposited; n side: negative side of the membrane from where protons are translocated. Solid single headed bold blue arrows indicate major electron flow pathways; solid single headed small blue arrows indicate entry of electrons into the PQ pool through different enzyme complexes. Dotted single headed blue arrows indicate suggested flow of electrons from Fd and FNR to Cyt *bf* complex. White arrows indicate translocation of protons across thylakoid membrane from n side to the p side of thylakoid membrane; single headed red arrow represents movement of electrons through the low-potential chain of Cyt *bf* complex via hemes. Orange arrows indicate metabolic pathways for production of carbohydrates. (Adapted from Kallas, 2012).

3.0 Linear Electron Flow

The PSII reaction center, a chlorophyll dimer called P680, becomes excited upon accepting a photon (from sunlight) and leaves its ground state. P680 then transfers the electron to a pheophytin molecule located within the PSII complex. From pheophytin, the electron is further transferred to a quinone molecule (Q_A), an iron atom, and finally to a plastoquinone molecule (Q_B) located on the cytoplasmic (n) side of the membrane. To replace the electrons removed from P680, electrons from water are donated by the oxygen evolving complex (OEC). This oxygen evolving complex consists of a tetranuclear manganese cluster which has been implicated as the catalytic site for water oxidation (Roelofs et al. 1995). Water oxidation by this manganese cluster results in the formation of molecular oxygen as a byproduct of photosynthesis.

During electron transfer, electron acceptors and donors undergo reduction and oxidation changes. Q_B, The terminal electron acceptor within PS II, is reduced after receiving two electrons. This plastoquinone molecule acquires two protons from the outer, electronegative (n) surface of the thylakoid membrane and forms a plastohydroquinone (PQH_2) molecule. The PQH_2 moves to the PQ pool and enters the quinol oxidase (Q_p) site of the Cyt *bf* complex. The Cyt *bf* complex is a 220kDa homodimeric, multi-subunit complex consisting of *PetA* (32kDa cytochrome *f*), *PetB* (25kDa cytochrome *b*), *PetC* (19kDa Reiske iron sulfur protein), *PetD* (17kDa subunit IV) along with several subunits (Yan et al. 2008; Kallas 1994; 2012). A bifurcation of electron flow occurs in the Cyt *bf* complex. One electron from the plastohydroquinol (PQH_2) passes through the high potential chain and another electron through the low

potential chain. The electron travelling through the low potential chain reaches two *b*-type hemes (b_P and b_N) and another *c*-type heme (c_n) and finally to the quinone reductase (Q_n) site of the Cyt *bf* complex. The b_P heme is situated closer to the electropositive side (p-side) of the thylakoid membrane whereas the b_N heme is situated closer to the electronegative side (n-side) of the membrane. After donating one electron through the high potential chain, PQH_2 becomes a highly reactive semiquinone ($PQH\bullet^-$) molecule. The semiquinone molecule is thought to shift from the distal to the proximal position of the Q_p site and passes its second electron to the low potential chain (Kurisu et al. 2003; Stroebel et al. 2003). Upon release of two protons into the thylakoid lumen, the semiquinone molecule is converted to a fully oxidized quinone (PQ) and moves to the Q_n site. This quinone (PQ) at the Q_n site receives electrons from the low potential chain and protons from the cytoplasmic (n) side of the membrane and becomes PQH_2. This PQH_2 can re-enter the PQ pool and cycle back to the Q_p site of the Cyt *bf* complex thus completing the Q-cycle (Figure 1 and 2).

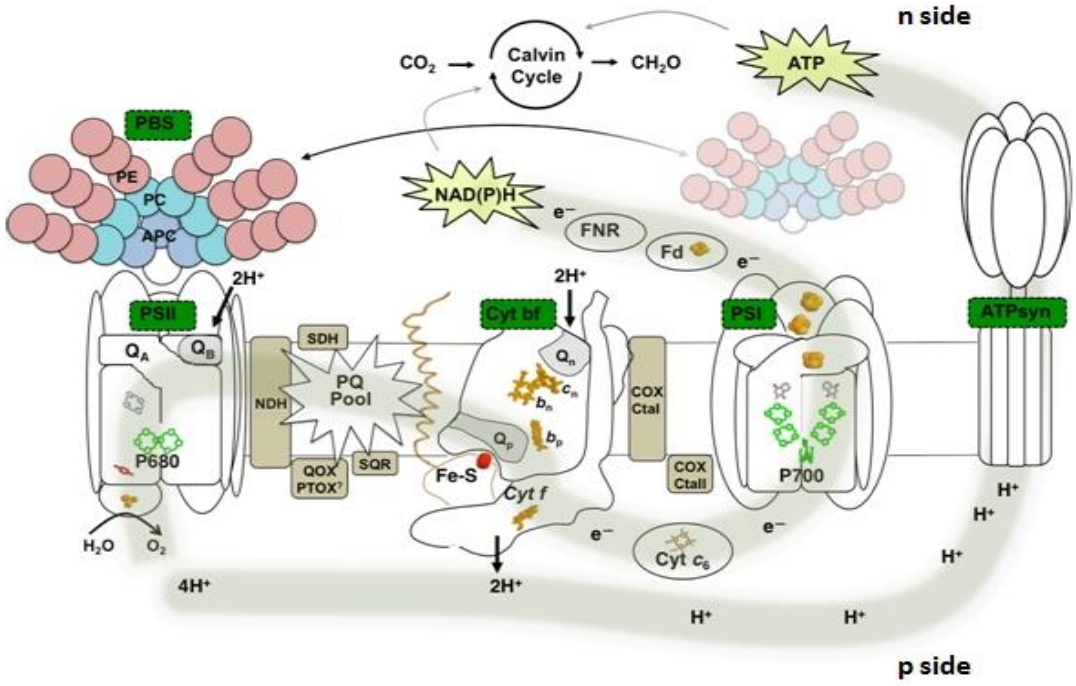

Figure 2. Linear electron flow in the cyanobacterial thylakoid membrane. PBS: phycobilisomes; PE: Phycoerythrin; PC: Phycocyanin; APC: Allo-phycocyanin; PSII and PSI: photosystem II and photosystem I; P 680: reaction center of photosystem II; Q_A and Q_B: plastoquinone A and plastoquinone B; PQ pool: plastoquinone / plastoquinol pool; NDH: NADH Dehydrogenase; SDH: Succinate Dehydrogenase; SQR: ; QOX: Quinol Oxidase; PTOX: Plastid Terminal Oxidase; Cyt *bf*: cytochrome *bf* complex; Q_p: plastoquinol oxidation site, also called as Q_o; Q_n: plastoquinone reduction site, also called as Q_i; Fe-S: Rieske iron-sulfur protein; Cyt *f*: cytochrome *f*; b_n, b_p and C_n: hemes b_n, b_p and c_n; Cyt c_6: cytochrome c_6; COX CtaI: Cytochrome oxidase encoded by *ctaI*; COX CtaII: Cytochrome Oxidase encoded by *ctaII*; P 700: reaction center of photosystem I; Fd: ferredoxin; FNR: Ferredoxin Oxido-reductase; ATP syn: ATP synthase enzyme; p side: positive side of thylakoid membrane where protons are translocated; n side: negative side of thylakoid membrane from where protons are translocated; e^-: electrons; H^+ : protons. Passage of electrons via the linear photosynthetic electron transport chain from PSII to PSI and flow of protons to ATP synthase are indicated by grey highlights. Bold single-headed black arrows indicate translocation of protons across the membrane. Double-headed black arrow indicates movement of PBS from PSII to PSI and back during state transitions. Faded arrows indicate that ATP and NADPH, end products of linear electron transport, are fed into cellular processes such as the Calvin-Benson cycle for CO_2 fixation. (Adapted from original figure by George Weir, Unpublished data)

Electrons travelling through the Cyt *bf* high-potential chain are carried by the Rieske iron sulfur protein (ISP). The Rieske ISP undergoes a large domain movement to transfer the first electron from PQH_2 oxidation in the Cyt *bf* quinol-oxidation (Q_p) site to the cytochrome *f* subunit (Heimann 2000; Kallas 1994; 2012). From cytochrome f the electron moves to a soluble copper-containing plastocyanin or a soluble c-type heme protein, cytochrome c_6 (Kallas 1994; 2012). Many cyanobacteria use only cytochrome c_6, which may be either acidic or basic, whereas plastocyanin occurs in other, rather diverse members of this group (Baymann et al. 2001). Cytochrome c_6 is present within the lumenal (p side) space and may be pre-bound to the PSI reaction center resulting in a rapid transfer of electrons (Baymann et al. 2001). Electrons from the cytochrome c_6 pool are donated to the PSI reaction center, P700. Sunlight energy excites PSI causing electrons to flow through a series of carriers, A_o (chlorophyll), A_1 (phylloquinone), F_x-F_A/F_B (iron-sulfur centers) within the PSI complex (Jordan 2001). The terminal electron acceptor for PSI is ferredoxin, which is present on the cytoplasmic (n) side of the membrane. Ferredoxin transfers electrons to $NADP^+$ (in a reaction catalyzed by Ferredoxin-$NADP^+$ oxidoreductase or FNR), generating NADPH, the ultimate and typical carrier of reducing power in photosynthesis. The protons translocated by the PSII and Cyt *bf* complexes generate a transmembrane hydrogen ion (ΔpH) gradient, which drives ATP synthesis through the ATP synthase complex in the thylakoid membrane (White 2002, and refer figure 2). Thus a linear electron flow through PSII, Cyt *bf* and PSI leads to production of ATP and NADPH.

In a variant of linear electron flow, molecular oxygen can also act as the terminal electron acceptor. In place of $NADP^+$, oxygen may readily accept electrons from ferredoxin (or other reduced carriers on the acceptor side of PSI) and is reduced completely back to water (Asada 2000; Allen 2003). In the cyanobacterium Synechocystis PCC 6803, dioxygen reduction by electrons from PSI occurs via NAD(P)H and the flavoproteins Flv1 and Flv3 (Helman et al. 2003). This observation that molecular oxygen can be used as an electron acceptor in photosynthesis was first noted by the late Alan Mehler, while studying chloroplasts (Mehler 1951). Hence the reaction was named the Mehler reaction. The underlying electron transport was named 'pseudocyclic electron transport' by Daniel Arnon (Arnon 1977). Further studies by Kozi Asada (Asada 1999; 2000) showed that intact chloroplasts contain ascorbate peroxidase and high concentrations of ascorbate (AA) instead of catalase. This represented an alteration of the original Mehler reaction scheme. This altered reaction sequence was termed the 'water-water cycle' (Asada 1999; Heber 2002), which is also used more generally to describe any reaction where electrons from water oxidation by PSII ultimately reduce oxygen to water on the acceptor side of PSI

4.0 Need for an 'Extra' ATP

The ATP and NADPH produced during linear electron flow are used by several cellular processes. Among these, a key process is carbon fixation by the Calvin-Benson-Bassham cycle (hereafter the Calvin cycle). The CO_2 fixed in this process is the precursor for biosynthesis of organic compounds. During the Calvin cycle, both NADPH and ATP

are used to regenerate ribulose-1,5-bisphosphate. For efficient carbon fixation, an ATP:NADPH ratio of 3:2 is required (Alric et al. 2010). Linear electron flow does not produce enough ATP to maintain this ratio. Hence, 'extra' ATP is required and this can be produced through several other mechanisms. Reactions such as the Mehler reaction (or water-water cycles more generally) or plastid terminal oxidase activity can participate either directly or indirectly, to form a proton-motive force at the level of the thylakoid membrane, and drive ATP synthesis (Alric et al. 2010). Another way would be synthesis of ATP in the mitochondria by exporting excess of NADPH towards mitochondria via the malate valve (Scheibe 1987). However, cyanobacteria do not have mitochondria, and even in plant cells, these reactions may not be fast enough to compete with linear electron flow. Hence, it may be more efficient to produce the additional ATP directly at the level of the thylakoid membrane.

5.0 Cyclic Electron Flow

In 1954, additional electron flow other than linear electron flow occurring in the thylakoid membranes of higher plants, green algae and cyanobacteria, and producing ATP was discovered by Arnon and co-workers (Arnon and Chain 1975). Since then, higher plants as well as cyanobacteria have been studied for occurrence of this additional electron flow. PSII does not play a role in this cyclic electron flow, which involves PSI and Cyt bf complex (Arnon and Chain 1975). Cyclic electron flow contributes toward production of the 'extra' ATP which is crucial for the proper balance of NADPH and ATP. In eukaryotes, external ATP can be obtained from cytosolic and mitochondrial

sources via chloroplast ATP/ADP translocators (Winkler and Neuhaus 1999). However, cyanobacteria lack such external sources of ATP; hence cyclic electron flow around PSI may be an important source of ATP required by these organisms (Thomas et al. 2001). In non-oxygenic photosynthetic bacteria, a form of cyclic electron flow occurring through a reaction center functionally analogous to PSI is the primary means by which light energy is converted to chemical energy (Herbert et al. 1990).

Initially, it was believed that cyclic electron flow around PSI occurred in cyanobacteria, algae and in bundle sheath cells of C_4 plants but did not show significant activity in C_3 plants (Carpentier et al. 1984; Herbert et al. 1990; Maxwell and Biggins 1976). Later, it became clear that in C_3 plants cyclic electron flow activity is also significant and is controlled by a redox poise requiring specific conditions (Golding et al. 2004). Accumulation of NADPH can act as a poise and trigger for cyclic electron flow (Golding et al. 2004). An imbalance of ATP/NADPH curtails CO_2 assimilation and leads to excessive accumulation of NADPH in the chloroplast stroma (equivalent to the cytoplasmic space in cyanobacteria) resulting in its over-reduction. Over-reduction of the stroma is avoided by cyclic electron flow, which is poised by a regulatory mechanism provided by the Cyt *bf* complex upon accumulation of NADPH (Arnon and Chain 1975; Joët et al. 2002). Pseudocyclic electron flow (the reduction of dioxygen by PSI) is also suggested to avoid over-reduction of PSI (Allen 2002; 2003; Heber and Walker 1992).

In some organisms, the redox poising of cyclic electron flow around PSI may be set by electrons derived from carbohydrate metabolism, a phenomenon known as chlororespiration (Bennoun 1982; Peltier 2002). In nutrient deprived cells, cyclic electron

flow may also occur via electrons derived from carbohydrate oxidation. The idea that respiratory and photosynthetic electron transport chains interact was initially suggested by Goedheer (1963) on the basis of studies on the green alga *Chlorella* and the cyanobacterium *Synechococcus* (Fork and Herbert 1993; Goedheer 1963). It has since become well established that in cyanobacteria the photosynthetic and respiratory electron transfer chains are linked via the PQ pool and Cyt *bf* complex (see e.g. Kallas 2012 and Yan et al. 2008 for reviews--). Thus in cyanobacteria reduced carbon pools could readily provide electrons for P700 reduction and an apparent cyclic electron transfer pathway (see Figure 3). In higher plants, chlororespiration seems to be a minor pathway compared to linear electron transport. However, it might play a role in the regulation of photosynthesis by modulating the activity of cyclic electron flow around PSI (Casano et al. 2000; Joet 2002; Ogawa 2007). One of the important enzymes in chlororespiration, plastid terminal oxidases (PTOX) (Aluru & Rodermel 2004; Kuntz 2004, Quiles 2006) controls the over-reduction of PQ pool during periods of high light and nutrient deprivation. (Kallas 2012; Quiles 2006). PTOX enzymes also occur in some but not all cyanobacteria (Kallas 2012) and apparently not in the *Synechococcus* sp. PCC 7002 used in this thesis. Another important enzyme in chlororespiration and in cyanobacteria is the NADH dehydrogenase complex (Quiles 1998; 2000; 2005; Rumeau 2005; Sazanov 1998b). Many studies suggest that it plays a role in the protection against photo-oxidative stress (Catala et al. 1997; Casano et al. 2001; Endo et al. 1999; Herbert et al. 1995; Martin et al. 1996; Teicher et al. 2000; and Quiles 2004).

Cyclic electron flow has been shown to proceed together with linear electron flow when oxaloacetate serves as electron acceptor for illuminated intact chloroplasts in addition to oxygen (Ivanov et al. 1998). Oxaloacetate is reduced to malate by NADP-dependent malate dehydrogenase, which is a light-controlled enzyme that becomes active at elevated NADPH/NADP ratios (Scheibe 1987; 1990). These observations demonstrate that cyclic electron transport can occur when oxidized NADP is still present (Heber 2002), at least in chloroplasts.

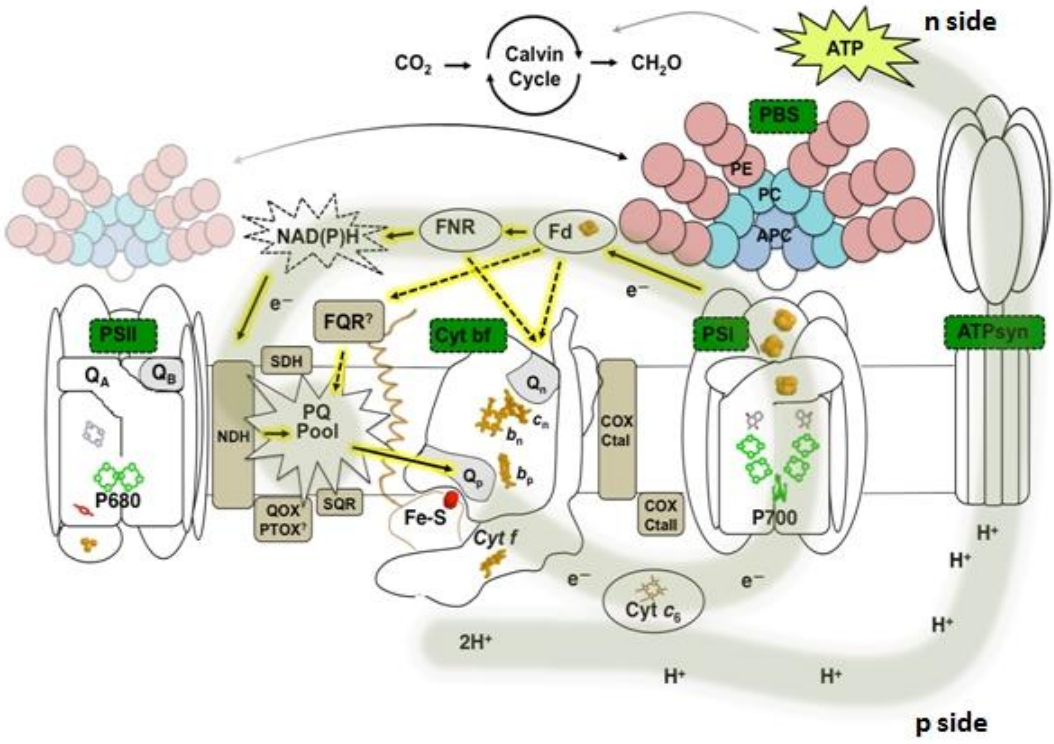

Figure 3. Cyclic electron flow in the cyanobacterial thylakoid membrane. Abbreviations are the same as those in Figure 2. Established cyclic electron flow pathways in cyanobacteria are indicated by bold black arrows with yellow highlights. Postulated cyclic pathways are indicated by dotted black arrows with yellow highlight. The main known (NDH) path of cyclic electron flow around PSI and flow of protons to ATP synthase is indicated by grey highlights. Double-headed black arrow indicates redistribution of PBS between PSII and PSI during state transitions. PBS located over PS

II are faded because PSII does not play a role in cyclic electron flow and cells are suggested to be in 'state 2' (majority of PBS associated with PSI). Faded arrow indicates that ATP, the end product of cyclic electron flow provides the 'extra ATP' to maintain the ATP:NADPH ratio required for efficient carbon fixation by the Calvin-Benson Cycle. (Figure adapted from George Weir, Unpublished data.)

6.0 Proposed Pathways of Cyclic Electron Flow

In principle, any pathway that accepts electrons from PSI and donates them to the PQ pool without the aid of ATP or other high-energy compounds could serve as a cyclic electron-transport pathway that generates a light-dependent proton gradient across the membrane (Howitt et al. 2001). Two main pathways have been proposed for cyclic electron flow around PSI in higher plants, algae and cyanobacteria (Figure 3). One is the Ferredoxin (Fd)-FQR pathway. In this pathway, the reduced Ferredoxin (Fd_{red}) donates electrons to Ferredoxin-quinone oxidoreductase (hereafter FQR) which deposits electrons back into the PQ pool and then the Cyt *bf* complex. Some evidence indicates that the Fd-FQR pathway is sensitive to Antimycin A (Munekage et al. 2004). This pathway is thought to operate concurrently with linear electron transfer in higher plants and green algae. A *pgr5* (Proton Gradient Regulator protein) dependent pathway was considered to be the main pathway in cyclic electron flow in higher plants (Munekage et al. 2004). It was demonstrated in *Arabidopsis thaliana* that *pgr5*, a chloroplast protein is essential for efficient photosynthesis and to prevent over-reduction of the stroma (Munekage 2004). However, further analysis revealed a regulatory rather than a catalytic role for this protein in the cyclic electron flow (Nandha et al. 2007). Cyanobacterial genomes appear to lack any *pgr5* homolog. Some studies have suggested that an Antimycin-A sensitive FQR

enzyme might operate in cyanobacteria (see Kallas 2012 for review), but compelling evidence is lacking and no FQR enzyme has been isolate. Thus the occurrence and significance of a Fd-FQR pathway remains unclear in cyanobacteria.

Another cyclic electron flow pathway is the NDH-dependent pathway. In this pathway, electrons are transferred from ferredoxin to FNR (Ferredoxin-NADP oxidoreductase) which further transfers the electrons to NAD(P)H which is oxidized by the NDH-1 complex. This NDH-1complex is a respiratory-type NAD(P)H dehydrogenase which reduces the PQ pool allowing electrons to cycle back to PSI through the PQ pool and Cyt *bf* complex. The NDH-dependent pathway is predominant in cyanobacteria at least under moderate light conditions (Ye et al., 1993; Mi et al., 1993; Alric, 2010), perhaps because the photosynthetic and respiratory chains share the same membrane. Some studies have demonstrated that in cyanobacteria, NDH-1 is the main site of entry of electrons into the PQ pool in the NDH- dependent cyclic electron flow as well as in respiratory electron flow (Mi et al 1992, Ogawa and Mi 2007). However, in other studies, notably those of Cooley et al. (Cooley et al. 2001) with *Synechocystis* PCC 6803, concluded that succinate dehydrogenase (SDH) is the main source for respiratory PQ pool reduction. The contribution of the NDH-dependent cyclic electron transport pathway in chloroplasts was considered to be relatively small, and only evident under stress conditions (Munekage et al. 2004). However, recent studies have demonstrated an important NDH-1 mediated cyclic activity in higher plants (Livingston et al. 2010).

The PsaE protein was found to have a role in the NDH-mediated cyclic electron flow pathway in *Synechococcus* PCC 7002 cyanobacteria (Yu et al. 1993). PsaE is one of

the polypeptides of the cyanobacterial PSI reaction center. The role of the PsaE protein was not known initially, but it was shown that the addition of PsaE to PsaE-deficient PSI complexes in vitro leads to higher rates of Fd and/or flavodoxin reduction (Golbeck 1992b; Strotmann and Weber 1993). Thus PsaE apparently aids in the binding of ferredoxin to the reducing side of PSI (Rousseau et al. 1993; Sonoike et al. 1993) and the lack of PsaE has been shown to greatly reduce the lifetime of the PSI/ ferredoxin complex (Barth et al. 1998). The physiological behavior of a *Synechococcus* PCC 7002 PsaE mutant suggests that the defect might reside in the cyclic electron flow pathway around PSI (Huang et al. 1993; Yu et al. 1993). PsaE-mediated cyclic electron flow is indicated to play a key role in efficient bicarbonate (HCO_3^-) utilization at low inorganic carbon concentrations in *Synechococcus* PCC 7002 (Sültemeyer 1993; Sültemeyer 1997).

7.0 Role of cyclic electron flow in Protection of the Photosynthetic Apparatus

Apart from maintaining the proper ratio of ATP/NADPH in photosynthetic organisms, cyclic flow is also considered to protect the photosynthetic apparatus against photoinhibition. During photosynthetic light-harvesting and electron transport, reactive oxygen species (ROS) are generated as normal byproducts (Muller 2000). Hence, the photosynthetic organisms must cope with photooxidative damage to PSII, PSI, and other components of the photosynthetic system. The most common type of photooxidative damage is caused to PSII and is called photoinhibition. Photoinhibition of PSII is rapidly repaired by partial disassembly of inactivated PSII complexes, lysis of the damaged D1 protein, de novo synthesis and replacement of D1, reassembly of PSII, and reactivation of

electron transport through the repaired PSII complex (Kyle 1984; Thomas et al. 2001). Cyclic electron flow around PSI has been proposed to protect PSII from photoinhibition (Canaani et al. 1989; Herbert et al. 1995; Thomas et al. 2001). In higher plants, PSI cyclic electron flow sustains a ΔpH across the membrane upon photoinhibition. Such a cyclic electron flow is also important to protect PSI from irreversible photodamage (Quiles 2006). Reactions such as the Mehler reaction or Water-water cycle can also maintain the ΔpH across the thylakoid membranes in higher plants. This ΔpH enhances non-photochemical quenching (NPQ) in higher plants and algae (Asada 1999; 2000; Makino et al. 2002; Osmond et al. 1997). Non-photochemical quenching (hereafter NPQ) is one of the photoprotective mechanisms employed by higher plants and algae. It refers to dissipation of excess absorbed energy as heat in the light-harvesting chlorophyll antenna (LHCII) of PS II. Since cyanobacteria do not have the integral membrane chlorophyll containing light-harvesting complex, LHCII, it was assumed that the NPQ mechanism is not exhibited by these organisms. However, studies have shown that an NPQ mechanism is apparently mediated by the Iron stress-induced A protein (IsiA) which is induced under iron starvation (Burnap et al. 1993; Laudenbach and Straus 1988) and other stress conditions (Havaux et al. 2005, Jeanjean 1993; Yousef et al. 2003;). More recently, a distinct blue light-induced NPQ mechanism that is associated with the orange carotenoid protein (OCP) and phycobilisomes has been discovered (El Bissati 2004). In the fresh-water cyanobacterium *Synechocystis* sp. PCC 6803, the Orange Carotenoid Protein (OCP) is required for this phycobilisomes-associated mechanism and

this appears to be the fundamental mechanism by which NPQ is triggered in cyanobacteria (Wilson et al. 2006).

8.0 State Transitions

'State transitions' (the re-distribution of light harvesting proteins) represent another important photoprotective mechanism. Cyanobacteria dynamically exhibit state transitions, which are both linked to and regulate the operation of cyclic electron flow around PSI (Herbert et al 1992; Satoh and Fork 1983; Schreiber et al. 1995). 'State transitions' (Bonaventura and Myers 1969) regulate the distribution of absorbed light energy between PSI and PSII occurring in plants (Allen 2004), algae (Cardol et al. 2009; Finazzi et al. 2002; Wollman 2001), and cyanobacteria to varying degrees (Joshua and Mullineaux 2004; McConnell et al. 2002). They are a rapid, dynamic process that adjusts the relative activities of PSI and PSII by regulating the distribution of excitation energy between them in response to imbalanced light regimes or other factors that influence the redox potential of the PQ pool (Huang et al. 2003). In higher plants and green algae, phosphorylation of the light harvesting complexes (LHCII), in response to PQ pool reduction, causes reversible transfer of a fraction of the LHCII from PSII to PSI (state 1 to state 2 transition) which is mediated by a stromal kinase associated with the Cyt *bf* complex (Allen 1981; Keren and Ohad 1998). Dephosphorylation of LHCII restores state 1. State 1 to state 2 transitions occurs when PSII activity exceeds that of PSI, which causes over-reduction of the PQ pool. Restoration of state 1 occurs when the PQ pool is

again oxidized (Allen et al. 1981; Horton and Black 1981; Vener et al. 1998), as in transitions from darkness to light in cyanobacteria.

In cyanobacteria and red algae, phycobilisomes (PBS) are the major light-harvesting antennae. The light energy absorbed by PBS can be delivered efficiently to either PSII or PSI. The regulatory mechanism for PBS-absorbed light energy distribution between PSI and PSII in these organisms is not fully understood. No apparent state-transition kinase exists in cyanobacteria; however, it has been proposed that the sensing site for imbalanced light distribution to the photosystems and the signaling mechanism involves the Cyt *bf* complex as indicated by mutational studies (Schneider et al. 2001; Volkmer et al. 2007) and inhibitor treatments (Brantmier-Kallas, unpublished). Binding of plastoquinol to the Cyt *bf* complex could trigger a conformation change in a sensor protein, leading to the state 2 transition (Huang et al. 2003). It should be noted that state transitions may strongly influence the relative activities of linear and cyclic electron flow. In state 2 (PQ pool reduced), more PBS antenna are associated with PSI and thus PSI activity, potentially including cyclic flow, should be increased. Conversely, in state 1 (PQ pool oxidized), PBS antenna move to PSII and PSI activity should decrease. In cyanobacteria in darkness or low light intensity, the PQ pool becomes more reduced because NAD(P)H dehydrogenase activity exceeds cytochrome oxidase activity (see e.g. Kallas 2011). At high light intensity, the PQ pool might again become more reduced because although both PSII and PSI activities should increase, PQH_2 oxidation by the Cyt *bf* complex is the usual rate-limiting step in electron transfer, resulting in PQ pool reduction.

In a photoinhibition study, *Synechocystis* sp. PCC 6803, wild-type, *ndhB* and *psaE* mutant strains showed similar rates of both photoinhibition damage and photoinhibition repair. The photoinhibitory treatments induced a high rate of PSI cyclic electron transport in all strains suggesting that PSI cyclic electron flow protects against photoinhibition. These results support the hypothesis that both Fd- and NDH-mediated cyclic electron pathways are present in cyanobacteria and are stimulated by strong light (Thomas et al. 2001). The ATP generated by cyclic electron flow is also used to drive active CO_2 uptake in cyanobacteria. Uptake of CO_2, driven by cyclic electron flow, would tend to protect against photoinhibition by providing a sink for electrons and supporting high rates of CO_2 assimilation (Thomas et al. 2001).

9.0 Cyclic electron flow under environmental stress conditions

Active cyclic electron flow around PSI is observed in plants and cyanobacteria under environmental stress conditions such as excessive light, salt stress, heat stress, iron stress or low CO_2 (Jia et al. 2008; Kohzuma et al. 2008; Baker and Ort 1992). This cyclic electron flow been proposed as a source of ATP for repair of PSII units damaged by environmental stress, since PSI is typically much less susceptible to damage than PSII (Canaani et al. 1989; Herbert et al. 1990). Higher PSI cyclic electron flow is observed in pea leaves exposed to heat stress in the presence of light. This heat-induced stimulation of cyclic electron transport through PSI is suggested to be an adaptive process, producing ATP under conditions when PSII activity is severely diminished. This ATP synthesis

could be important for survival of the plant and necessary for repair of stress-damaged processes (Havaux et al. 1991; Canaani et al. 1989).

Several studies indicate that application of stress to cyanobacterial cells leads to an increase in the level of cyclic electron flow. Significant increases in PSI cyclic electron flow and dark respiration has been demonstrated in the halotolerant cyanobacterium *Synechocystis* sp. PCC 6803 and other strains grown in high salt media (Hibino et al. 1996; Jeanjean 1993; Joset et al. 1996; Tanaka et al. 1997; Murakami et al. 1997). It is hypothesized that flavodoxin, a soluble electron carrier and functional analog of ferredoxin, might be primarily involved in cyclic electron flow in salt-acclimated *Synechocystis* sp. PCC 6803 cells (Hagemann et al. 1999). Alternatively, flavodoxins such as Flv1 and Flv3 may offer protection by catalyzing dioxygen reduction by PSI in a 'water-water' reaction (Helman et al. 2003) as mentioned above. In *Synechococcus* sp. PCC 7942 grown under iron-stress, linear electron transport is impaired apparently because of an altered structure and content of cytochrome *f*. Under these iron-stress conditions, it is hypothesized that growth rate is maintained because of ATP generated through PSI cyclic electron flow (Ivanov et al. 2000). However, this role of a damaged cytochrome *f* protein in this process is questionable because an active Cyt *bf* complex is required for all known cyclic electron flow pathways.

Genetic manipulations of acyl-lipid desaturase genes have demonstrated that cyanobacteria modulate unsaturation of their membrane lipids to establish tolerance to low temperature in the presence of excessive light (Gombos et al. 1992; 1994; Tasaka et al. 1996; Wada et al. 1992). Low-temperature has a synergistic effect with irradiation in

provoking photoinhibition (Powles 1984). The recovery of photosynthetic activity after photoinhibition damage by high-intensity illumination at low temperature is reduced when the saturation level of membrane lipids increases (Gombos et al. 1994). It has been proposed that membrane lipid desaturation may facilitate the repair of the PSII complex after photoinhibition at low temperature (Gombos et al. 1992; Gombos et al. 1994; Tasaka et al. 1996), although no direct experimental evidence has yet been obtained to suggest a molecular mechanism for this hypothesis (Somerville 1995; Sakamoto and Bryant 1998).

10.0 Tolerance of High light Intensity

High light intensity is a stress condition for many photosynthetic organisms. Absence of appropriate acceptors for electron at high light intensity can increase the formation of reactive oxygen species (ROS) at specific sites within the photosynthetic apparatus. ROS production can cause harmful effects such as damage of DNA, lipid peroxidation, oxidation of amino acids and oxidative de-amination of specific enzymes (Muller 2000, Horn, Master's Thesis, UWOshkosh). These effects can lead to irreversible damage of cellular functions and result in cell death (Herman and D'Ari 1998). Photosynthetic organisms have developed mechanisms for adaptation to excess light. These include photoinhibition, non-photochemical quenching, and state transitions. Inspite of these mechanisms, very few photosynthetic organisms are able to survive and grow under high light intensity. One such organism, which grows under extremely high light intensities, is the marine cyanobacterium *Synechococcus* sp. PCC 7002 (hereafter,

Synechococcus PCC 7002) (Figure 4 and 5), which was used for the studies presented in this thesis.

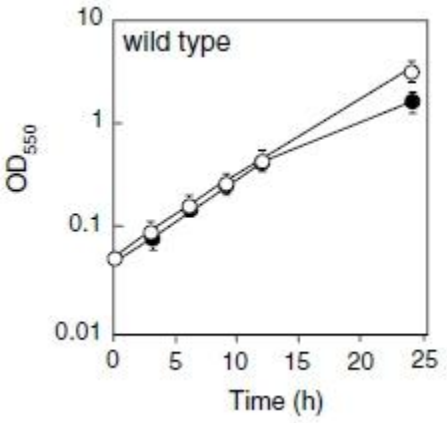

Figure 4. Growth of *Synechococcus* sp. PCC 7002 under high light intensity. Exponentially growing wild type cells under standard conditions (250 µmol photons m^{-2} s^{-1}, 1% CO_2, 38° C) were diluted to an OD_{550} of 0.05 and grown at either 250 µmol photons m^{-2} s^{-1} or 4500 µmol photons m^{-2} s^{-1} constant illumination. Open circles represent cells grown under 250 µmol photons m^{-2} s^{-1}. Filled circles represent cells grown under 4500 µmol photons m^{-2} s^{-1}. Standard deviations are indicated as error bars on the graph (Nomura et al. 2006)

The mechanism of high-light tolerance in *Synechococcus* PCC 7002 is not well understood. Oxygen should be consumed to avoid formation of reactive oxygen species. Cytochrome oxidases are among the proteins that can consume oxygen and lower cellular oxygen concentrations (Kelly 1990). Cytochrome oxidases are present in both the respiratory and photosynthetic electron transport chains in cyanobacteria. Studies indicate that *Synechococcus* PCC 7002 uses cytochrome oxidase as a sink for removing excess electrons not accounted for by PSI activity (Schubert 1995). Two cytochrome oxidase operons, CtaI and CtaII have been cloned and characterized from *Synechococcus* PCC

7002. Studies by Nomura et al. (Nomura et al. 2006a; 2006b) demonstrate that both the CtaI and CtaII oxidases are important for high light tolerance in *Synechococcus* PCC 7002. Further, this cyanobacterium has an exceptionally efficient energy transfer from PBS to PSI that requires the allophycocyanin ApcD protein of the phycobilisome complex (Dong et al. 2009). The occurrence of this efficient energy transfer to PSI implies an important role for PSI activity, and quite likely cyclic electron flow, in high light tolerance.

11.0 Model organism for this thesis

As stated previously, cyclic electron flow increases under stress conditions. Studies have suggested that exposure to high light might increase the rate of cyclic electron flow (Baker and Ort 1992). The exact role of elevated cyclic electron flow under high light condition remains incompletely understood. The present study attempts to examine cyclic electron flow pathways in the marine cyanobacterium *Synechococcus* sp. PCC 7002 grown under high light conditions. This cyanobacterium was first isolated in 1961 from mud-flat pens in Magueyes Island, Puerto Rico (Van Baalen 1961). *Synechococcus* PCC 7002 is among the fastest growing cyanobacteria with a doubling time of 3.5 hrs. *Synechococcus* PCC 7002 is the model organism for this study of cyclic electron flow under high light intensity because of its tolerance and growth under extreme high light conditions. This organism can grow well at extremely high light up to 5000 μmol photons m^{-2} s^{-1} (Figure 4). This light intensity is more than twice that of full-sunlight on a bright day. *Synechococcus* PCC 7002 is a unicellular; rod shaped

cyanobacterium (Figure 5) and is capable of photoheterotrophic growth on glycerol (Lambert and Stevens 1986).

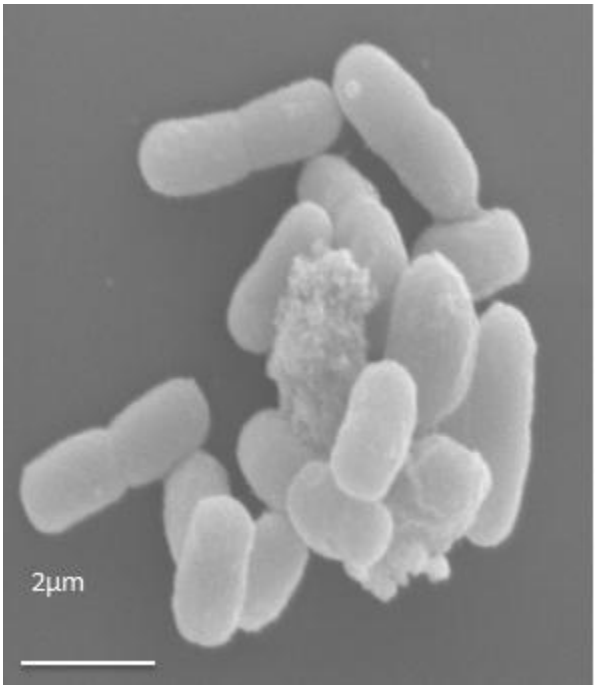

Figure 5. Scanning electron micrograph showing rod-shaped *Synechococcus* PCC 7002 cells. (Courtesy of George Weir, Pers. Comm.)

12.0 *Synechococcus* sp. PCC 7002 wild type and mutant strains

In the current cyclic electron flow study, experiments were performed on laboratory grown wild type *Synechococcus* PCC 7002 and two mutant strains. The mutant strains used were NdhF (Schluchter et al. 1993) and PetB-R214H (Nelson et al. 2005). The NdhF mutant has a non-functional NAD(P)H dehydrogenase (NDH) enzyme complex. As mentioned above, the NDH enzyme plays an important role in cyclic electron flow, especially in cyanobacteria. Previous studies have demonstrated the

importance of the NDH-mediated cyclic electron pathway in cyanobacteria (Yu et al., 1993; Mi et al., 1993). In the present study, experiments were performed with the NdhF mutant to elucidate the role of the NDH-mediated pathway in cyclic electron flow under high light conditions. The PetB-R214H mutant has a mutation in the quinone reductase or Q_n site of the Cyt *bf* complex (Nelson et al. 2005). In this mutant, an arginine (R) in the cytochrome b_6 (PetB) polypeptide at position 214 near the Q_n site is substituted with a histidine (H). The PetB-R214H mutant has an electron transfer rate through the Cyt *bf* complex (Cyt f/c_6 reduction) ~3 times slower than the wild type and impaired electron flow through the *b* hemes to the Q_n site. This mutant grows ~3 times slower than the wild type (under 200 µmol photons m^{-2} s^{-1}, 3% CO_2). The PetB-R214H mutant also overproduces superoxide radicals and these cause damage, which accounts in part for the slow growth of this strain (Ouyang et al. 2004; Brantmier, MS thesis, UW Oshkosh). These studies suggest that superoxide formation may result from a prolonged lifetime plasto-semiquinone at the Cyt *bf* Q_p site resulting in reduction of dioxygen to superoxide. In the current research, experiments were designed with the PetB-R214H mutant to investigate the proposed site of entry for electron flow in a possible direct cyclic pathway from PSI to the Cyt *bf* quinone-reductase (Q_n) site.

13.0 Electron transfer kinetics and measurements of linear and cyclic electron flow

Electron transfer kinetics were studied using a Joliot-type (Biologic JTS-10) spectrophotometer. To estimate the total electron flow (linear plus cyclic) through PSI, the kinetics of P700 re-reduction were measured following P700 oxidation in wild-type

as well as the mutant cells. To measure cyclic electron flow, two approaches are commonly used. One approach involves steady state measurements performed by measuring the fluorescence comparing PSI and PSII turnover across a range of conditions (Herbert et al. 1990; Golding et al. 2004). But this method does not give an absolute measure of photosystem turnover and conflicting results have been obtained. In steady state kinetics measurement studies with chloroplasts, some authors have found substantial rates of cyclic electron flow (Harbinson and foyer 1991; Golding 2003) whereas others have found no evidence for the pathway (Sacksteder and Kramer 2000).

Another approach to measure cyclic electron flow is to examine P700 reduction following its oxidation under conditions that suppress PSII turnover. PSII turnover can be suppressed in two ways. One, by use of a PSII inhibitor such as 3-(3,4-dichlorophenyl)-1,1-dimethylurea (DCMU), which blocks the Q_B site of PSII and thus inhibits electron flow through linear electron transport chain (Golding et al. 2004; Yu et al. 1993). Two, by use of far-red light for illumination, which exclusively or primarily excites only PSI (Golding et al. 2004; Herbert et al. 1990). In the study presented here, P700 kinetic and cyclic electron flow measurements were made with the aid of both of these methods to suppress PSII turnover. My objectives were 1) to compare cyclic electron flow in *Synechococcus* PCC 7002 wild type and the NdhF and PetB-R214H mutants under optimal and high light growth conditions, and 2) To investigate the role of cyclic electron flow under high light conditions.

In addition to DCMU, several other inhibitors were used. These include 2,5 Dibromo-3-methyl-6-isopropyl-p-benzoquinone (DBMIB), potassium cyanide (KCN),

MV (methyl viologen) and 4(1H)-quinolone (4-1HQ). All inhibitors blocked different sites and served different functions in this cyclic electron transport study as will be further discussed below. Kinetics experiments were also carried out following pre-illumination to investigate possible differences in cyclic electron flow in cyanobacteria pre-adapted under darkness versus photosynthetic illumination. Since the Cyt *bf* complex is essential for all known cyclic electron transfer pathways around PSI, Cyt *bf* kinetics were also measured together with P700 kinetics under all conditions in the wild-type as well as mutant cultures. Studies have also shown that 'state transitions' (the redistribution of light harvesting proteins between PSII and PSI) are involved in the switch between linear and cyclic electron flow (Finazzi et al. 2002). These 'state transitions' are triggered by the redox state of the PQ pool or Cyt *bf* complex by mechanisms that are not fully understood, particularly in cyanobacteria (see Kallas, 2012 and references therein). Measurements of Cyt *bf* kinetics in the wild type and mutant strains under optimal and high-light conditions were performed to reveal the activity and contributions of the Cyt *bf* complex to cyclic electron flow pathways and their regulation.

Apart from the NAD(P)H dehydrogenase (NDH) complex, another respiratory enzyme complex has a possible role in cyclic electron flow. Studies on *Synechocystis* sp. PCC 6803 have shown that succinate dehydrogease (SDH) is a major source of electrons for reduction of the PQ pool, especially under darkness (Cooley et al. 2001). Therefore, inactivation of the *sdhB* gene, encoding the Fe-S subunit of the SDH enzyme complex in *Synechococcus* PCC 7002, and characterization of the SdhB mutant was an important, initial objective of the thesis research. Unfortunately, all the attempts towards knocking

out this gene ultimately failed (see Appendix D for a description of the strategy and progress of this work). Electron transfer kinetics studies of the SdhB mutant were intended to elucidate the contribution of succinate dehydrogenase to cyclic electron flow in *Synechococcus* PCC 7002 under optimal as well as high light conditions.

14.0 Photosystem I – cytochrome *bf* supercomplexes

Preliminary data from our laboratory shows that at a high light intensity (1400 µmol photons m^{-2} s^{-1}, or ~3/4 full sunlight) relative to optimal light intensity (~200 µmol photons m^{-2} s^{-1}), cyclic electron flow in *Synechococcus* PCC 7002 wild type increased dramatically to ~30% of total electron flow. This was an unexpectedly high percentage of cyclic electron flow. Under typical laboratory growth conditions (~200 µmol photons m^{-2} s^{-1}), cyclic electron flow has been reported to play a minor role, only ~5% of total electon flow in *Synechococcus* PCC 7002 (Yu et al. 1993 and Hagemann et al. 1998) cyanobacteria. The apparent, elevated cyclic electron flow in *Synechococcus* 7002 at high light intensity might occur via several different pathways. Alternative cyclic electron pathways active under high light might involve 1) a direct PSI – Cyt *bf* pathway mediated by soluble electron carriers, or 2) a direct PSI – Cyt *bf* pathway mediated by the formation of a possible PSI – Cyt *bf* supercomplex under high light intensity. A variety of supercomplexes have been found in the photosynthetic apparatus of higher plants, green algae, as well as cyanobacteria and some of these play specific roles under stress conditions. For instance, a PSI-CP43´ light harvesting supercomplex is found in some cyanobacteria (Melkozernov et al. 2006). The PSI- CP43´ supercomplex increases the

light-harvesting capacity of the cyanobacteria specifically under low-light and iron-deficiency. A PSI-LHCI supercomplex is found in green algae and higher plants (Melkozernov et al. 2006). This PSI-LHCI supercomplex functions in accessory light harvesting and efficient delivery of the excitation to the PSI core complex before it dissipates and converts into long lived triplet states giving rise to the deleterious singlet oxygen species (Melkozernov et al. 2006). Most importantly, a PSI- LHCI-LHCII-FNR-Cyt bf-PGRLI supercomplex was recently isolated from the green alga, Chlamydomonas reinhardtii (Iwai et al., 2010). This protein supercomplex consisted of PSI with its own light-harvesting complex (LHCI), the PSII light-harvesting complex (LHCII), the Cytochrome b_6f complex (Cyt *bf*), ferredoxin (Fd)-NADPH oxidoreductase (FNR), and integral membrane protein PGRL1. There is evidence that this supercomplex is involved in cyclic electron flow and in regulating electron flow and redox balance between two photosystems.

There has been no previous evidence for a PSI - Cyt *bf* supercomplex in cyclic electron flow in cyanobacteria. However, our preliminary data suggests the possible formation of such supercomplex in *Synechococcus* PCC 7002, especially under high light conditions. This thesis research was undertaken to obtain further evidence for a PSI- Cyt *bf* supercomplex or other alternative cyclic electron flow pathways active in *Synechococcus* PCC 7002 cyanobacteria under high light conditions.

15.0 Objectives of the thesis research

1. To compare the contributions of cyclic versus linear electron flow in the wild type, NdhF, SdhB, and PetB-R214H mutants of *Synechococccus* sp. PCC 7002 grown under optimal and high light intensity conditions
2. To investigate the impacts of the NdhF, SdhB, and PetB-R214H mutations on Cyt *bf* electron transfer kinetics under optimal and high light intensity conditions.
3. To investigate the occurrence of a direct PSI – Cyt *bf* cyclic electron flow and formation of a PSI – Cyt *bf* supercomplex in *Synechococcus* sp. PCC 7002 cyanobacteria.

16.0 Expected Outcomes

The NdhF mutant is expected to have a much less active and smaller proportion of cyclic electron flow, and thus show a slower re-reduction of PSI in presence of DCMU or far-red illumination than the wild type. This is because the major, known cyclic electron route in cyanobacteria is mediated by the NDH-1 enzyme complex. Since this complex is inactive in the NdhF mutant, cyclic electron flow should be impaired in this mutant and this will lower the rate of entry of electrons into PSI. If an Fd-dependent, direct PSI – Cyt *bf* cyclic electron transfer pathway exists in *Synechococcus* sp. PCC 7002, then this should be unaffected in the NdhF mutant because this pathway does not require the NDH-1 complex. Moreover, if a direct PSI – Cyt *bf* pathway exists, then the PetB-R214H mutant may show impaired cyclic electron flow because the R214H mutation occurs in the quinone-reductase (Q_p) domain, which is the likely site of electron entry from PSI. In

Cyt *bf* kinetics experiments, electron flux through the Cyt *bf* complex is known to be slower in the PetB-R214H mutant compared to wild type *Synechococcus* PCC 7002 (Nelson et al. 2005). Further, my preliminary results show that electron flow through the Cyt *bf* complex is also slower in the NdhF mutant than in the wild type. The reasons for this are less obvious, but perhaps suggest a more important contribution of NDH-mediated cyclic flow that previously estimated. Under high light intensity conditions, faster re-reduction of PSI in the NdhF mutant might indicate either the formation of a PSI – Cyt *bf* supercomplex and a direct PSI – Cyt *bf* electron flow under these conditions or complete reduction of the acceptor side of PSI. This can be further evaluated by experiments with methyl viologen (paraquat), which accepts electrons from the acceptor side of PSI. Overall, this work will contribute for understanding photosynthetic electron transfer pathways in cyanobacteria and their biological significance. The work will further be important for developing biofuel production pathways.

CHAPTER II

CYCLIC ELECTRON FLOW UNDER HIGH LIGHT INTENSITY

1.0 Introduction

Photosynthesis is the biological process converting the electromagnetic energy emitted by the sun (in the form of sunlight) into biochemical energy and thus acting as the direct or indirect source of energy for nearly all life on earth. Photosynthetic organisms convert carbon dioxide into organic compounds, evolve oxygen through photosynthesis and play an important role as the primary producers of food in every ecosystem. Cyanobacteria are the ubiquitous and most genetically diverse group of photosynthetic organisms which drastically changed the Earth by oxygenating the atmosphere. They account for approximately 25% of the global photosynthetic activity and some of them are also involved in nitrogen fixation. Other than oxygenating the atmosphere, cyanobacteria have played one more important role in the evolution. Several lines of evidence indicate that modern plant chloroplasts evolved from ancestral, endosymbiotic cyanobacteria (McFadden 2001).

In cyanobacteria, photosynthesis occurs in internal thylakoid membranes encompassing components of the respiratory as well as photosynthetic electron transport. The cyanobacterial light harvesting antennae are attached to the thylakoid membranes and are called phycobilisomes (PBS). Photosystem II (PSII), photosystem I (PSI) and cytochrome *bf* (Cyt *bf*) complexes are the major complexes in this photosynthetic apparatus. Light energy captured by the PBS is funneled to chlorophyll reaction centers

in PSII and starts a linear electron flow through PSII, Cyt *bf* and PSI producing ATP and NADPH as end products (Whitmarsh and Govindjee 1995). Oxidation of water provides the electrons for this electron flow. ATP and NADPH produced during the linear electron flow are used for several cellular reactions. Carbon fixation through the Calvin-Benson-Bassham cycle (Calvin cycle) is an important step and requires an ATP:NAD(P)H ratio of 3:2. However, studies show that, in oxygenic photosynthesis, linear electron transfer from water to $NADP^+$, produces ATP and NAD(P)H in a ratio of only 9:7 (Alric et al. 2010). Moreover, many cellular reactions require ATP and this further imbalances the ATP to NAD(P)H ratio required for carbon fixation. Several mechanisms may be considered, that produce the 'extra' ATP to meet the demands of carbon fixation (Alric et al. 2010). Reactions such as the Mehler reaction (Mehler 1951) or Plastid Terminal Oxidase (PTOX) activity (Bennoun 1982) may directly or indirectly participate to form a thylakoid membrane proton gradient for ATP synthesis. In green plants and algae, ATP can also be synthesized in mitochondria (Lemaire et al. 1988). However, these reactions may not be fast enough to compete with linear electron flow. Thus it may be more efficient, and essential in cyanobacteria, to produce additional ATP directly at the level of the thylakoid membrane. Several studies have reported that cyclic electron flow around PSI is involved in production of the additional ATP (Allen 2003). Cyclic electron flow thus seems to be crucial for the proper balance of NAD(P)H and ATP in photosynthetic organisms (Alric et al. 2010) and is also thought to protect the photosynthetic apparatus from photodamage (Shikanai 2007).

Two primary pathways have been proposed for cyclic electron flow: 1) the Ferredoxin (Fd)-FQR pathway and 2) The NAD(P)H dehydrogenase (NDH)-dependent pathway.

In the Ferredoxin (Fd)-FQR pathway, reduced Ferredoxin (Fd_{red}) donates electrons to ferredoxin-quinone oxidoreductase (hereafter FQR) which cycles the electrons back to the PQ pool through the Cyt *bf* complex. The electrons cycled back through this pathway may enter Cyt *bf* complex through Q_n (Quinone reductase) site. In the NDH-dependent pathway, NDH mediates NAD(P)H oxidation and plastoquinone (PQ) pool reduction in the same way that complex I (NDH dehydrogenase) does in mitochondria (Ogawa 1991). According to previous studies, cyclic electron flow mediated by the NDH-1 complex appears to be the major cyclic electron route in cyanobacteria (e.g. Yu et al., 1993). The NDH-I (NADH dehydrogenase) complex oxidizes NAD(P)H and delivers electrons to the PQ pool (Schluchter et al. 1993).

Several studies indicate that application of stress to cyanobacterial cells leads to an increase in the level of cyclic electron flow. High light intensity is a stress condition for many photosynthetic organisms. It can increase the formation of reactive oxygen species (ROS) at specific sites inside the photosynthetic apparatus (Muller 2000). ROS production can cause harmful effects such as damage of DNA, lipid peroxidation, oxidation of amino acids and oxidative de-amination of specific enzymes. These effects can lead to irreversible damage of cellular functions and result in cell death (Herman and D'Ari 1998). Photosynthetic organisms have developed mechanisms for adaptation to

excess light such as non-photochemical quenching, and state transitions (Niyogi 1999). But inspite of these mechanisms, very few photosynthetic microrganisms are able to survive and grow under high light intensity. One such organism which grows under extremely high light intensities is the marine cyanobacterium *Synechococcus* sp. PCC 7002 (hereafter, *Synechococcus* PCC 7002). Though steady state kinetics measurements suggest that exposure to high light might increase the rate of cyclic electron flow (Herbert et al . 1990; 1995; Thomas et al. 2001), the exact role of elevated cyclic electron flow under high light condition remains poorly understood. The present study attempts to examine cyclic electron pathways and their role in the marine cyanobacterium *Synechococcus* sp. PCC 7002 grown under high light conditions.

In this study, experiments were performed on laboratory-grown, wild type *Synechococcus* PCC 7002 strain and two mutant strains, NdhF and PetB-R214H. The NdhF mutant (Schluchter et al. 1993) has a non-functional NDH-1 (NADH dehydrogenase) enzyme complex. Previous studies have provided evidence for the involvement and importance of an NDH-mediated cyclic electron pathway in cyanobacteria (Yu et al. 1993; Mi et. al., 1993, Ogawa and Mi 2007) In the current study, experiments with the NdhF mutant were designed to elucidate the role of the NDH-1 complex in cyclic electron flow under high light conditions.

The PetBR-214H mutant has mutation in the quinone reductase, or Q_n, site of the Cyt *bf* complex (Nelson et al. 2005). In comparison to the wild type, the PetB-R214H mutant shows ~2.5 times slower electron transfer through the *b* hemes to the Q_n site and a

~3 fold slower growth rate. Experiments with the PetB-R214H mutant were designed to investigate the proposed site of entry for electrons into the Cyt *bf* quinone-reductase (Q_n) site during a possible direct cyclic electron flow pathway from PSI.

Cyclic electron flow was measured by examining PSI P700 re-reduction following its light-induced oxidation under conditions that prevent PSII turnover. PSII turnover was inhibited or minimized in two ways. Namely: 1) by use of the PSII inhibitor 3-(3,4-dichlorophenyl)-1,1-dimethylurea (DCMU), which blocks the Q_B site of PSII and thus inhibits PQ pool reduction by PSII and linear electron flow (Herbert e t al .1990), and 2) by use of far-red (700 to 740 nm) light for illumination, which primarily excites only PSI (Joliot and Joliot 2002).

To further investigate cyclic electron flow back to PSI, in relation to possible alternative electron pathways, experiments were performed using KCN in addition to DCMU. The cyanide ions from KCN inhibit cytochrome oxidase activity and thus block electron flow from the Cyt *bf* complex to cytochrome oxidase and oxidative phosphorylation (Yu et al. 1993) (refer Figure 1). To cells inhibited with DCMU and KCN, methyl viologen (also known as paraquat) was also added, as a further test of cyclic electron flow activity through PSI. The herbicide methyl viologen (Paraquat) accepts electrons from the acceptor side of PSI, thus intercepting electron flow from PS I before electrons cycle back into PQ pool or reduce $NAD(P)^+$ (Fork and Herbert 1993). Maximal cyclic electron flow through PSI should thus occur in the presence of DCMU, KCN, and methyl viologen.

Since the Cyt *bf* complex also clearly plays an important role in the cyclic electron flow around PSI, Cyt *bf* kinetics were measured along with P700 kinetics under all conditions in wild type as well as the mutant cultures. Experiments with DBMIB and 4-1HQ were designed to investigate the contribution of electron flow through the Cyt *bf* complex and to compare Cyt *bf* turnover under optimal and high light conditions. DBMIB is a potent inhibitor of Cyt bf complex, which binds to the Q_p (Quinol Oxidase) site of Cyt *bf* complex and slows down the Cyt *bf* turnover (Cramer et al 1991). DBMIB does not behave as a good inhibitor when it is reduced, hence another inhibitor 4-1HQ was used in addition to the DBMIB. The 4-1HQ inhibitor also binds to the Q_p (Quinol Oxidase) site of Cyt *bf* complex and its functioning does not depend on its oxidation state.

Data presented here showed that the NDH-I route accounted for most of the cyclic flow (~10% of linear) under optimal light as observed previously. At high light intensity, PSI content decreased but cyclic electron flow increased markedly in both the wild type and NdhF mutant. Cyclic flow also increased in the PetB-R214H mutant at high light but PSI content did not decline, suggesting a defect in Cyt *bf* – mediated regulation. Most interestingly, at high light intensity in the NdhF mutant, cyclic electron flow accounted for 50% or more of linear flow. This active, cyclic flow in the NdhF mutant indicates the activation of an NDH-independent cyclic pathway. These data suggest that this efficient cyclic flow is catalyzed by the formation of a Cyt *bf* – PSI supercomplex that is important for adaptation and growth of *Synechococcus* 7002 at extreme, high-light intensities.

Further experiments will be needed to define the supercomplex and its implications for biofuels.

2.0 Materials and Methods

2.1 Cyanobacterial strains and culture conditions.

Synechococcus sp. PCC 7002 (formerly known as *Agmenellum quadruplicatum* PR-6) is a rod shaped, gram-negative, unicellular marine cyanobacterium originally cultured by Van Baalen in 1961 (Van Baalen 1961). *Synechococcus* cells perform oxygenic photosynthesis and require vitamin B_{12} for growth. The mutant strains used in the study were, NdhF mutant (Schluchter et al. 1993) kindly provided by Don Bryant, Penn State University) and PetB-R214H mutant (Nelson et al. 2005). Table 1 summarizes the media requirements and antibiotics used during the study.

Synechococcus stock strains were grown in liquid A(D7) medium and/or A^+(P1) medium as well as on agar plates containing A(D7) medium and/or A^+(P1) medium (Appendix A). Agar plates were incubated at 32 °C in a temperature controlled growth chamber with light intensity of 40 to 80 μmol photons m^{-2} s^{-1} (Percival Scientific, Perry, IA.). Liquid cultures were grown with shaking (ca. 100-200 rpm) on an Orbital Shaker located on the floor of the growth chamber. Stock cultures were maintained at room temperature (RT) at a light intensity of approximately 13 μmol photons m^{-2} s^{-1} under a cool-white fluorescent lamp.

Table 1: Cyanobacterial strains, media requirements and antibiotics

Cyanobacterial cultures	Growth Medium	Antibiotics	Vit B_{12}
WT	A(D7), A^+(P1)	-	+
NdhF	A^+(P1)	Km^{100}	+
PetBR214H	A(D7)	Sm^{50}/Sp^{50}	+

WT, Wild-type Synechococcus PCC 7002 (UWO strain); NdhF, NdhF mutant (PSU strain); PetBR214H, PetBR214H mutant (UWO strain); +, requires Vitamin B12 for growth; -, antibiotic not needed; Km^{100}, 100µg/ml Kanamycin, Sm^{50}/Sp^{50}, 50µg/ml Streptomycin & 50µg/ml Spectinomycin

2.2 Experimental set-up for spectroscopic measurements.

In order to perform spectroscopic measurements, experimental cultures were grown in 300ml of medium in sterile Roux flasks with 3% CO_2/air bubbled along with constant stirring at 38°C. For optimal light conditions, cultures were grown under light intensity of 200 µmol photons m^{-2} s^{-1}. For high light conditions, cultures were initially grown under light intensity of 200 µmol photons m^{-2} s^{-1}, and were shifted to high light after they reached an $O.D_{750}$ of 0.3. These cultures were then grown under light intensity of 2000 µmol photons m^{-2} s^{-1} for two hours. The high light intensity of 2000 µmol photons m^{-2} s^{-1} was reached by using a Magna, white-light, LED, light bank.

All the spectroscopic measurements were done with a Biologic JTS-10, Joliot-type spectrophotometer (hereafter Joliot JTS-10). This is a pump-probe LED (Light Emitting Diode) instrument which allows direct measurements of photosynthesis reactions within living cells by measuring time-resolved, light-induced spectral changes associated with oxidation or reduction of electron carriers. Turnover of these electron carriers and thus of photosynthetic electron transfer complexes can be calculated from the obtained results. For spectroscopic measurements, typically 20 mL samples were collected from experimental cultures, pelleted by centrifugation, and suspended in 5mM Hepes (at pH7.9), 10mM NaCl and 10mM $NaHCO_3$ buffer to an $O.D_{750}$ in the range of 3-5 (see protocol in Appendix B).

2.3 Photosystem I P700 Reduction Kinetics

For measuring total electron flow (linear + cyclic) through PSI, oxidation and re-reduction of PSI P700 was observed with the Joliot JTS-10 spectrophotometer (Joliot and Joliot 2002; 2005). Microsecond flashes or continuous illumination with green actinic light (530 nm) at 300 μmol photons m^{-2} s^{-1} were provided to excite both PS I and PS II. Absorbance changes at 705 and 740 nm (10 nm filter bandwidth) were detected using 705nm and 740nm interference filters with 'P700' cutoff filters (6mm thick). The 'P700' cutoff filters are 6mm thick filters placed in front of the reference as well as the measurement photodetectors. These cutoff filters allow signals of a certain wavelength to enter the photodetectors. The instrument operated with a time constant of 1 ms. An

illumination period of 10 seconds followed by a dark decay period of 20 seconds permitted full oxidation and re-reduction of PSI. Cyclic electron flow was measured by addition of the PS II inhibitor DCMU. 10 μM DCMU was added to 1 ml cell samples to inhibit electron flow from PS II. P700 reduction kinetics were measured as described above.

In other experiments, 1 mM KCN (Potassium cyanide) and 100 μM MV (Methyl Viologen) were added to cells treated with DCMU. After addition of each inhibitor, P700 Reduction Kinetics was measured. Potassium cyanide blocks electron flow to Cytochrome Oxidase and MV accepts electrons from the electron acceptor side of PSI. Cells were also treated with 10 μM DBMIB, 10 μM and 20 μM 4-1HQ in separate experiment to measure electron flow to PSI originating from the Cyt *bf* complex. DBMIB and 4-1HQ both act as quinone analogs and bind to the Q_p (Quinol Oxidase) site of the Cyt *bf* complex.

2.4 Photosystem I P700 Measurements with Far-red Illumination

An alternative way of measuring cyclic electron flow is by using Far-red light for illumination. The Far-red light (~700 – 740 nm) illumination at 2500 μmol m^{-2} s^{-1} light intensity was typically provided for 10 s. This primarily excites PS I and oxidizes the P700 reaction center. P700 oxidation-reduction Kinetics were measured on the wild type and mutants under optimal and high light, with and without the addition of inhibitors, as described above.

Most experiments with the Joliot JTS-10 spectrophotometer require harvesting and concentration of culture samples. The optical density of cell samples is adjusted before performing experiments. Consequently there is a time gap between sampling and experimental runs during which the cell samples might sit in the dark. The PQ pool typically becomes reduced in cyanobacteria during darkness (Cooley et al. 2001). Therefore to see whether dark conditions and PQ pool reduction influence P700 reduction kinetics and cyclic electron flow, pre-illumination experiment were performed during which cell samples were exposed to green actinic light (300 μmol m^{-2} s^{-1}) for periods up to 5 min. P700 reduction kinetics were measured immediately after pre-illumination.

2.5 Cytochrome *bf* Kinetics

Cytochrome *bf* kinetics was measured in wild type and mutant cell samples under optimal and high light intensity, with and without addition of inhibitors, and with and without pre-illumination with green actinic light**.** To measure Cyt *bf* kinetics, cells were typically exposed to Green actinic light (520 nm) at 300 μmol m^{-2} s^{-1} light for flashes totaling 9 ms or a 10 s illumination period followed by a 10 s or 20 s dark decay. Light-induced absorbance changes were recorded via interference filters (6 nm band width) at 546 nm, 554 nm, 563 nm and 573 nm to monitor time-resolved *b* heme (cytochrome b_6) and cytochrome f/c_6 redox changes. 'BG39' (3mm) cut-off filters allowed the reference and sample photodetectors to detect light only in the 300 – 700 nm wavelength range. The kinetics data were deconvoluted using a function of the BioLogic JTS-10 operating

software to obtain individual kinetics traces for cytochrome b_6 (at 563 nm) and cytochrome f/c_6 (at 554 nm).

2.6 Data Analysis

For PSI P700 kinetics, 740 nm traces were subtracted from 705 nm traces. Half-times of the final traces were determined by a function in the BioLogic JTS-10 operating software. From the reaction half-times, the turnover number (electrons per second) of PSI complexes was calculated was calculated according to the formula:

K (Turnover of PSI in electrons/second) = 0.693/ half time of P700 reduction in seconds.

The turnover of PSI in the presence of DCMU (reflecting cyclic electron flow) was divided by the turnover of PSI in the absence of DCMU (reflecting total or linear + cyclic electron flow) to obtain the contribution of cyclic electron flow (expressed as percentage) relative to total electron flow. Cytochrome *bf* reaction half-times and turnover numbers were calculated similarly from deconvoluted *b* heme and cytochrome f/c_6 kinetics data.

3.0 Results

3.1 P700 kinetics in wild type and mutant *Synechococcus* PCC 7002

The light-induced oxidation and dark re-reduction of PSI P700 reaction centers in the wild type and NdhF mutant of *Synechococcus* PCC 7002 is shown in Figure 6.

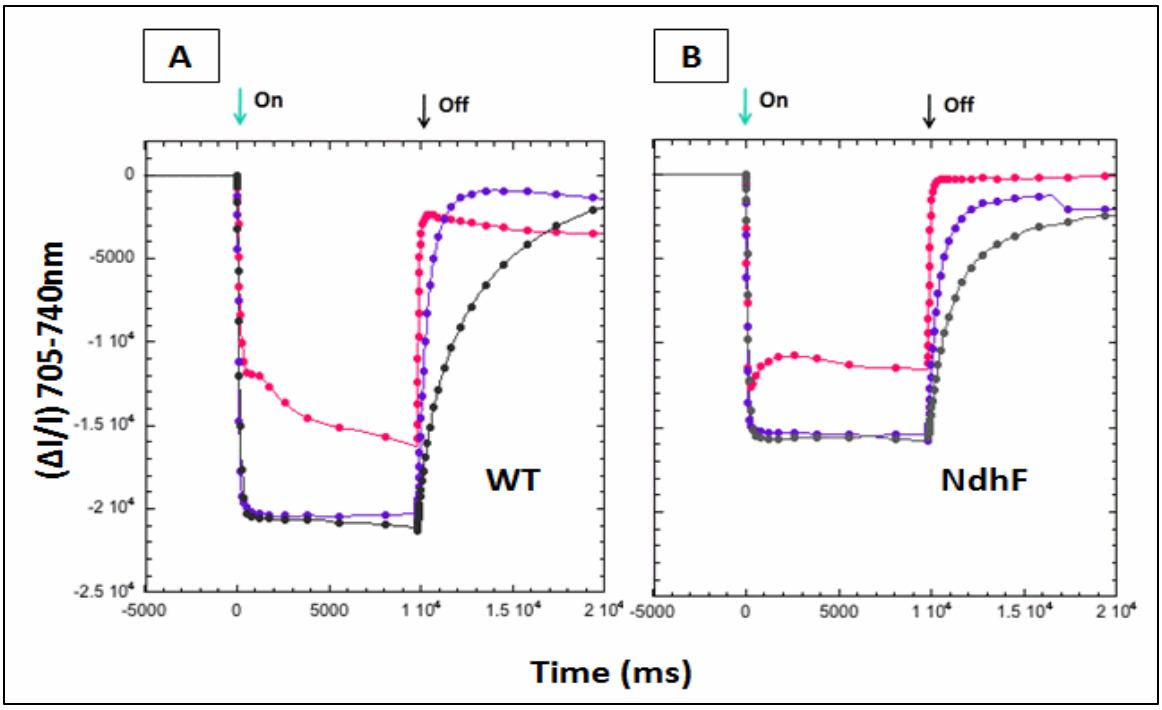

Figure 6. P700 kinetics in *Synechococcus* wild type and NdhF strains grown under optimal light. Panel A and B represents P700 kinetics of the wild type and NdhF mutant, respectively, grown under optimal light. The x-axis shows time in milliseconds (ms) and the y-axis shows relative absorbance (ΔI/I) after subtracting the 740 nm traces from 705 nm traces. Pink traces indicate samples without addition of inhibitors. Purple traces indicate samples upon addition of DCMU. Black traces indicate samples after addition of DCMU and DBMIB. Green arrows indicate the onset of actinic light and black arrows indicate the end of the actinic light period. Oxidation (downward deflection) of P700 was observed when the actinic light was turned on followed by re-reduction (upward deflection) of P700 when the light was turned off. Green actinic light (~530 nm) was 300 µmol photons m^{-2} s^{-1}. Final concentrations of DCMU and DBMIB were 10 µM.

The onset and termination of actinic illumination is indicated by green and black downward arrows, respectively. P700 becomes oxidized during illumination because plastoquinol (PQH_2) oxidation by the Cyt *bf* complex is the usual rate limiting step during photosynthetic electron transfer (Kallas 1994; 2012). Re-reduction ('dark decay') occurs as electrons are resupplied to P700 via the Cyt *bf* complex and pool of Cyt c_6 proteins

that carry electrons to PSI. P700 re-reduction kinetics in the absence of inhibitors is a measure of the total, net electron flow (linear + cyclic) through PSI. Because PQH_2 oxidation by the Cyt *bf* complex is the rate-limiting step, P700 remains oxidized during illumination, and electron flow during illumination should occur no faster than P700 re-reduction in darkness.

To measure cyclic electron flow in the wild-type and mutant cultures, 10 μM DCMU was added to the cell samples. In the presence of DCMU, electrons available for P700 reduction are expected to be derived predominantly from NADH dehydrogenase (NDH) via the NDH-mediated cyclic electron flow pathway from PSI (Yu et al. 1993) and see also Figure 3. In the presence of DCMU, P700 reduction in wild type Synechococcus PCC 7002 showed a half-time of 260 ms, a rate nearly 7-fold slower than that in untreated wild-type cells (Table 2 and Figure 6). In the NdhF mutant treated with DCMU, the half-time of P700 reduction increased dramatically to 1513 ms, or ~24-fold slower than in untreated NdhF cells (Table 2 and Figure 6). These data indicate that the NDH complex plays a predominant role in cyclic electron flow under optimal light conditions as observed previously (Yu et al. 1993; Mi et al. 1993). Moreover, this cyclic pathway represents a relatively small fraction (at best ~15%) of the total electron flow (Table 3).

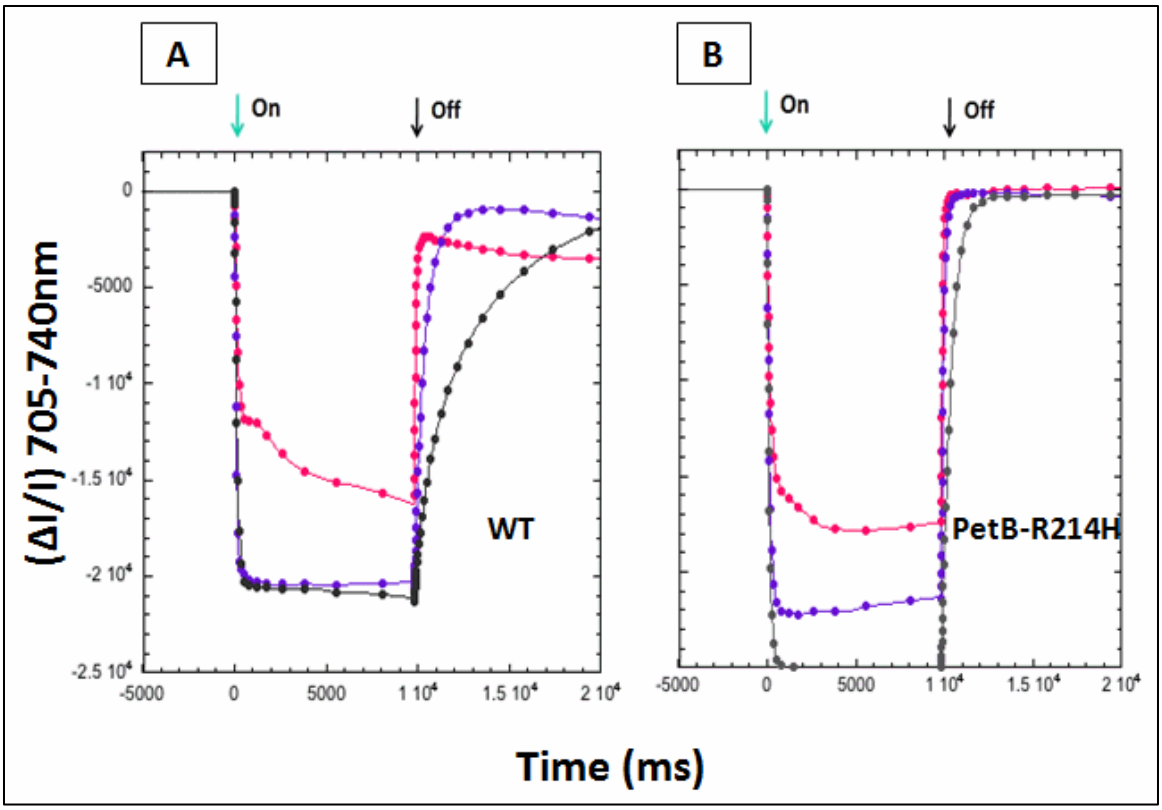

Figure 7. P700 kinetics in the *Synechococcus* wild type and PetB-R214H mutant grown under optimal light. Panels A and B represent P700 kinetics of the wild type and PetB-R214H mutant, respectively, grown under optimal light. The x- and y-axes show time (ms) and absorbance changes as in Figure 6. Pink traces indicate samples without addition of inhibitors. Purple traces indicate samples upon addition of DCMU. Black traces indicate samples after addition of DCMU and DBMIB. Green arrows indicate onset of actinic light and the black arrows indicate the end of actinic light illumination. Downward deflections indicate oxidation of P700 and upward deflections indicate re-reduction. Green actinic light (~530 nm) was 300 µmol photons m^{-2} s^{-1}. Final concentrations of DCMU and DBMIB were 10 µM.

The untreated WT and PetB-R214H mutant showed 42 ms half-time of P700 re-reduction (Table 2). Upon addition of DCMU, the PetB-R214H mutant showed a faster P700 re-reduction (117 ms) compared to the wild type cells (260 ms) (Table 2 and Figure

7). This mutant showed less than a 3-fold decline in the P700 reduction rate upon addition of DCMU. These data indicate that, in contrast to the wild type and NdhF mutant, the PetB-R214H mutant has a very active cyclic electron flow under optimal light intensity, and that this cyclic flow approaches 35% of the total electron flow (Table 3).

Table 2. P700 reduction kinetics +/- DCMU in *Synechococcus* wild type, NdhF and PetB-R214H mutants grown under optimal and high light.

Condition	Optimal light		High light	
	$t_{1/2}$ (ms) [a]	e^-/sec [b]	$t_{1/2}$ (ms) [a]	e^-/sec [b]
WT	42	16.3	39	17.8
WT + DCMU [c]	260	2.6	82	8.5
NdhF	65	10.6	64	10.8
NdhF + DCMU [c]	1513	0.5	86	8.0
PetB-R214H	42	16.5	35	20.0
PetB-R214H + DCMU [c]	117	5.9	41	16.8

[a] Half-times are in milliseconds (ms). [b] PSI P700 turnover (electrons per second) is noted as e^-/sec. [c] DCMU was used at a final concentration of 10μM.

Table 2 summarizes the turnover of the PSI complex measured in cells grown under optimal light (200 μmol photons m^{-2} s^{-1}) and high light (2000 μmol photons m^{-2} s^{-1}) conditions. PSI turnover was faster, as expected, in untreated cells than in inhibitor-treated cells because inhibitors that impede either PSII or the Cyt *bf* complex slow electron flow through PSI. All of the untreated samples (whether wild type, NdhF or

PetB-R214H mutants) showed a higher PSI turnover under both optimal as well as high light conditions relative to inhibitor-treated samples under the same condition (Table 2).

The half-times of P700 reduction were similar in untreated wild type (control) (42 ms) and PetB-R214H (42 ms) and slightly faster compared to NdhF (65 ms) (Table 2). These data are from a single, typical experiment. In another experiment, half-times of P700 reduction were slightly faster in wild type (control) untreated cells (35 ms) relative to NdhF (62 ms) and PetB-R214H (49 ms).

Table 3. Cyclic electron flow as a percentage of total electron flow in *Synechococcus* wild type, NdhF and PetB-R214H mutants grown under optimal and high light.

	Optimal light	High light
Strain	% Cyclic	% Cyclic
WT	15	47
NdhF	4	74
PetB-R214H	35	84

3.2 Electron transfer kinetics under high light conditions

Cultures for high light experiments were shifted to high light (2000 μmol photons m^{-2} s^{-1}) for 2 hours after they had first grown exponentially to ~0.3 OD_{750nm} under

optimal light intensity (200 μmol photons m^{-2} s^{-1}). Both the wild type and mutants showed either similar or much faster P700 reduction kinetics (Table 2) compared to the same strain grown under optimal light intensity (200 μmol photons m^{-2} s^{-1}). Upon treatment with DCMU, the half-time of P700 reduction in wild type cells increased to 82 ms relative to the half-time in the untreated wild type (39 ms). This is a 2-fold decrease in the P700 reduction rate relative to untreated cells. However, this P700 reduction rate (82 ms) in DCMU-treated wild type cells grown under high light was much faster than P700 reduction (260 ms) in DCMU-treated wild type cells grown under optimal light (Table 2). This represents a 3-fold increase in the P700 reduction rate relative to the cells grown under optimal light (Table 2 and Figure 8). These data suggest an active cyclic electron flow in the wild type cells grown under high light intensity.

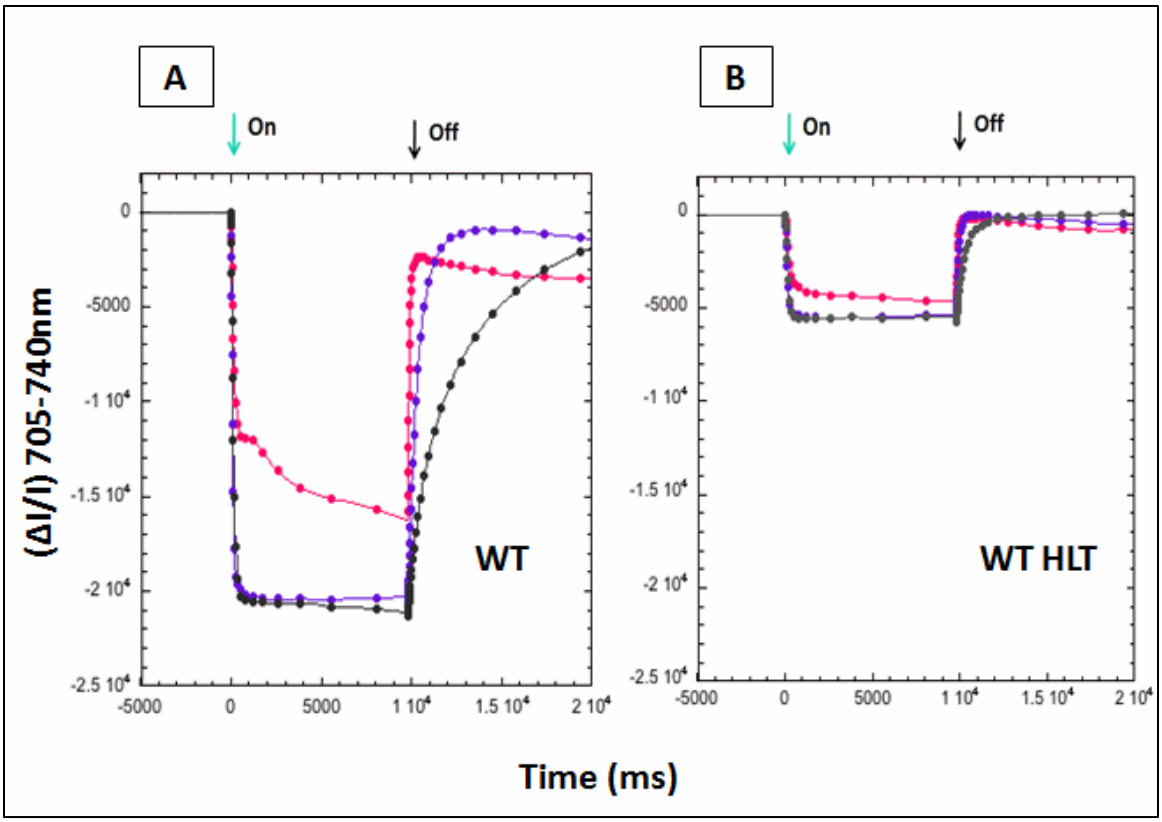

Figure 8. P700 kinetics in the *Synechococcus* wild type grown under optimal and high light. Panels A and B represent P700 kinetics of the wild type sample grown under optimal and high light, respectively. The x- and y-axes show time (ms) and absorbance changes as in Figure 6. Pink traces indicate samples without addition of inhibitors. Purple traces indicate samples upon addition of DCMU. Black traces indicate samples after addition of DCMU and DBMIB. Green arrows indicate onset of actinic light and the black arrows indicate the end of actinic light illumination. Downward deflections indicate oxidation of P700 and upward deflections indicate re-reduction. Green actinic light (~530 nm) was 300 µmol photons m^{-2} s^{-1}. Final concentrations of DCMU and DBMIB were 10 µM.

In the NdhF mutant grown at high light intensity and treated with DCMU, the half-time of P700 reduction decreased dramatically to 86 ms relative to the half-time (1513 ms) of NdhF cells grown at optimal light intensity and treated with DCMU. This

rate in high-light grown NdhF cells in the presence of DCMU is only ~1.5-fold slower than in untreated NdhF cells grown under high light (64 ms) (Table 2 and Figure 9). Therefore, surprisingly and interestingly, in contrast to the NdhF mutant grown at optimal light intensity, NdhF cells under high light conditions showed a remarkably fast cyclic electron flow. Because the NAD(P)H dehydrogenase complex is inactivated in this mutant, cyclic electron flow must occur by a pathway other than the NDH pathway (see Figure 1 for reference). The mostly likely alternative is a direct PSI – Cyt *bf* pathway possibly mediated by the formation of a PSI- Cyt *bf* supercomplex that catalyzes this active cyclic electron flow under high light conditions.

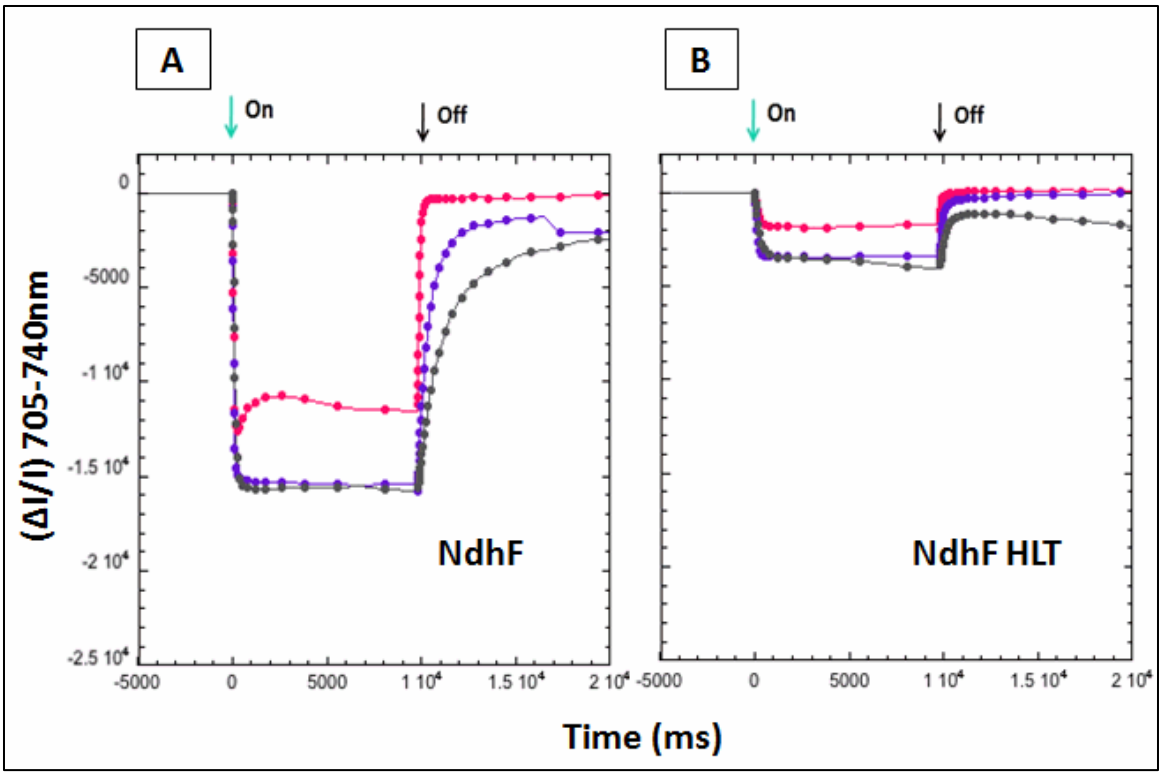

Figure 9. P700 kinetics in the *Synechococcus* NdhF mutant grown under optimal and high light. Panels A and B represent P700 kinetics of the NdhF mutant grown under optimal and high light, respectively. The x- and y-axes show time (ms) and absorbance changes as in Figure 6. Pink traces indicate samples without addition of inhibitors. Purple traces indicate samples upon addition of DCMU. Black traces indicate samples after addition of DCMU and DBMIB. Green arrows indicate onset of actinic light and the black arrows indicate the end of actinic light illumination. Downward deflections indicate oxidation of P700 and upward deflections indicate re-reduction. Green actinic light (~530 nm) was 300 µmol photons m^{-2} s^{-1}. Final concentrations of DCMU and DBMIB were 10 µM.

In the PetB-R214H mutant grown under high light intensity and treated with DCMU, the half-time of P700 reduction increased to 41 ms relative to this mutant grown at optimal light intensity and treated with DCMU. The rate in the high-light, DCMU-

treated cells, is nearly similar to that of the untreated PetB-R214H cells under high light (35 ms) (Table 2 and Figure 10). Thus a much faster P700 reduction (41 ms) was observed in DCMU-treated PetB-R214H cells from high light relative to P700 reduction (117 ms) in DCMU-treated mutant cells from optimal light (Table 2). This result indicates that the contribution of cyclic electron flow to total electron flow in this mutant is higher at high light intensity than at optimal light intensity. However, other experiments with the PetB-R214H mutant (data not shown) showed a much slower cyclic electron flow at high light intensity. Therefore the data presented in Table 2 for the PetB-R214H mutant may not be representative.

All of the *Synechococcus* 7002 cultures grown under high light conditions showed faster P700 reduction rates relative to the same strain and treatment at lower (optimal) light intensity. Also the PSI content (or quantity) at high light intensity was lower in all of the strains than at optimal light intensity, at least as indicated by the lower extent of P700 oxidation upon illumination (Figure 8, 9 and 10).

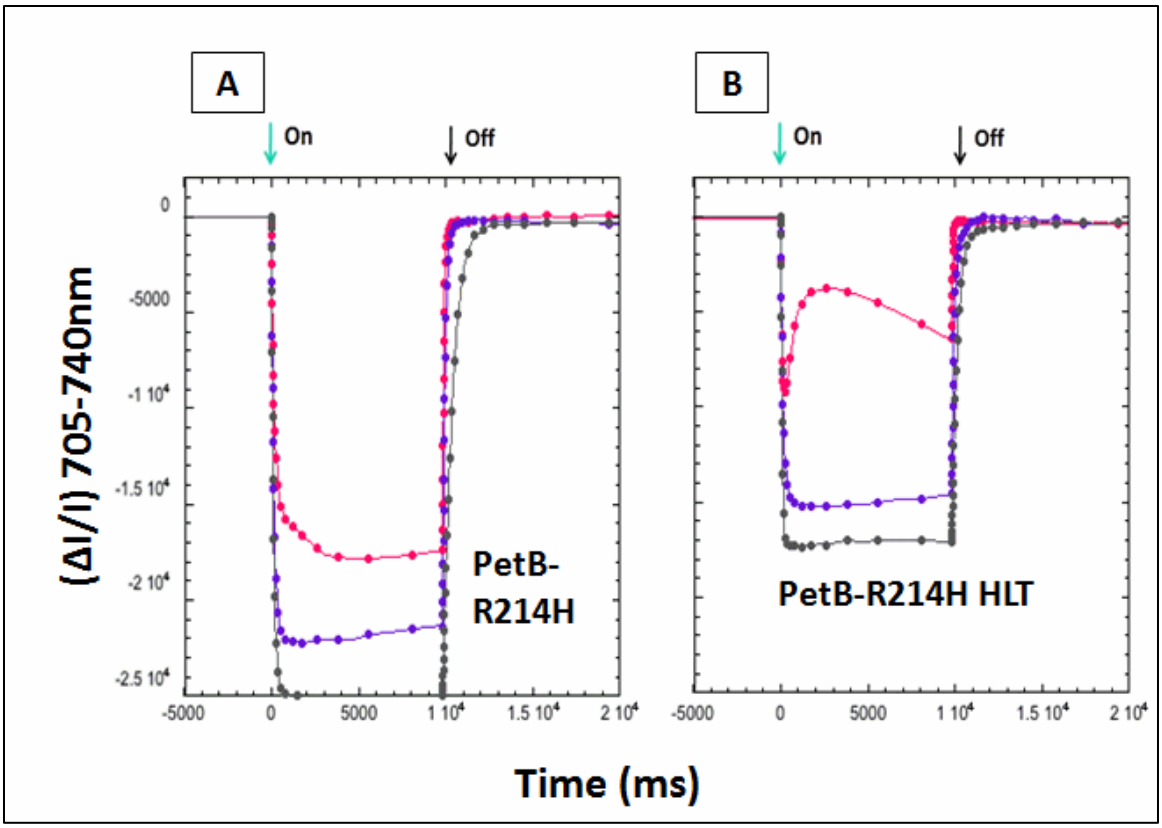

Figure 10. P700 kinetics in the *Synechococcus* PetB-R214H mutant grown under optimal and high light. Panels A and B represents P700 kinetics of the PetB-R214H mutant grown under optimal and high light, respectively. The x- and y-axes show time (ms) and absorbance changes as in Figure 6. Pink traces indicate samples without addition of inhibitors. Purple traces indicate samples upon addition of DCMU. Black traces indicate samples after addition of DCMU and DBMIB. Green arrows indicate onset of actinic light and the black arrows indicate the end of actinic light illumination. Downward deflections indicate oxidation of P700 and upward deflections indicate re-reduction. Green actinic light (~530 nm) was 300 µmol photons m^{-2} s^{-1}. Final concentrations of DCMU and DBMIB were 10 µM

3.3 Contribution of cyclic electron flow at optimal and high light intensities

Table 3 summarizes the percentage of cyclic electron flow in *Synechococcus* PCC 7002 wild type, NdhF and PetB-R214H cells grown under optimal and high light

conditions. As expected, the contribution of cyclic electron flow was lowest in the NdhF mutant grown under optimal conditions. In both the wild type and NdhF mutant, the contribution of cyclic electron flow increased dramatically in cells grown under high light intensity. According to the data shown in Tables 2 and 3, the PetB-R214H mutant showed a higher percentage of cyclic electron flow in cells grown under high light intensity than at optimal light intensity. However, as mentioned above, other data contradict this. In another experiment, the PetB-R214H mutant showed a higher percentage of cyclic electron flow in cells grown under optimal light intensity than at high light intensity (data not shown). Also, the PetB-R214H mutant showed no corresponding decrease in the PSI content under high light as compared to the wild type and NdhF mutant. These data from the PetB-R214H mutant suggest that the PetB-R214H mutation changes the conformation and signaling role of the Cyt *bf* complex. These data are further consistent with previous observations that the Cyt *bf* complex plays a central role in sensing redox changes in electron transport and signaling that adjusts photosynthesis (see Kallas 2012 for a review).

Since the Cyt *bf* complex participates in all known cyclic electron transfer pathways, it was important to confirm that the observed P700 kinetics data represent electrons flowing through the Cyt *bf* complex rather than from some other source. To test this, I measured electron flow in cells after treatment with DBMIB, a classical inhibitor of the quinol oxidase (Q_p) site of the Cyt *bf* complex (Cramer et al. 1991). Under both optimal and high light conditions, all of the experimental cultures showed a significant decrease in P700 reduction rates (longer half-times) upon addition of DBMIB (Table 4).

These data confirm that the observed P700 reduction kinetics, and cyclic electron flow estimations in the presence of DCMU, represent electron flow through the Cyt *bf* complex. Note, however, that DBMIB slowed electron flow from the Cyt *bf* complex to PSI to a much greater extent under optimal light intensity than under high light intensity (Table 4). This may be attributed to a higher electron flux and expected greater reduction of the PQ pool at high light intensity leading to greater reduction of DBMIB. DBMIB in the reduced state becomes ineffective as an inhibitor (Kramer and Crofts 1994) and this might explain the faster observed P700 reduction rates in the presence of DBMIB at high light intensity than at lower, optimal light intensity. This question is discussed further below.

Table 4. P700 reduction kinetics +/- DCMU and DBMIB in *Synechococcus* wild type, NdhF and PetB-R214H mutants grown under optimal and high light.

Inhibitors used	Optimal light $t_{1/2}$ (ms)			High light $t_{1/2}$ (ms)		
	WT	NdhF	PetB-R214H	WT	NdhF	PetB-R214H
No inhibitors	42	65	42	39	64	35
DCMU[a]	260	1513	117	82	86	41
DCMU+DBMIB[a]	1402	1617	419	354	184	233

[a] Final concentrations of DCMU and DBMIB were 10 μM.

3.4 Possible alternative pathways of Cyt *bf* oxidation or PSI reduction?

Electrons from the Cyt *bf* complex can flow to either PSI or a terminal, CtaI or CtaII, cytochrome oxidase (Navarro et al., 2005) as illustrated in Figure 1. To investigate the possible role of a cytochrome oxidase and determine maximum rates of electron flow through PSI, potassium cyanide (KCN) was used to block electron flow to cytochrome oxidases (Yu et al. 1993). P700 reduction was measured in the absence of inhibitors, after the addition of DCMU alone, and after the addition of KCN to the DCMU-treated cells. Excess electrons not accounted for PSI activity may be removed by the CtaI or CtaII cytochrome oxidases. Hence, acceleration in P700 reduction would be expected after

inhibition of cytochrome oxidases by KCN if a significant part of the electron flow from the Cyt *bf* complex goes to these oxidases. Both the NdhF and PetB-R214H mutants showed accelerated P700 reduction rates after addition of KCN to cells treated with DCMU (Table 5). The half-times for P700 reduction decreased (i.e. the reduction rates increased) ~2.5-fold (to 154 ms) and ~1.5-fold (to 188 ms) in the NdhF mutant after KCN addition to cells grown under optimal and high light, respectively. In the PetBR-214H mutant grown under optimal light, the half-times of P700 reduction decreased ~2-fold (to 123 ms) and ~2.5-fold (to 114 ms) after KCN additions to cultures grown under optimal and high light, respectively. These data indicate that a significant fraction of the electrons from the Cyt *bf* complex flow to the cytochrome oxidases under both optimal and high light conditions in the NdhF and PetB-R214H mutants. Wild type *Synechococcus* cells grown at high light intensity also showed a small ~1.2-fold decrease (to 183 ms) in the P700 reduction half-time (Table 5) after KCN addition. In contrast, wild-type grown under optimal light showed a significantly increased P700 reduction half-time (decreased rate) of almost 3-fold (to 238 ms) after KCN addition (Table 5). This result is not readily understandable because there is no apparent reason why KCN, which should not inhibit PSI or the Cyt *bf* complex, should slow P700 reduction. This experiment was performed only once and will need to be repeated.

Table 5. P700 reduction kinetics +/- DCMU, KCN, and MV in *Synechococcus* wild type, NdhF and PetB-R214H mutants grown under optimal and high light.

Inhibitors used	Optimal light $t_{1/2}$ (ms)			High light $t_{1/2}$ (ms)		
	WT	NdhF	PetB-R214H	WT	NdhF	PetB-R214H
No inhibitors	30	142	71	73	60	65
DCMU[a]	82	396	244	221	311	286
DCMU+KCN[a]	238	154	123	183	188	114
DCMU+KCN+MV[a]	1576	764	303	1012	437	228

[a] Final concentrations of inhibitors were 10 μM DCMU, 1 mM KCN, and 100 μM MV.

From the data presented here, I assume that the P700 reduction observed in the presence of DCMU and KCN reflects a cyclic electron flow that involves electron flow from PSI either into the PQ pool (e.g. by way of NAD(P)H dehydrogenase), or directly into the Cyt *bf* complex, and then back to PSI. A further test of this would be to intercept electrons from the acceptor side of PSI (Yu et al. 1993), which should then prevent cyclic electron flow. Hence, the herbicide methyl viologen (paraquat) was used in addition to DCMU and KCN. Methyl viologen (MV) accepts electrons from the acceptor side of PSI (Yu et al. 1993). The wild type as well as both mutant strains showed a significant decrease in the rate of P700 reduction after addition of methyl viologen (Table 5). Wild type cells treated with MV showed increases of ~6.6-fold (to 1576 ms) and ~5.5-fold (to

1012 ms) in P700 reduction half-times (thus much slower reduction rates) under optimal and high light conditions, respectively (Table 5). After the same treatment, the NdhF mutant showed ~5.0-fold (to 764 ms) and ~2.3-fold (to 437 ms) increases in P700 reduction half-times under optimal and high light growth, respectively. After MV treatment, the PetB-R214H mutant showed smaller but still significant increases in P700 reduction half-times of ~2.4-fold (to 303 ms) and ~2-fold under optimal and high light conditions, respectively (Table 5). These results are consistent with an active cyclic electron flow around PSI in the *Synechococcus* wild type and NdhF and PetB-R214H mutant cultures grown under optimal as well as high light conditions. The kinetics traces used to derive the data shown in Table 5 are displayed in Appendix E (pg 109).

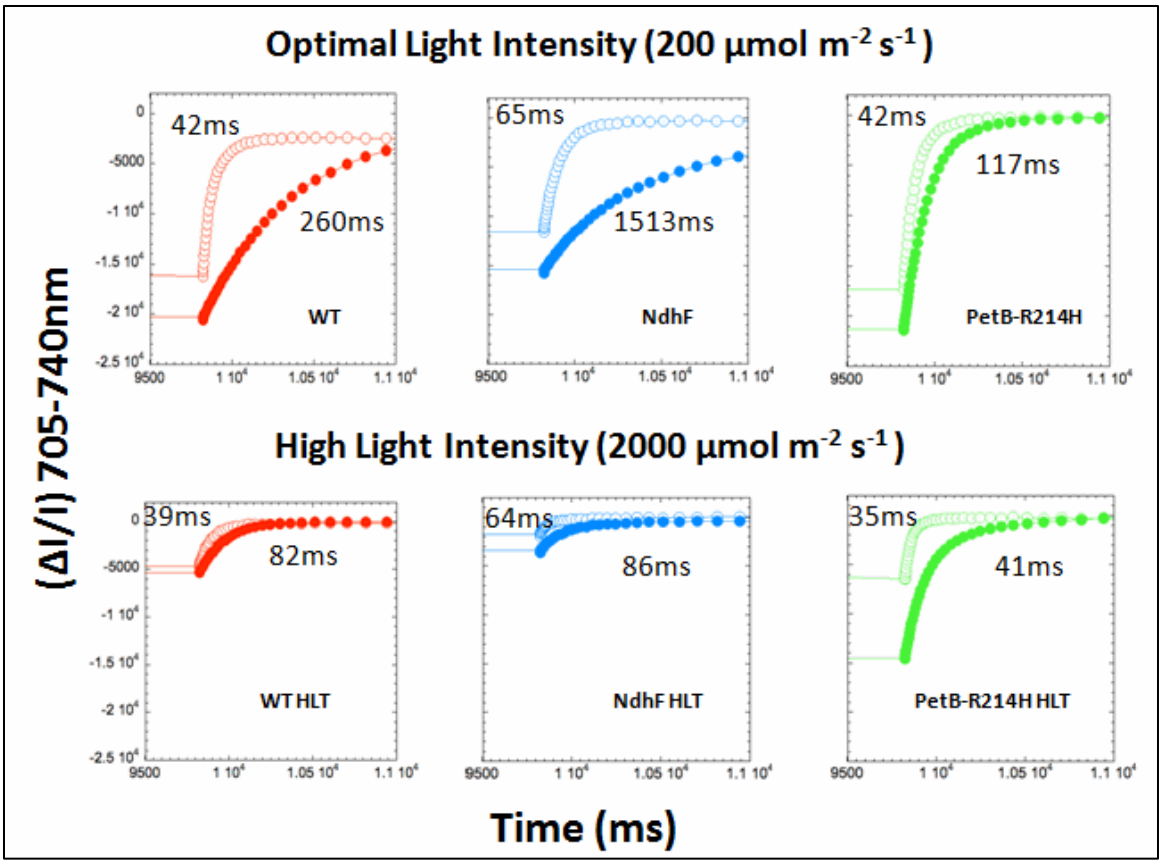

Figure 11. P700 reduction kinetics in the *Synechococcus* wild type, NdhF and PetB-R214H strains grown under optimal and high light. Panels A and B represent P700 re-reduction kinetics of the wild type, NdhF and PetB-R214H mutant grown under optimal and high light, respectively. The x-axes denote time in milliseconds (ms) and y-axes denote relative absorbance (ΔI/I) after subtracting the 740 nm traces from 705 nm traces. Red traces represent wild type samples; Blue traces represent NdhF mutant samples; and green traces represent PetB-R214H mutant samples. Open circles indicate redox kinetics of untreated samples. Closed circles indicate redox kinetics of samples treated with DCMU. Green actinic light (~530 nm) was 300 µmol photons m^{-2} s^{-1}. Final concentration of DCMU was 10 µM.

Figure 11 shows the reduction phases of P700 kinetics in *Synechococcus* wild type, NdhF and PetB-R214H mutant strains grown under optimal and high light. P700 reduction was slowest in the DCMU-treated NdhF mutant grown under optimal light

(1513 ms) (Figure 11, Panel A). These data indicate that the NDH-mediated pathway is the major pathway for cyclic electron flow in *Synechococcus* sp. PCC 7002 grown under optimal light intensity. The high-light grown wild type and NdhF mutant showed faster P700 reduction rates in the presence of DCMU (Figure 11, Panel B) compared to these strains grown under optimal light (Figure 11, Panel A). These data indicate a faster cyclic electron flow in these strains under high light than under optimal light intensity. Since the NdhF mutant shows a high cyclic electron flow rate under high light, and the NDH pathway is inactivated in this mutant, these results indicate that another cyclic electron pathway must have become activated. These findings suggest a direct cyclic electron flow via a PSI – Cyt *bf* supercomplex.

Under optimal light conditions, the PetB-R214H mutant showed faster P700 reduction compared to both the wild type and NdhF mutant (Table 2). Faster P700 reduction in the PetB-R214H mutant was also observed in another experiment. Data from these experiments indicate a faster cyclic electron flow in PetB-R214H mutant than the wild type or NdhF mutant under these conditions. This faster cyclic electron flow may be mediated either by the NDH complex or by possible, alternative electron pathways. The PetB-R214H mutant showed an even faster cyclic electron flow at high light intensity, which was nearly as fast as the total electron flow (Table 2). Based on these data, the PetB-R214H mutant exhibited an extremely high percentage of cyclic electron flow (84%) relative to total electron flow at high light intensity (Table 3). However, further experiments will be needed to support this conclusion.

3.5 Far-red illumination and pre-illumination experiments

Another approach to measure cyclic electron flow is to use far-red actinic illumination, which primarily excites PSI, with little excitation of PSII. For the experiments reported here, a far-red actinic source was used that emits light in the ~700 – 740 nm range. Thus P700 reduction after far-red illumination specifically reflects cyclic electron flow activity, with little contribution from PSII-derived linear electron flow. Figure 12 shows P700 oxidation-reduction traces of experimental cultures after far-red illumination. Untreated wild type *Synechococcus* PCC 7002 cells grown at optimal light intensity showed very little P700 oxidation upon illumination in contrast to the NdhF mutant. This is consistent with an active cyclic flow in the wild type that efficiently re-supplies electrons to P700 during far-red illumination and prevents extensive P700 oxidation. In untreated NdhF cells, P700 becomes oxidized during illumination because the NAD(P)H dehydrogease (NDH) pathway, the major cyclic electron pathway under optimal light, is not available. Untreated PetB-R214H cells grown at optimal light intensity showed only a very small P700 oxidation during far-red illumination, consistent with an active cyclic electron flow in these cells, as observed from the green light data (Figure 10).

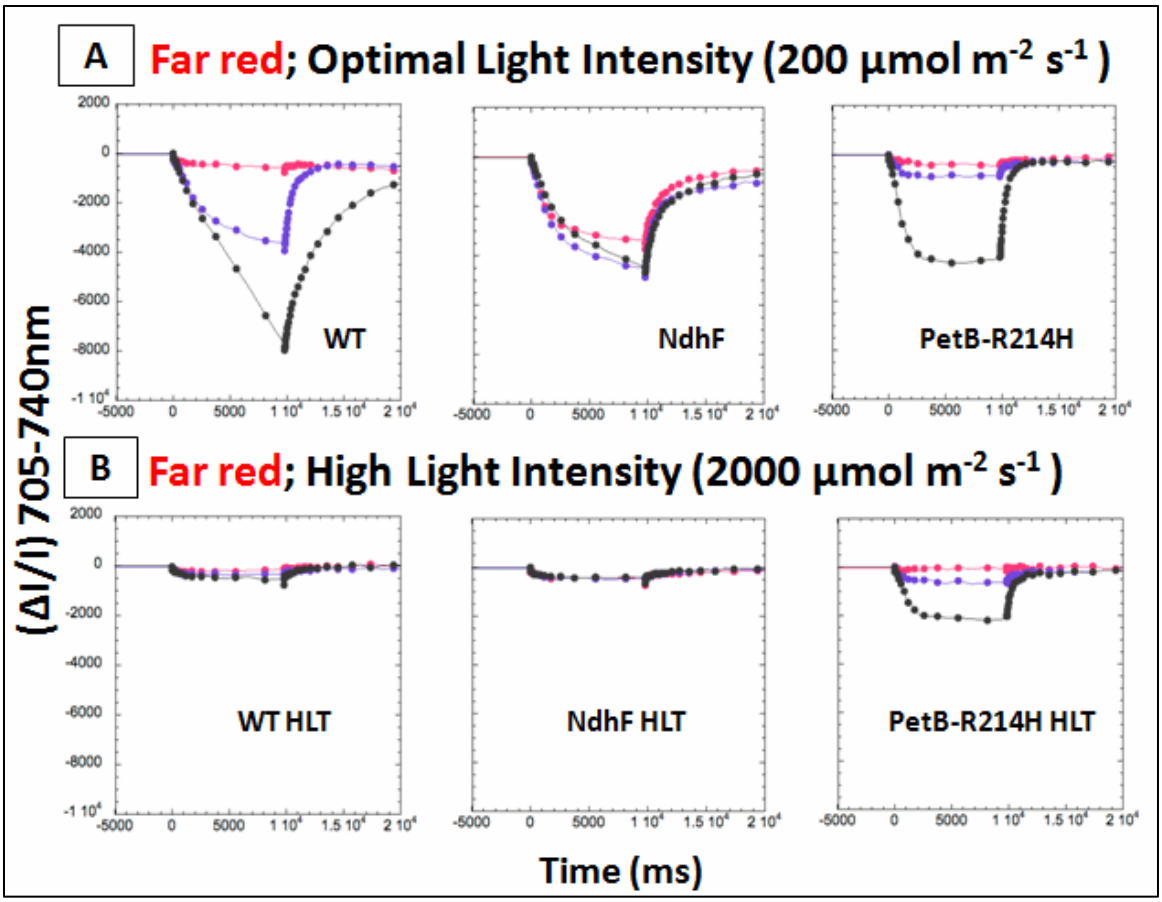

Figure 12. P700 kinetics with far-red illumination in the *Synechococcus* wild type, NdhF and PetB-R214H strains grown under optimal and high light. Panels A and B represent P700 kinetics of the wild type, NdhF and PetB-R214H mutant grown under optimal and high light, respectively. The x-axes denote time in milliseconds (ms) and y-axes denote relative absorbance (ΔI/I) as in Figure 11. Pink traces indicate samples without addition of inhibitors. Purple traces indicate samples upon addition of DCMU. Black traces indicate samples after addition of DCMU and DBMIB. Downward deflections indicate oxidation of P700 and upward deflections indicate re-reduction. Far-red actinic light (~700 – 740 nm) was 2500 µmol photons m^{-2} s^{-1}. Final concentrations of DCMU and DBMIB were 10 µM.

In far-red illumination experiments with high-light grown PetB-R214H cells, the addition of DBMIB resulted in a larger oxidation signal relative to untreated or DCMU-

treated cells, consistent with an active cyclic electron flow in these cells. However, far-red illumination of high-light grown wild type or NdhF cells, produced very little P700 oxidation, regardless of whether cells were untreated or treated with DCMU or DBMIB (figure 12). These data may reflect a low content of PSI and very high cyclic electron flow rates in these cultures. However, the signals are small and thus no clear conclusions can be drawn. Since reductant pools may be larger in high-light grown cultures, DBMIB may become reduced when added to these cells. Since DBMIB becomes inactive when reduced *(Kramer and crofts 1994)*, DBMIB may not have inhibited electron flow from the Cyt *bf* complex in the high-light grown cells. If so, we cannot assess the maximum extent of P700 oxidation (detected when electron flow from the Cyt *bf* complex is blocked), and therefore cannot draw conclusions about PSI content nor cyclic electron flow from these particular far-red illumination experiments.

In preparations for kinetics experiments, there is often a time gap of as much as several hours between sample preparation and experimental runs and samples may sit in the dark during this period. Because the plastoquinone pool typically becomes reduced in cyanobacteria during darkness (Cooley et al 2001), dark incubation may result in accumulation of reductant pools that may supply electrons for P700 reduction and thus result in overestimation of cyclic electron flow rates. To determine whether dark incubations influenced cyclic electron flow data, I did experiments during which cells were pre-illuminated with green actinic light (300 μmol m^{-2} s^{-1}) for different periods of time prior to kinetics runs. P700 kinetics traces were obtained after pre-illumination of samples for 0, 1, and 5 min. Table 6 summarizes P700 reduction half-times before and

after pre-illumination of wild type and NdhF mutant cultures grown under optimal and high light conditions. The half-times of P700 reduction did increase (and therefore the reduction rates decreased) by ~60% after 5 min pre-illumination of both wild type and NdhF cultures grown at optimal light intensity. However, there was no significant difference in P700 reduction half-times in the optimal light cultures after treatment with DCMU or in any of the high-light grown cultures. These data indicate that dark incubations prior to kinetics runs did not significantly alter P700 kinetics results or conclusions drawn about cyclic electron transfer rates.

Table 6. P700 reduction kinetics after pre-illumination of *Synechococcus* wild type and NdhF mutant grown under optimal and high light.

Condition	Optimal light $t_{1/2}$ (ms)			High light $t_{1/2}$ (ms)		
Pre-illumination	0	1 min	5 min	0	1 min	5 min
WT	36	61	57	60	72	58
WT + DCMU[a]	223	224	260	69	69	64
NdhF	33	45	52	52	65	71
NdhF + DCMU[a]	625	429	419	51	59	65

[a] DCMU was used at a final concentration of 10μM.

3.6 Cytochrome *bf* Kinetics

To investigate the role of the Cyt *bf* complex in cyclic electron flow around PSI, and to analyze the central role it plays in photosynthesis, Cyt *bf* kinetics were measured in all of the experimental cultures. Two kinds of experiments were performed, with actinic illumination of either 9 milliseconds (ms) ms or 10 seconds (s). The 9 ms green (530 nm) actinic, excitation results in approximately one (or only a few) turnovers of the Cyt *bf* complex, and thereby provides an estimation of the maximum rates of electron transfer reactions in the complex. Longer (e.g. 10 second) actinic illumination results in complete oxidation of the Cyt c_6 acceptor pool that carries electrons from the Cyt *bf* complex to PSI (see Figure 1), and therefore multiple turnovers of the Cyt *bf* complex are required to re-fill the Cyt c_6 pool and all of the PSI P700 reaction centers. This results in much longer reaction half-times (i.e. slower apparent rates) that are good indicators of steady state turnover and electron flow rates through the Cyt *bf* complex or PSI.

At high light intensity, the 9 ms Cyt *f*/c_6 oxidation-reduction signals were very small (data shown in Appendix E, pg 110) in the wild type and NdhF mutant making determination of the reduction rates and estimation of cyclic flow rates difficult. These small signals suggest a much lower content of the Cyt *bf* complex at high light intensity, consistent with a lower PSI content. However, this question is addressed better in the 10 second Cyt *bf* oxidation-reduction experiments presented below. Figure 13 shows Cyt *bf* oxidation-reduction kinetics, during and after 10 s actinic (green light) excitation, in *Synechococcus* wild type cultures grown under optimal as well as high light intensities.

Figures 14 and 15 show Cyt bf oxidation-reduction kinetics, in the NdhF and PetB-R214H mutants, respectively, grown under optimal and high light intensities.

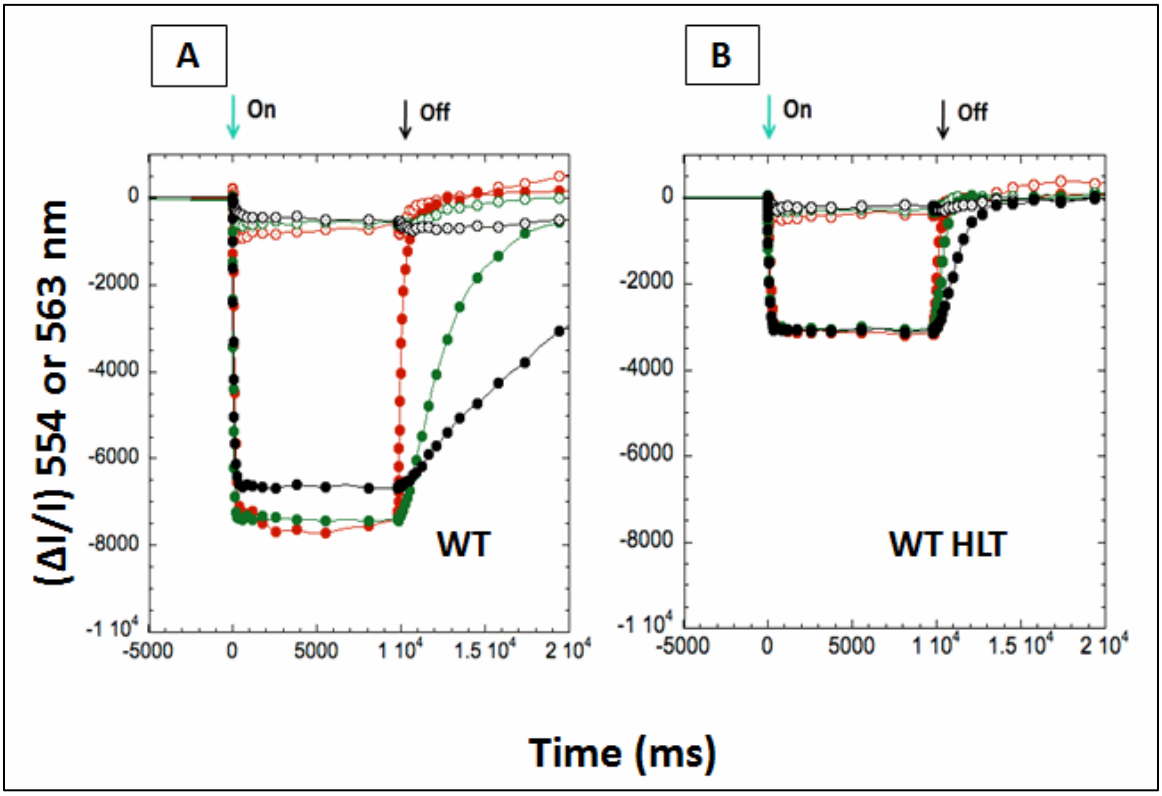

Figure 13. Cyt *bf* kinetics in the *Synechococcus* wild type grown under optimal and high light. Panels A and B represent Cyt *bf* kinetics of the wild type grown under optimal and high light, conditions. The x-axes denote time in milliseconds (ms) and the y-axes denotes relative absorbance (ΔI/I) at 554 nm and 563 nm. Open circles represent *b* heme redox changes (563 nm) and closed circles represent Cyt *f*/c_6 redox changes (554 nm). Red traces indicate samples without addition of inhibitors. Green traces indicate samples upon addition of DCMU. Black traces indicate samples after addition of DCMU and DBMIB. Green arrows indicate the onset of actinic light and black arrows indicate the end of actinic light illumination. Oxidation (downward deflection) of Cyt *f*/c_6 is observed when the actinic light is turned on followed by re-reduction (upward deflection) when the light is turned off. Cells were exposed to green actinic light (~530 nm, 300 µmol photons m^{-2} s^{-1}) for 10 seconds. Final concentrations of DCMU and DBMIB were 10 µM.

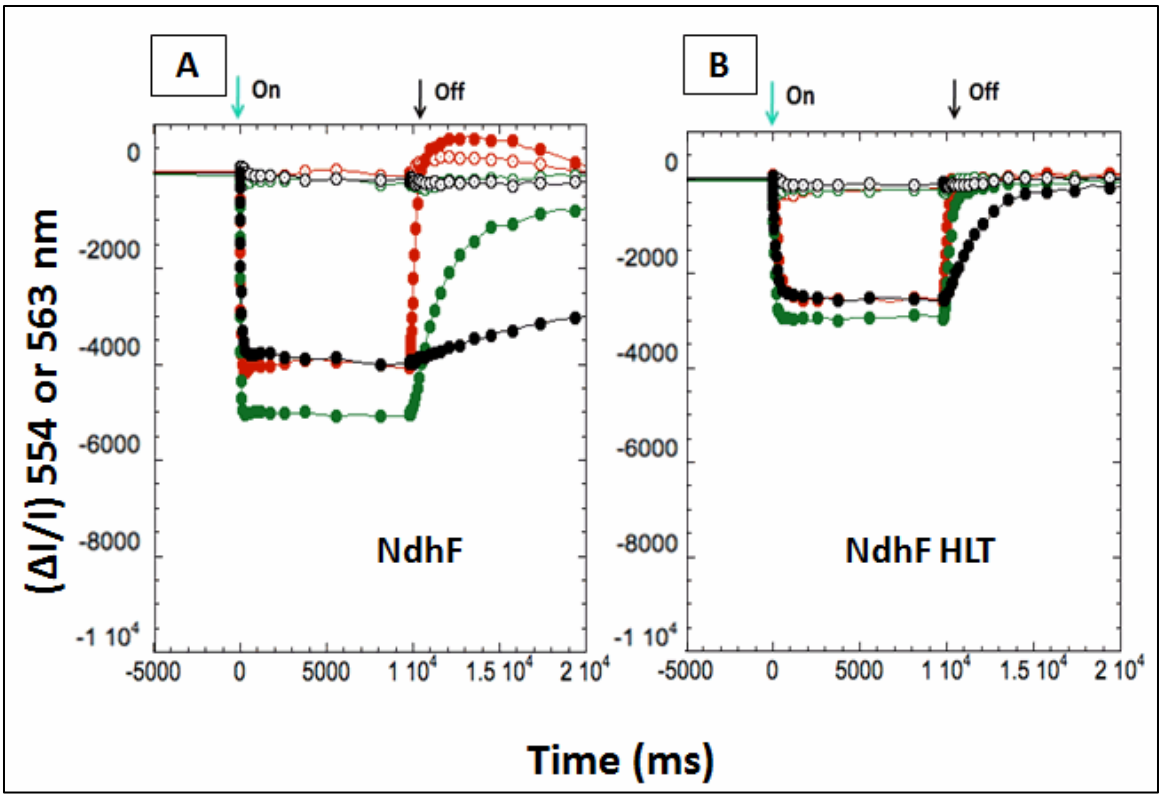

Figure 14. Cyt *bf* kinetics in the *Synechococcus* NdhF mutant grown under optimal and high light. Panels A and B represent Cyt *bf* kinetics of the NdhF mutant grown under optimal and high light, respectively. The x-axis denotes time in milliseconds (ms) and the y-axis denotes relative absorbance (ΔI/I) at 554 nm and 563 nm. Open circles represent *b* heme redox changes (563 nm) and closed circles represent Cyt *f*/c_6 redox changes (554 nm). Red traces indicate samples without addition of inhibitors. Green traces indicate samples upon addition of DCMU. Black traces indicate samples after addition of DCMU and DBMIB. Green arrows indicate the onset of actinic light and black arrows indicate the end of actinic light illumination. Oxidation (downward deflection) of Cyt *f*/c_6 is observed when the actinic light is turned on followed by re-reduction (upward deflection) when the light is turned off. Cells were exposed to green actinic light (~530 nm, 300 µmol photons m^{-2} s^{-1}). Final concentrations of DCMU and DBMIB were 10 µM.

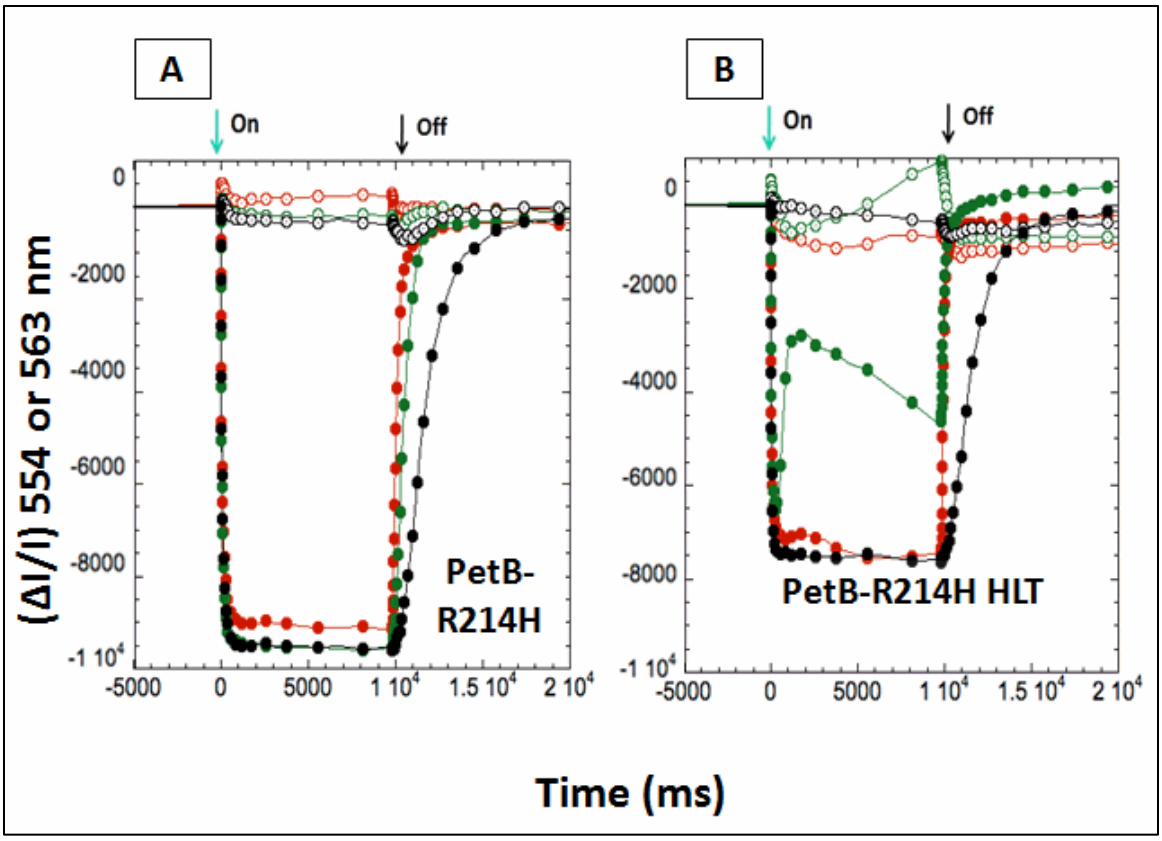

Figure 15. Cyt *bf* kinetics in the *Synechococcus* PetB-R214H mutant grown under optimal and high light. Panels A and B represent Cyt *bf* kinetics of the PetB-R214H mutant grown under optimal and high light, respectively. The x-axis denotes time in milliseconds (ms) and the y-axis denotes relative absorbance (ΔI/I) at 554 nm and 563 nm. Open circles represent *b* heme redox changes (563 nm) and closed circles represent Cyt *f*/c_6 redox changes (554 nm). Red traces indicate samples without addition of inhibitors. Green traces indicate samples upon addition of DCMU. Black traces indicate samples after addition of DCMU and DBMIB. Green arrows indicate the onset of actinic light and black arrows indicate the end of actinic light illumination. Oxidation (downward deflection) of Cyt *f*/c_6 is observed when the actinic light is turned on followed by re-reduction (upward deflection) when the light is turned off. Cells were exposed to green actinic light (~530 nm, 300 µmol photons m^{-2} s^{-1}). Final concentrations of DCMU and DBMIB were 10 µM.

The half-time of Cyt *f*/c_6 reduction in untreated wild type cells grown under optimal light was 177 ms. Upon addition of DCMU, Cyt *f*/c_6 reduction slowed greatly (2384 ms). The half-time of Cyt *f*/c_6 reduction in untreated NdhF mutant cells from optimal light was 227 ms. Upon addition of DCMU, Cyt *f*/c_6 reduction slowed greatly in the this mutant (1380 ms) (Table 7). The data from DCMU-treated wild type and NdhF cells grown at optimal light intensity are consistent with a relatively low rate of cyclic electron flow through the Cyt *bf* complex.

Under high light, the Cyt *f*/c_6 content became lower in both the wild type and NdhF mutant. (Figures 13 and 14, Panel B). The half-time of Cyt *f*/c_6 reduction in untreated wild type cells grown under high light was 233 ms. Upon addition of DCMU, Cyt *f*/c_6 reduction slowed to 479 ms in these wild type cells. The half time of Cyt *f*/c_6 reduction in untreated NdhF mutant cells grown under high light was 169 ms. Upon addition of DCMU, Cyt *f*/c_6 reduction in this mutant slowed to 340 ms. The DCMU-treated wild type and NdhF mutant grown under high light did not show a large decreases in their Cyt *f*/c_6 reduction rates compared to the same strains grown under high light and not treated with DCMU (Table 7). These data from high-light grown cells suggest an active cyclic electron flow that involves, as expected, the Cyt *bf* complex. The wild type and NdhF Cyt *bf* kinetics data are thus consistent with the PSI kinetics data summarized in Tables 2 and 3.

In the PetB-R214H mutant grown at high-light intensity, the Cyt *f*/c_6 oxidation signal was only slightly smaller than in cells grown at optimal light intensity, indicating that the Cyt

bf content remained relatively unchanged. The Cyt f/c_6 reduction rate in the PetB-R214H mutant from high light (102 ms, prior to DCMU treatment) was ~2-fold faster than in these cells grown at optimal light intensity (200 ms, prior to DCMU treatment, Table 7). The Cyt f/c_6 reduction rate in the PetB-R214H mutant grown at high light intensity and treated with DCMU (133 ms) did not slow significantly relative to the high-light, untreated cells (102 ms) as it did in these mutant cells grown under optimal light and treated with DCMU (570 ms relative to 200 ms, Table 7). These data indicate a much faster and higher proportion of cyclic electron flow in the PetB-R214H mutant grown at high light intensity and are consistent with the conclusion drawn from the P700 reduction data (Tables 2 and 3). Note that in the PetB-R214H mutant, the *b*-hemes (Figure 15, open circles) generally became more reduced (upward signal deflection) relative to the wild type and NdhF mutant. This is consistent with a greater reduction of the Cyt *bf* low-potential chain in this mutant as originally described (Nelson et al. 2005).

Table 7: Cyt *bf* kinetics +/- DCMU and DBMIB in *Synechococcus* wild type, NdhF and PetB-R214H mutants grown under optimal and high light.

Inhibitors used	Optimal light $t_{1/2}$ (ms)			High light $t_{1/2}$ (ms)		
	WT	NdhF	PetB-R214H	WT	NdhF	PetB-R214H
No inhibitors	177	227	200	233	169	102
DCMU[a]	2384	1380	570	479	340	133
DCMU+DBMIB[a]	6275	6831	1656	1178	1500	1551

[a] Data shown represent half times (ms) of Cyt *f*/c_6 reduction after 10 s illumination with green (530 nm) actinic light (300 μmol m^{-2} s^{-1}). Final concentrations of DCMU and DBMIB were 10 μM.

In the 9 ms and 10 second actinic illumination experiments, the addition of DBMIB greatly slowed Cyt *f*/c_6 reduction rates in all of the cultures grown at both optimal and high light intensities. DBMIB is a potent, classical inhibitor of the Cyt *bf* complex (Cramer et al. 1991) that binds the quinol oxidation (Q_p) site of the *bf* complex. DBMIB is expected to slow both Cyt *bf* and PSI turnover during both linear and cyclic electron flow because the *bf* complex is an essential component of both pathways. The data in Figures 13, 14, and 15 showing DBMIB inhibition of Cyt *f*/c_6 reduction in DCMU-treated cells are consistent with a cyclic electron pathway that relies on electron flow from the Cyt *bf* complex. The 9 ms illumination data are shown in Appendix ___.

Based on the Cyt *bf* kinetics experiments with 10 second actinic illumination (Figures 13, 14, and 15), Cyt *bf* contents were lower at high light intensity in both the

wild type and NdhF mutant, ~40% and ~60% of the optimal light content, respectively. In contrast, in the PetB-R214H mutant, the Cyt *bf* content declined only slightly at high light intensity (Figure 15, Panel B). Cyclic electron flow rates, measured as Cyt f/c_6 reduction rates in the presence of DCMU, again increased dramatically in the wild type and NdhF mutant cells grown at high light intensity (Figure 13 and 14, Panel B). These data are entirely consistent with the rapid cyclic electron flow rates and high proportions of cyclic flow relative to total electron flow in high-light grown cultures determined from P700 oxidation-reduction kinetics (see Figures 8, 9, and 10). Similarly the PetB-R214H mutant showed an even faster rate of cyclic electron flow at high light intensity than its already high rate at optimal light intensity (Figure 15, Panel B). Again these data are consistent with the P700 kinetics data for this mutant.

An unexpected finding from the PSI kinetics data (Figures 9, 10, and Table 4) was that DBMIB, which should be a potent inhibitor of the Cyt *bf* complex, did not greatly inhibit P700 reduction in all cases in cells grown at high light intensity. This was particularly evident in the PetB-R214H mutant (Figure 10, Panel B). There are a couple of possible interpretations. First, the PetB-R214H mutation, or perhaps exposure to high light more generally, may change the conformation of the Cyt *bf* complex such that DBMIB no longer effectively binds to block the Q_p (quinol oxidase) site. Second, if DBMIB still binds and inhibits electron flow through the Cyt *bf* complex, then these data suggest an alternative, previously undiscovered electron transfer pathway, for example one that bypasses the Cyt *bf* complex. Third, the least interesting, but perhaps the most likely explanation is (as already mentioned above) that under high-light intensity growth

conditions the cyanobacteria accumulate reductant pools that effectively reduce DBMIB rendering it much less effective as an inhibitor. As mentioned, only the oxidized form of DBMIB is an effective inhibitor of the Cyt *bf* complex

To further test these possibilities, especially to ensure that DBMIB was still active, 4-1HQ, another inhibitor of the Cyt *bf* quinol-oxidase (Q_p) site, was tested as an inhibitor in both P700 and Cyt *bf* kinetics experiments. 4-1HQ is an analog of NQNO and has recently been synthesized by Sandra Zulegar, Jason Coplien, and Drs. Brant Kedrowski and Linfeng Xie (UW Oshkosh Chemistry Department) in collaboration with the Kallas group. As far as we know, inhibition by 4-1HQ is not dependent on its redox state. Figures in the appendix (pg 111) show the results of 10 second Cyt *bf* kinetics experiments. Table 8 summarizes the half-times of P700 reduction after treatments with DBMIB and 4-1HQ. In wild type and NdhF cultures grown under optimal light conditions, 4-1HQ at 20 μM was a more effective inhibitor than DBMIB at 10 μM. However, at least in the experiments shown in Table 8, for the PetB-R214H mutant grown either at optimal or high light intensity, and for the wild type and NdhF mutant at high light intensity, DBMIB was more effective than 4-1HQ.

Table 8. P700 reduction kinetics +/- DBMIB and 4-1HQ of *Synechococcus* wild type, NdhF and PetB-R214H mutants grown under optimal and high light.

Inhibitors used	Optimal light $t_{1/2}$ (ms)			High light $t_{1/2}$ (ms)		
	WT	NdhF	PetB-R214H	WT	NdhF	PetB-R214H
No inhibitors	30	140	71	73	60	65
DBMIB[a]	57	403	390	362	463	414
10μM 4-1HQ[a]	180	383	142	76	135	91
20 μM 4-1HQ[a]	314	579	224	107	136	169

[a] Final concentrations of inhibitors were 10 μM DBMIB and 10 μM or 20 μM 4-1HQ.

In these experiments comparing DBMIB and 4-1HQ, DBMIB inhibited electron flow through the Cyt *bf* complex more effectively in high-light grown rather than optimal light grown cells. Unlike other P700 kinetics experiments where DBMIB was added after the addition of DCMU, in the experiments shown in Table 8, DBMIB was used alone, which might explain its better performance. Because of these conflicting results, no definitive conclusions can be drawn. However, the lack of significant inhibition of P700 reduction in cultures grown at high light intensity and treated with 4-1HQ, might suggest 1) that binding and inhibition by 4-1HQ is also sensitive to the redox state of the inhibitor or 2) that indeed a conformational change occurs in the quinol-oxidase (Q_p) site of the Cyt *bf* complex in high-light grown cells such that some inhibitors, such as 4-1HQ and DBMIB, no longer bind very efficiently.

4.0 Discussion

In this thesis, I compared the contributions of cyclic versus linear electron flow in the wild type, NdhF and PetB-R214H mutants of *Synechococcus* PCC 7002 grown under optimal and high light conditions. The very slow P700 reduction rate (1512 ms, Table 2) in the DCMU-treated NdhF mutant grown under optimal light suggested that the NDH-mediated cyclic electron pathway (see Figure 1) plays a major role in these cyanobacteria under optimal light conditions as noted previously (Yu et al. 1993; Mi et al. 1993). The contribution of cyclic electron flow (Table 3) in the NdhF mutant grown under optimal light was only 4%. This increased dramatically to as much as 74% in the same mutant grown under high light intensity (Table 3). In other, similar trials, the contribution of cyclic electron flow was also very high (50 – 60%) under high light conditions. These cyclic rates are much higher than previously reported, in which cyclic flow accounted for only ~5% of the total electron flow (Yu et al. 1993; Hagemann et al. 1999). However, that previous studies were performed on cyanobacteria grown at optimal light intensities, ~250 μmol photons m^{-2} s^{-1} in the Yu et al. (1993) work with *Synechococcus* PCC 7002. In wild type *Synechococcus* 7002 grown under optimal light, I found a cyclic contribution of ~15%, which is higher than in these previous studies but still quite low relative to total electron flow. My discovery of apparently, remarkably high cyclic electron flow activities in *Synechococcus* PCC 7002, and especially in the NdhF mutant, grown at high light intensity has several, possible explanations. 1) An alternative, non-NDH-mediated, cyclic electron pathway may become active in cells grown under high light intensity. 2) A possible likely pathway is a direct PSI – Cyt *bf* mediated by the formation of a PSI –

Cyt *bf* supercomplex as recently demonstrated by the isolation of such a supercomplex from *Chlamydomonas* chloroplasts (Iwai et al. 2010). 3) Alternatively, and less interestingly, a lower content of PSI observed in *Synechococcus* wild type and the NdhF mutant grown at high light intensity (Figures 8 and 9) would result in more rapid P700 reduction rates as long as the content of Cyt *bf* complexes and Cyt c_6 electron donors did not decrease as well. However, The Cyt *bf* content also decreased in high-light grown wild type and NdhF cells (Figures 13 and 14). Moreover, P700 reduction rates did not increase in high-light grown wild type and NdhF cells, relative to optimal-light grown cells, in linear electron flow measurements (i.e. green actinic illumination without DCMU treatment, Table 2). These observations suggest that a direct PSI – Cyt *bf* electron pathway, perhaps mediated by a PSI – Cyt *bf* supercomplex, may provide the most likely explanation for the observed, rapid P700 reduction rates observed in the presence of DCMU in high-light grown *Synechococcus* PCC 7002 cyanobacteria.

Supercomplexes have been found in cyanobacteria, green algae, and higher plants under stress conditions. Also several studies have reported elevated cyclic electron flow under stress conditions, such as drought (Jia et al. 2008; Kohzuma et al. 2008), salt-stress (Hagemann et al. 1999), high light (Baker and Ort 1992) or during the induction of photosynthesis after prolonged dark adaptation (Joët et al. 2002; Joliot and Joliot 2002). The data presented here are consistent with these previous studies reporting elevated cyclic electron flow under stress conditions. Since there is evidence of formation of supercomplexes under stress conditions, the elevated cyclic electron flow in *Synechococcus* sp. PCC 7002 under high light might be the outcome of formation of a

PSI-Cyt *bf* supercomplex involved in cyclic electron flow. Such a PSI-Cyt *bf* supercomplex has been isolated from green alga *Chlamydomonas reinhardtii* (Iwai et al. 2010). This supercomplex is not only active in cyclic electron flow, but also plays a role in regulating the balance of electron flow between the two photosystems. Supercomplexes active in cyclic electron flow have not yet been found in cyanobacteria. However, the present study suggests the formation of a possible PSI-Cyt *bf* supercomplex active in cyclic electron flow under high light conditions. Further experiments, such as efforts to isolate a PSI – Cyt *bf* supercomplex from cultures grown under high light intensity, will be needed to confirm the formation of such a cyclic electron flow supercomplex from *Synechococcus* PCC 7002 cyanobacteria.

Formation of a supercomplex involved in cyclic electron flow may offer several advantages to photosynthetic organisms such as cyanobacteria. Cyclic electron flow and linear electron flow share many redox carriers and they are potentially in competition with one another (Allen 2003). Formation of a supercomplex active in cyclic electron flow should compartmentalize cyclic electron flow by localizing mobile electron carriers (plastoquinone, ferredoxin, and cytochrome *f*), which would lead to the formation of an efficient, functional pool of cyclic electron flow components. Formation of a supercomplex might also enable cyclic electron flow to operate independently of linear electron flow (Iwai et al. 2010). This would be an advantage, if photodamage to PSII curbs linear electron flow under high light conditions, cyclic electron flow associated with the PSI-Cyt *bf* supercomplex would still operate and provide ATP for maintenance and repair.

Although the data presented here primarily point toward a putative PSI-Cyt *bf* supercomplex, the possible presence of an alternative cyclic electron flow cannot be overlooked. It remains possible that electrons are donated by other enzymes such as succinate dehydrogenase (SDH) to reduce the PQ pool and that these electrons then flow via the Cyt *bf* complex to reduce P700 (see Figure 1). There is strong evidence for the involvement of the SDH enzyme complex in PQ pool reduction in *Synechocystis* sp. PCC 6803, especially under dark conditions (Cooley et al. 2001). Thus a study should be conducted to investigate the involvement of the SDH enzyme complex in cyclic electron flow in *Synechococcus* sp. PCC 7002. A mutant having a non-functional SDH enzyme complex in Synechococcus sp. PCC 7002 should be constructed and electron transfer kinetics observed under optimal as well as high light. It would also be useful to create a double mutant defective in both NDH and SDH complexes. Studies on such a double mutant would help reveal the role of any other existing alternative cyclic pathway in *Synechococcus* sp. PCC 7002.

The contribution of a Fd-dependent direct PSI-Cyt *bf* cyclic electron pathway in cyanobacteria is still unknown. Such a pathway might be mediated either by soluble electron carriers or the formation of a supercomplex. In a direct PSI-Cyt *bf* pathway, electrons are thought to enter the Cyt *bf* complex via the quinone-reductase (Q_n) site (Yan et al. 2008; Kallas 2012; Kurisu et al. 2003; Stroebel et al. 2003). Kinetics studies were performed on the PetB-R214H mutant to test this hypothesis. The PetB-R214H mutant has a mutation in the Q_n site, which impairs electron flow through the *b* hemes to the Q_n site (Nelson et al. 2005). This mutant grows ~3 times slower than the wild type. Kinetics

experiments with the PetB-R214H mutant might provide insight into possible electron flow from PSI through the Cyt *bf* Q_n site. The contribution of cyclic electron flow in the PetBR214H mutant grown under optimal light conditions was 35 – 48 % (Table 3). This percentage of cyclic flow in the PetB-R214H mutant under optimal light is very high compared to the wild type (1 – 15%) under the same conditions. These data therefore suggest either 1) that a Fd-dependent, PSI – Cyt *bf* cyclic pathway may not be the major cyclic pathway or 2) that the PetB-R214H mutation in the Cyt *bf* Q_n site might not hinder electron flow through this site in a Fd-dependent, direct PSI-Cyt *bf* pathway. Under high light conditions the contribution of cyclic electron flow in the PetB-R214H mutant ranged from 25 – 84 % (Table 3). Since the PetB-R214H mutation did not impede cyclic electron flow, these data do not provide further insight into the role of a possible Fd-dependent, direct PSI-Cyt *bf* cyclic electron pathway in *Synechococcus* sp. PCC 7002.

Microarray studies have reported a general increase in the ratio of PSII/PSI gene expression levels upon a shift to high light in *Synechocystis* PCC 6803 cyanobacteria (Hihara et al. 1998). A lower PSI content would be expected to lower the susceptibility of the cells to high light damage, particularly under prolonged exposure (Hihara 1998). The kinetics data from high-light grown *Synechococcus* 7002 presented here corroborate this. I found a lower content of PSI in all the cultures grown under high light conditions (Figures 8, 9, and 10). These results are nonetheless somewhat puzzling, as PSI is known to be much more resistant to photodamage than PSII (Canaani et al. 1989; Fork and Herbert 1993; Golding et al. 2004). However, PSI is also known to be a major site of superoxide production *(DH MS thesis)*, and this might explain the advantage of a lower

PSI content under high light. It might further be possible that there are two types of PSI centers: 'cyclic' PSI centers and 'linear' PSI centers. Decreased linear electron flow under high light might inactivate or reduce the number of 'linear' PSI centers leaving the 'cyclic' PSI centers functioning under high light conditions. The 'cyclic' PSI centers are suggested to be present as monomers rather than trimers. Affinity-binding chromatography can help in finding out the differences in these structures. Fluorescence kinetics experiments, which can provide information about PSII content and state transitions, might provide insight into this interesting possibility.

Since electrons from the Cyt *bf* complex can either enter the PSI complex or a CtaI, CtaII Cytochrome oxidase (Navarro et al. 2005), electron flow to cytochrome oxidase should be blocked in order to get an accurate estimate of the number of electrons entering PSI and thus involved in cyclic flow around PSI. Therefore it would be interesting to investigate cyclic electron flow by analyzing P700 reduction rates when cells are inhibited with DCMU and KCN (Yu et al. 1993). KCN prevents electron flow to cytochrome oxidase (Yu et al. 1993). Hence, P700 reduction in the presence of KCN should provide a measure of the maximum PSI cyclic electron flow rate. For these measurements, electron flow from PSII should also be inhibited by the addition of DCMU. All of the *Synechococcus* 7002 strains, except wild-type grown under optimal conditions, showed faster P700 reduction upon addition of KCN (refer to Table 5). Faster P700 reduction in the presence of KCN provides evidence that some electrons are normally diverted to cytochrome oxidases. To further verify whether the electrons that are not diverted to cytochrome oxidases, enter the PSI complex, methyl viologen (MV)

was added to the DCMU and KCN treated cells. Methyl viologen efficiently accepts electrons from the acceptor side of PSI (Yu et al. 1993), thus a slower apparent P700 reduction is expected because electrons are more rapidly removed by MV than can be returned by any PSI cyclic pathway to re-reduce P700. All of the cultures (except the PetB-R214H mutant grown under high light and treated with DCMU alone) showed the expected outcome upon addition of methyl viologen (Table 5). Slower P700 reduction upon addition of methyl viologen provides evidence that in DCMU treated cells (with PSII inactivated) the electrons for P700 re-reduction flow via a PSI cyclic pathway that requires reduction of electron carriers on the acceptor side of PSI. These data provide further evidence that a cyclic electron flow around PSI is active under optimal and high light conditions.

The data from far-red illumination experiments are consistent with conclusions with conclusions drqwn from green actinic light experiments (Figure 12 and Table 3). In the NdhF mutant grown under optimal light, untreated as well as DCMU and DBMIB-treated cells showed a deeper P700 oxidation relative to the wild type. Since far-red light primarily excites PSI, a deep oxidation of P700 in untreated NdhF cells indicates a minimal cyclic electron flow in this mutant grown under optimal light. In contrast, very little P700 oxidation was seen in either the wild type or PetB-R214H mutant, in the absence of DCMU or DBMIB treatments, in cells grown under optimal light. These data are consistent with an active cyclic electron flow in these cultures. The wild type shows a deeper oxidation upon addition of DCMU (Figure 12, Panel A). This was unexpected as it suggests that the far-red actinic illumination also excited PSII to at least a small extent.

Thus even under far-red illumination, electron flow to P700 apparently slowed down upon addition of DCMU, thus inhibiting electrons from PSII and resulted in a deeper oxidation of P700. In both the wild-type and NdhF mutant cultures grown under high light, the P700 oxidation-reduction signals were very small (Figure 12, Panel B), which make it difficult to interpret these results. On the other hand, untreated, high-light grown PetB-R214H showed little P700 oxidation, which hardly changed upon addition of DCMU (Figure 12, Panel B). These data indicate a highly active cyclic electron flow in the PetB-R214H mutant grown under high light and are consistent with the conclusions from experiments with green actinic light illumination (e.g. Table 2).

Because of variations in some of the PetB-R214H kinetics data, some of the results are difficult to interpret. In some experiments with this mutant, but also with the wild type and NdhF mutant, particularly in cells grown at high light intensity, the P700 re-reduction kinetics after 10 second green actinic illumination did not slow appreciably upon addition of DBMIB (Figures 8, 9, and 10). In contrast, the data in Table 4 for these mutants indicated significant decreases of at least 4-fold in P700 reduction rates after DBMIB addition. Since DBMIB is a known inhibitor of electron flow through the Cyt *bf* complex (Cramer et al. 1991), the absence of a significant inhibition of P700 reduction by DBMIB, in some experiments, was not expected. If DBMIB still bound the Cyt *bf* quinol-oxidation (Q_p) site and inhibited electron flow through the *bf* complex in these experiments, then these data might indicate an interesting, alternative electron pathway that bypasses the Cyt *bf* complex. This possibility may be supported by a study showing that plastoquinol can directly reduce cytochrome *c* (Kruk et al. 2003), which could in turn

reduce P700. Alternatively, these data might indicate that DBMIB was non-functional in cells grown under high light. Studies have shown that if DBMIB becomes reduced, it does not bind to the Cyt *bf* quinol-oxidation (Q_p) site (ref). This might have occurred especially in the PetB-R214H mutant, which has a slower turnover of the Cyt *bf* complex (Nelson et al. 2005) and thus a more reduced PQ pool. Moreover, growth at high light intensity is expected to increase reductant pools, which could in turn over-reduce the PQ pool leading to DBMIB reduction. Finally, the absence of consistent DBMIB inhibition in cells grown at high light intensity might reflect a conformational change of the Cyt *bf* complex that occurs under these conditions and prevents DBMIB binding. One interesting possibility could be the formation of the suggested PSI – Cyt *bf* supercomplex that impedes access of DBMIB, and perhaps other Q_p-site inhibitors.

To further test these possibilities, additional studies were performed with 4-1HQ, a novel inhibitor of the Cyt *bf* Q_p-site that has recently been synthesized by Sandra Zulegar, Jason Coplien, and Drs. Brant Kedrowski and Linfeng Xie (UW Oshkosh Chemistry Department). The results of these experiments are summarized in Table 8 and kinetics traces are shown in Appendix E pg 111. In these experiments, 4-1HQ was a better inhibitor than DBMIB of P700 reduction in wild type cells grown at optimal light intensity. However, DBMIB was a better inhibitor in cells grown at high light intensity, and in all cases, 4-1HQ was a more effective inhibitor in cells grown in optimal light intensity than at high light intensity. Some of these data appear to be conflicting. However, the absence of a significant inhibition by 4-1HQ of P700 reduction in cells grown at high light intensity may be consistent with a conformational change of the

Cyt *bf* complex that occurs in high-light grown cells, again perhaps the result of supercomplex formation, that prevents the efficient binding of quinol-oxidation inhbitors.

The Cyt *bf* complex is the major and essential route for PQ pool oxidation in cyanobacteria, and also plays a central role in sensing the redox potential of electron transport and signaling adjustments in photosynthesis. Many cyanobacteria, such as *Synechococcus* PCC 7002, do not have alternative plastoquinol oxidases (QOX or PTOX) to help prevent dangerous over-reduction of the PQ pool (Nomura et al. 2006). Thus the activity of the Cyt *bf* complex in regulating state transitions and cyclic versus linear electron fluxes is crucial for maintaining redox balance in the PQ pool (see Kallas, 2012 for a review). Cyt *bf* kinetics data from *Synechococcus* PCC wild type and the NdhF and PetB-R214H mutants are shown in Figures 13 – 15, respectively, and summarized in Table 7. Cyt f/c_6 reduction kinetics in the PetB-R214H mutant grown either under optimal or high light, and treated with DCMU, were quite rapid relative to untreated cells indicating active cyclic electron flow rates under both conditions (Figure 15 and Table 7). In addition, and in contrast to the wild type and NdhF mutant, the Cyt *bf* content in PetB0R214H declined only slightly at high light intensity (Figure 15, Panel B). These data suggest that the PetB-R214H mutation changes the conformation of the Cyt *bf* complex in ways that alter the signaling role of the complex. Previous studies have provided evidence for signaling pathways linked to the stromal (or cytoplasmic) quinone-reductase (Q_n) domain of the Cyt *bf* complex (reviewed by Kallas, 2012).

Overall, the conclusions from the Cyt *bf* kinetics data are consistent with the P700 kinetics data. Cyt f/c_6 reduction kinetics were considerably faster in DCMU-treated NdhF cells from high light intensity than in comparably-treated NdhF cells from optimal light intensity. These data from the high light grown NdhF mutant indicate the activation of an active cyclic electron flow pathway that does not require the NDH complex, which is inactivated in the NdhF mutant. The dramatically elevated cyclic electron flow in the high light grown NdhF mutant is consistent with the formation of a possible PSI- Cyt *bf* supercomplex that may account for this remarkably active cyclic electron flow. It remains possible, however, that another cyclic electron flow may become activated under these high light conditions. The succinate dehydrogenase (SDH) complex is one candidate that may be involved in an alternative cyclic pathway and has been shown to be important in PQ pool reduction in the cyanobacterium *Synechocystis* PCC 6803 (Cooley et al., 2001). Kinetics experiments with and SDH mutant should be very interesting to investigate the role of this enzyme complex in cyclic electron flow as well as PQ pool reduction in *Synechococcus* PCC 7002. Finally, attempts should be made to isolate an actual PSI-Cyt *bf* supercomplex from high light grown *Synechococcus* PCC 7002 cells to further investigate the occurrence of such a complex in a direct PSI – Cyt *bf* electron flow pathway in cyanobacteria.

5.0 Conclusion

Supercomplexes such as the PSI-CP43´ supercomplex have been found in the photosynthetic apparatus of higher plants, green algae as well as cyanobacteria and play specific roles under stress conditions (Melkozernov et al. 2006). Recently, a protein supercomplex composed of PSI with its own light-harvesting complex (LHCI), the PSII light-harvesting complex (LHCII), the Cyt *bf* complex, ferredoxin (Fd)-NADPH oxidoreductase (FNR), ferredoxin, and the integral membrane protein PGRL1, was isolated from the green alga, *Chlamydomonas reinhardtii* (Iwai et al. 2010). This supercomplex catalyzes an active cyclic electron flow. A comparable supercomplex involving the PSI and Cyt *bf* complexes has not been identified in cyanobacteria. The current study was conducted to investigate the role of cyclic electron transfer in adaptation and rapid growth of the cyanobacterium, *Synechococcus* sp. PCC 7002 at high light intensity. Data presented here revealed a surprisingly active cyclic electron flow (up to 74 % of total electron flow) in the NdhF mutant grown under high light (Figure 9 and Table 3). Under optimal light the NDH pathway is the primary cyclic electron transfer pathway in cyanobacteria and typically represents only a small fraction of total electron flow (Yu et al., 1993). Consistent with this, I found only a very small contribution of cyclic electron flow (4%) in the *Synechococcus* 7002 NdhF mutant grown under optimal light. However, cyclic flow increased dramatically when this mutant was shifted to high light intensity (Figure 9 and Table 3). Cyt *bf* kinetics data from the NdhF mutant (Figure 14 and Table 7) support the findings from P700 kinetics data. Together, these data provide the first compelling evidence for the formation of a possible PSI-Cyt *bf*

supercomplex active in cyclic electron flow under high light conditions in cyanobacteria. The formation of a PSI – Cyt *bf* supercomplex would provide a direct, efficient pathway for electron flow from PSI to the Cyt *bf* complex that would not depend on NAD(P)H dehydrogenase or other more circuitous routes. Finally, inhibitor studies with DBMIB and 4-1HQ revealed a surprising absence of inhibition of electron flow through the Cyt *bf* complex by these inhibitors. These data might reflect conformational changes occurring in the Cyt *bf* complex at high light intensity, perhaps as the result of supercomplex formation with PSI.

APPENDIX A

Cyanobacterial and Microbial Media

A] A medium with D7 micronutrients

1. Add following ingredients to ~990 ml ddH_2O in a 2000 ml conical flask.

Ingredients	Amount	Final Concentration
NaCl	17.53 g	300 mM
KCl	0.6 g	8.0 mM
$NaNO_3$	1.02 g	12.0 mM
$MgSO_4 .7H_2O$	5.0 g	20.0 mM
$CaCl_2$	0.3 g	2.5 mM
FeEDTA[a]	1.0 ml	15 µM
10X D7 micronutrients (Tbl. A-2)	1.0 ml	1 X

[a] use 15mM solution of FeEDTA since 0.0062 grams would need to be weighed to reach the desired final concentration per liter (FeEDTA+$2.5H_2O$: m.w. = 412.1. Add 0.62 grams to 100ml ddH_20 and autoclave).

2. Add a teflon coated stir bar to the flask and heat on a hot plate to dissolve salts prior to autoclaving.

3. Let the medium cool to about 50°C after autoclaving and add these separately sterilized compounds: 10ml of an 0.83M Tris-HCl solution (pH8.2), 370µl of a 1.0M KH_2PO_4 solution, and 1.0ml of a 6.0µM (8 mg/l) vitaminB_{12} solution (stored in the dark at -20°C). Add antibiotics or other supplements that are required and store at 4ºC.

4. To make A(D7) agar plates, add above ingredients to ~500 ml ddH_2O to make 2X A base solution, then add 15g bacto agar/liter, 2 g $Na_2S_2O_3$/liter to 500 ml ddH_2O.

5. Autoclave agar and base separately for 40-50 min. Wait to cool down to 50-55ºC, then add Vitamin B_{12}, appropriate antibiotic(s) and the remaining compounds for A medium and add agar and medium together. Pour thick plates (1 liter makes approximately 20-25 thick (40ml) 1.4 % agar plates) and let them solidify. Store the solidified plates at 4ºC.

B] 10 X D7 Micronutrients: (Aron D7 Trace minerals)

Trace Metals (Dissolve in the following order)	Amount (g/L)
H_3BO_3	2.86 g/l
$MnCl_2 \bullet 4H_2O$	1.81 g/l
$ZnSO_4 \bullet 7H_2O$	0.22 g/l
$Na_2MoO_4 \bullet 2H_2O$	1.26 g/l
$CuSO_4 \bullet 5H_2O$	0.079 g/l
$NaVO_3$	0.239 g/l
$CoCl_2 \bullet 6H_2O$	0.04 g/l

C] A+ medium with P1 micronutrients

1. Add following ingredients to appropriate amount of ddH_2O in a conical flask.

Ingredients	Amount in 1liter	Amount in 4 liter
NaCl	18 g	72 g
KCl	0.6 g	2.4 g
$NaNO_3$	1.0 g	4.0 g
$MgSO_4 .7H_2O$	5.0 g	20.0 g
KH_2PO_4 (50g/L)	1.0 ml	4.0 ml
$CaCl_2$ (37g/L)	7.2 ml	29 ml
NaEDTA tetra (3g/L)	10.0 ml	40.0 ml
$FeCl_3.6H_2$ (3.89g/1 liter 0.1N HCL)	1.0 ml	4.0 ml
Tris (100g/L, pH 8.2)	1.0 ml	40.0 ml
P1 Metals (1000X)	1.0 ml	4.0 ml
ddH_2O	to 1 liter	to 4 liters

2. Autoclave and cool down to room temperature, then add 1 ml Vitamin B_{12} (4mg/L) to 1 liter medium and 4 ml Vitamin B_{12} (4mg/L) to 4 liters.

3. Add appropriate antibiotic(s) and store at 4ºC.

4. To make A+ (P1) agar plates, add above ingredients to ~500 ml ddH_2O to make 2X solution, then add 15g bacto agar/liter, 2 g $Na_2S_2O_3$/liter to 500 ml ddH_2O.

5. Autoclave agar and medium separately for 40-50 min. Wait to cool down to 50-55ºC, then add Vitamin B_{12} and appropriate antibiotic(s) and add agar and base together. Pour thick plates (1 liter makes approximately 20-25 thick (40ml) 1.4 % agar plates) and let them solidify. Store the solidified plates at 4ºC.

D] P1 metals (to make 1 liter 1000X stock solution)

Trace Metals (Dissolve in the following order)	Amount (g/L)
H_3BO_3	34.26 g/l
$MnCl_2 \bullet 4H_2O$	4.32 g/l
ZnCl	0.315g/l
MoO_3 (85%)	0.03 g/l
$CuSO_4 \bullet 5H_2O$	0.003 g/l
$CoCl_2 \bullet 6H_2O$	0.01215 g/l

E] Luria Bertani (L.B.) agar medium (1 liter)

1. Add following ingredients to 500ml dH_2O in a 2000ml conical flask.

Ingredients	Quantity (g)
Tryptone	10.0
Yeast extract	5.0
NaCl	10.0
Agar	15.0

2. Adjust the pH to 7.0 using 200µl 5.0M NaOH solution and add 15.0g Bacto agar. Stir well and bring the final volume to 1000ml.
3. Autoclave the medium for 20 minutes. Pour 25ml of the medium into each sterile Petri plate. Let the medium in plates cool down to room temperature before placing lids and store the plates at 4^0C.

Appendix B

Buffers and Reagents

A] 5 X TAE (Tris-acetate/EDTA) Buffer

In one liter final volume add 24.2 grams Tris base, 57.1ml glacial acetic acid, 100ml 0.5M EDTA (pH 8.0). Stir until dissolved and store at room temperature.

B] 5 X TBE (Tris-borate/EDTA) Buffer

Combine 54 grams of Tris base (Tris [hydroxymethyl] aminomethane, FW: 121.1), 27.5 grams boric acid and 20ml EDTA (0.5M, pH 8.0) in one liter of ddH_2O. This is suction filtered through a Whatman #5 or #6 filter for fine crystal retention and diluted 1:5 prior to use. 25ml of 1 X TBE is used in each gel preparation. Occasionally after prolonged storage a precipitate will form. If bottle was capped tightly so no fluid volume was lost, the solution can be heated to almost boiling and the crystals will go back into solution.

C] Antibiotics

Antibiotics were typically formed as 1000 x stock solutions. Kanamycin (100mg/ml), Streptomycin (50mg/ml) and Spectinomycin (50mg/ml) are dissolved in sterile ddH_2O and filter sterilized through a 2.0cm Acrodisk Syringe Filter with a 0.2-micron pore size (Gelman Laboratory, HT Tuffryn membrane, Ref: 4192). Erythromycin stock is prepared as a 20mg/ml solution in 100% EtOH and is filter sterilized. All are stored at -20°C protected from light (wrapped in aluminum foil).

D] 10T/0.1E buffer

Add following DEPC treated ingredients to a sterile 50ml conical tube.

Ingredients	Quantity (g)
1.0M Tris-HCl, pH 8.2	0.5
0.5M Na_2EDTA, pH 8.0	0.01
Nuclease free water	49.49

* While preparing 10T/0.1 E buffer with pH 7.5, use 1.0M Tris with pH adjusted to 7.5 using HCl.

E] 5mM HEPES, 10mM NaCl, 10mM $NaHCO_3$ buffer

Add 150 µl of 1M HEPES solution, 300 µl of 1M NaCl and 300 µl of 1M $NaHCO_3$. Add ddH_2O to reach 30 ml total volume. While preparing HEPES solution maintain pH 7.9.

APPENDIX C

Protocols

A] P700 reduction Kinetics with and without inhibitors

1. Grow the wild type, NdhF and PetBR214H cultures to 0.5 $O.D_{750}$ under optimal photosynthetic conditions. For measurement of kinetics under high light conditions, grow the cultures to 0.3 $O.D_{750}$ and shift them under high light (2000 $\mu M\ m^{-2}\ s^{-1}$) and let them grow for two hours. Harvest 20ml culture volumes using 5mM HEPES, 10mM NaCl and 10mM $NaHCO_3$ buffer, pH 7.9 and adjust the final $O.D_{750}$ to 3.0 – 5.0.
2. Using a syringe, load 1ml of the concentrated cultures into cuvette adaptable with the Biologic's JTS-10 spectrophotometer without forming any bubbles.
3. Using the operating software for the spectrophotometer either set or select a program that involves 115 seconds dark phase for dark adaptation of cyanobacterial cells followed by continuous actinic light illumination phase for 10 seconds which is followed further by dark phase e.g. 230 seconds. The program should include exposure of the sample to 200 ms intense pulses of 7900$\mu E\ m^{-2}s^{-1}$ followed by short detecting pulses of 10 μs. Set the voltage required for detection of absorption signal between 3 and 4, but preferably close to 4 Volts.
4. Insert PSI specific 'P700' (6mm wide) cut off filter in front of the reference detector and the sample detector. Use 705 nm intereference filter to measure PSI redox changes and 740 nm intereference filter as reference.
5. For far-red experiments select the Actinic I (far-red ring, 2500 μE). For pre-illumination experiments turn Actinic II (green ring, 300 μE) on. For all other experiments select Actinic II (green ring, 300 μE). Final trace is obtained by

subtracting 740 nm trace from 705 nm. Calculate half times of re-reduction for all of the final PSI traces obtained. Convert the data obtained into Microsoft Excel format.

6. For every trace obtained calculate the turnover of PSI by calculating electrons passing through the complex per second. By comparing, the turnover of PSI in presence and absence of DCMU, % cyclic electron flow can be calculated.

B] Cyt *bf* Kinetics with and without inhibitors

1. Grow the wild type, NdhF and PetBR214H cultures to 0.5 $O.D_{750}$ under optimal photosynthetic conditions. For measurement of kinetics under high light conditions, grow the cultures to 0.3 $O.D_{750}$ and shift them under high light (2000 $\mu M\ m^{-2}\ s^{-1}$) and let them grow for two hours. Harvest 20ml culture volumes using 5mM HEPES, 10mM NaCl and 10mM $NaHCO_3$ buffer, pH 7.9 and adjust the final $O.D_{750}$ to 3.0 – 5.0.
2. Using a syringe, load 1ml of the concentrated cultures into cuvettes adaptable with the Biologic's JTS-10 spectrophotometer without forming any bubbles.
3. Using the operating software for the spectrophotometer either set or select a program that involves 50 milliseconds dark phase for dark adaptation of cyanobacterial cells followed by 9 milliseconds continuous illumination phase and followed further by 180 seconds dark phase. Set the voltage required for detection of absorption signal between 3 and 4, but preferably close to 4 Volts.

Insert ‘BG39’ (3mm wide) cut off filters in the light paths, before the reference as well as sample detectors.

4. For the strains under study; record redox spectra using 546nm, 554nm, 563nm and 573nm interference filters
5. Using a function of the operating software, deconvolute the spectra obtained with 546, 554, 563 and 573nm to obtain individual spectra for cytochrome *f and* b hemes. Convert the data into Microsoft Excel format.

APPENDIX D

SdhB Gene Inactivation

Succinate dehydrogenase is an enzyme complex in the photosynthetic electron transport chain. It has been proposed that this enzyme plays an important role in the electron transport. Studies also suggest that the enzyme has a major effect on the PQ redox poise. The succinate dehydrogenase enzyme has two subunits. One is a flavoprotein subunit and another is the iron-sulfur subunit. The flavoprotein subunit is encoded by *sdhA* gene whereas the iron-sulfur subunit is encoded by *sdhB* gene. We were interested in studying the role played by succinate dehydrogenase complex in the photosynthetic electron transfer. For this purpose, we aimed at creating a mutant lacking the functional succinate dehydrogenase complex. In order to create a mutant which has inactivated succinate dehydrogenase enzyme we targeted the Fe-S subunit of the enzyme complex, encoded by *sdhB* gene. Instead of using the traditional cloning techniques to create a knockout mutant, we decided to use megaprimer PCR method to create a gene inactivation construct.

In megaprimer PCR, primers are designed which amplify upstream region and some portion of the target gene. This fragment is called as fragment A or forward fragment. Primers are also designed to amplify downstream region and some portion of the target gene. This fragment is called as fragment B or reverse fragment. The forward and reverse primers which amplify the antibiotic resistance gene (in this case it is *ermc* gene encoding the Erythromycin gene resistance cassette) are located on the 5' ends of the two primers amplifying the upstream and downstream flanking regions. Fragments A and B are then used as megaprimers to amplify the antibiotic resistance gene. A gene inactivation construct is obtained at the end of this second PCR reaction. This gene

inactivation construct should be inserted into the *Synechococcus* sp. PCC 7002 cell through natural transformation.

Primer designing was successful. The primers were highly specific and did not bind to any other region in the gene. We successfully obtained the gene inactivation construct; this took us closer to the original goal of achieving the SdhB mutant. Unfortunately, we lost this gene inactivation construct during further purification steps. Further attempts at repeating the megaprimer PCR failed; hence we decided to attempt ligation method. We had a success in individually purifying Fragment A, B and *ermc* gene fragment. The ligation of these three fragments was also a success. After obtaining a gene inactivation product through ligation, we attempted natural transformation of *Synechococcus* PCC 7002 wild-type UWO strain. We achieved transformants able to grow on A(D7)/ Em^{20} plates, but none of them had the inactivated *sdhB* gene. Hence the transformation needs to be repeated with the ligation product again.

APPENDIX E

Supplementary Kinetics Data

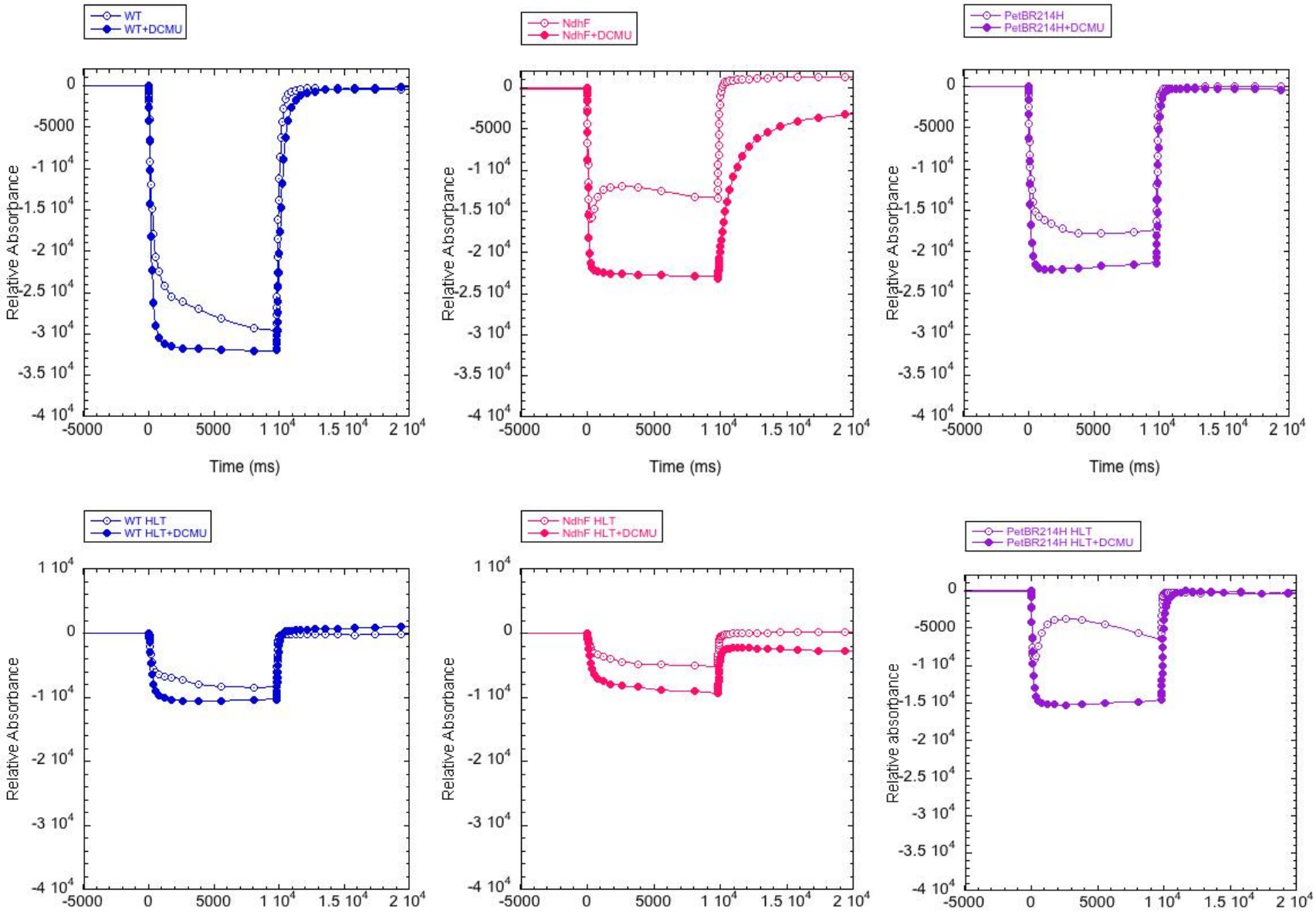

Figure 6: P700 kinetics with and without DCMU in WT, NdhF and PetBR214H cultures grown under optimal and high light conditions. Upper panel consists of optimal light grown cultures; lower panel consists of high light grown cultures. The x-axes denote time in milliseconds (ms) and y-axes denote relative absorbance (ΔI/I). Open circles indicate untreated samples and closed circles indicate DCMU-treated samples. Green actinic light (~530 nm) was used at 300 µmol m^{-2} s^{-1}. Final concentration of DCMU was 10 µM.

108

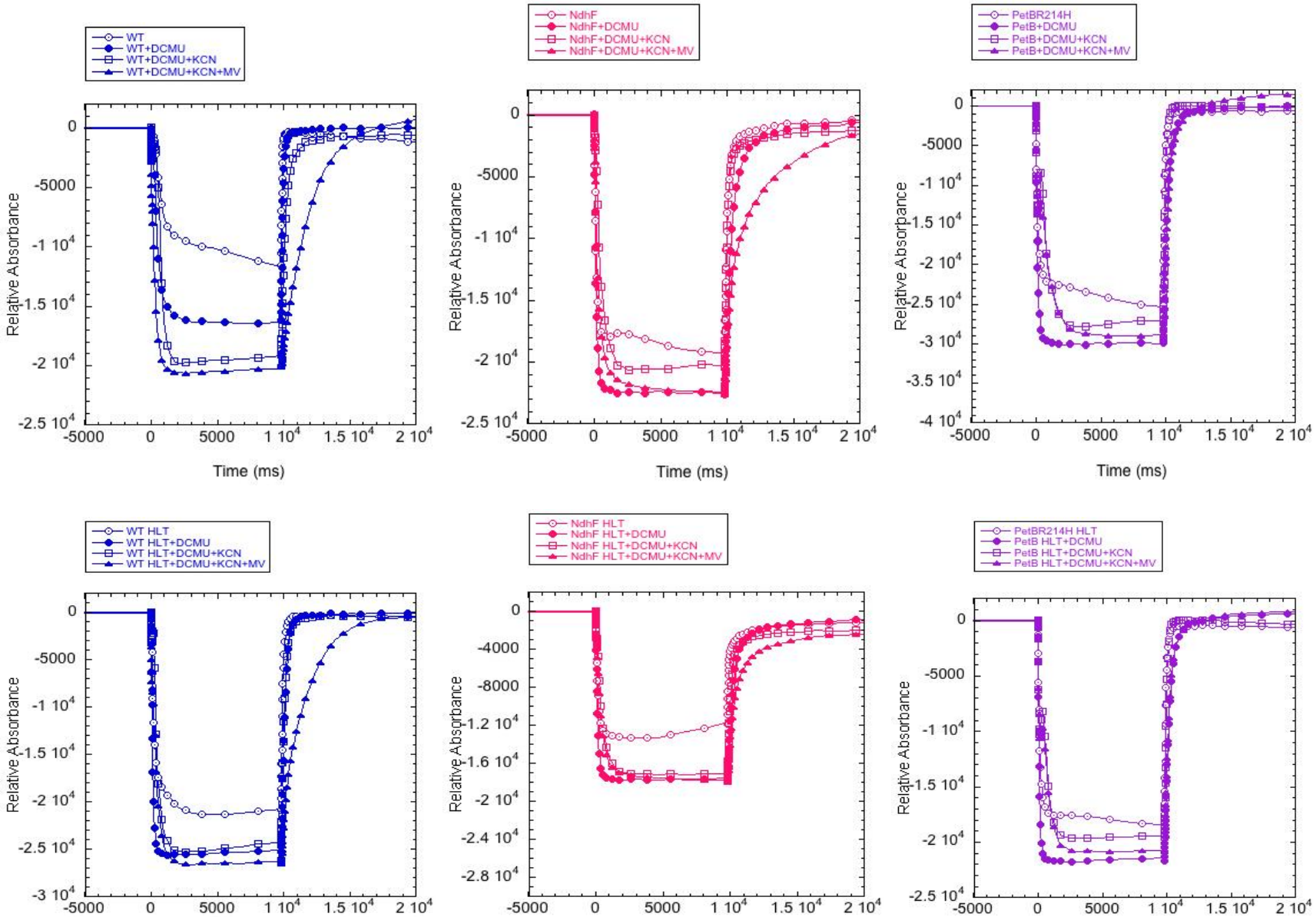

Figure 7: P700 kinetics with DCMU, KCN and MV in WT, NdhF and PetBR214H cultures grown under optimal and high light conditions. Upper panel consists of optimal light grown cultures; lower panel consists of high light grown cultures. The x-axes denote time in milliseconds (ms) and y-axes denote relative absorbance (ΔI/I). Open circles: untreated samples; closed circles: DCMU-treated samples; Open squares: DCMU+KCN treated samples; Closed triangles: DCMU+KCN+MV treated samples. Green actinic light (~530 nm) was used at 300 µmol m^{-2} s^{-1}. Final concentration of DCMU was 10 µM, KCN was 1mM and MV was 100 µM.

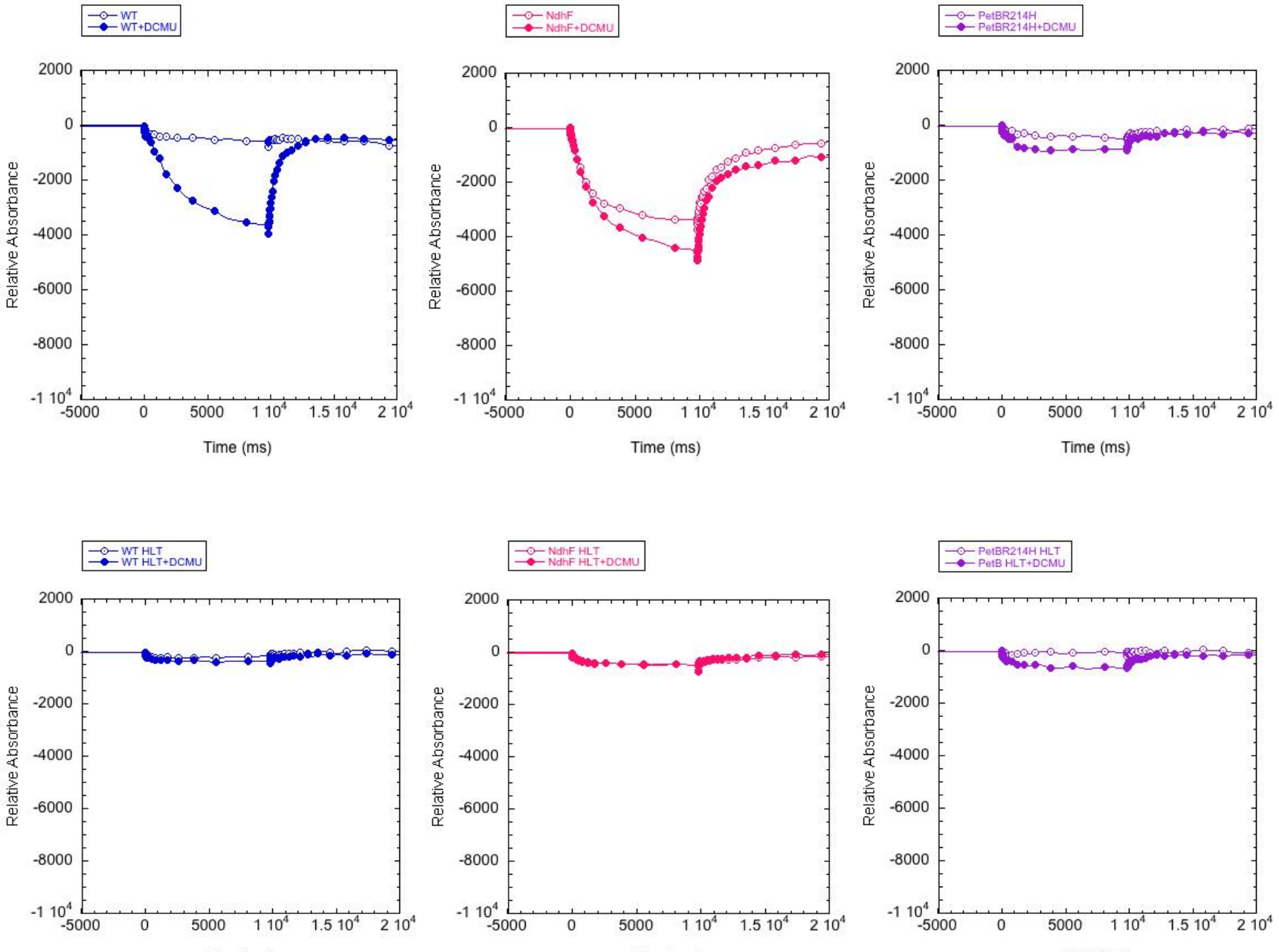

Figure 8: P700 kinetics with DCMU using Far red illumination in WT, NdhF and PetBR214H cultures grown under optimal and high light conditions. Upper panel consists of optimal light grown cultures; lower panel consists of high light grown cultures. The x-axes denote time in milliseconds (ms) and y-axes denote relative absorbance (ΔI/I). Open circles indicate untreated samples and closed circles indicate DCMU-treated samples. Far-red actinic light (~700 – 740 nm) was used at 2500 µmol m^{-2} s^{-1}. Final concentration of DCMU was 10 µM.

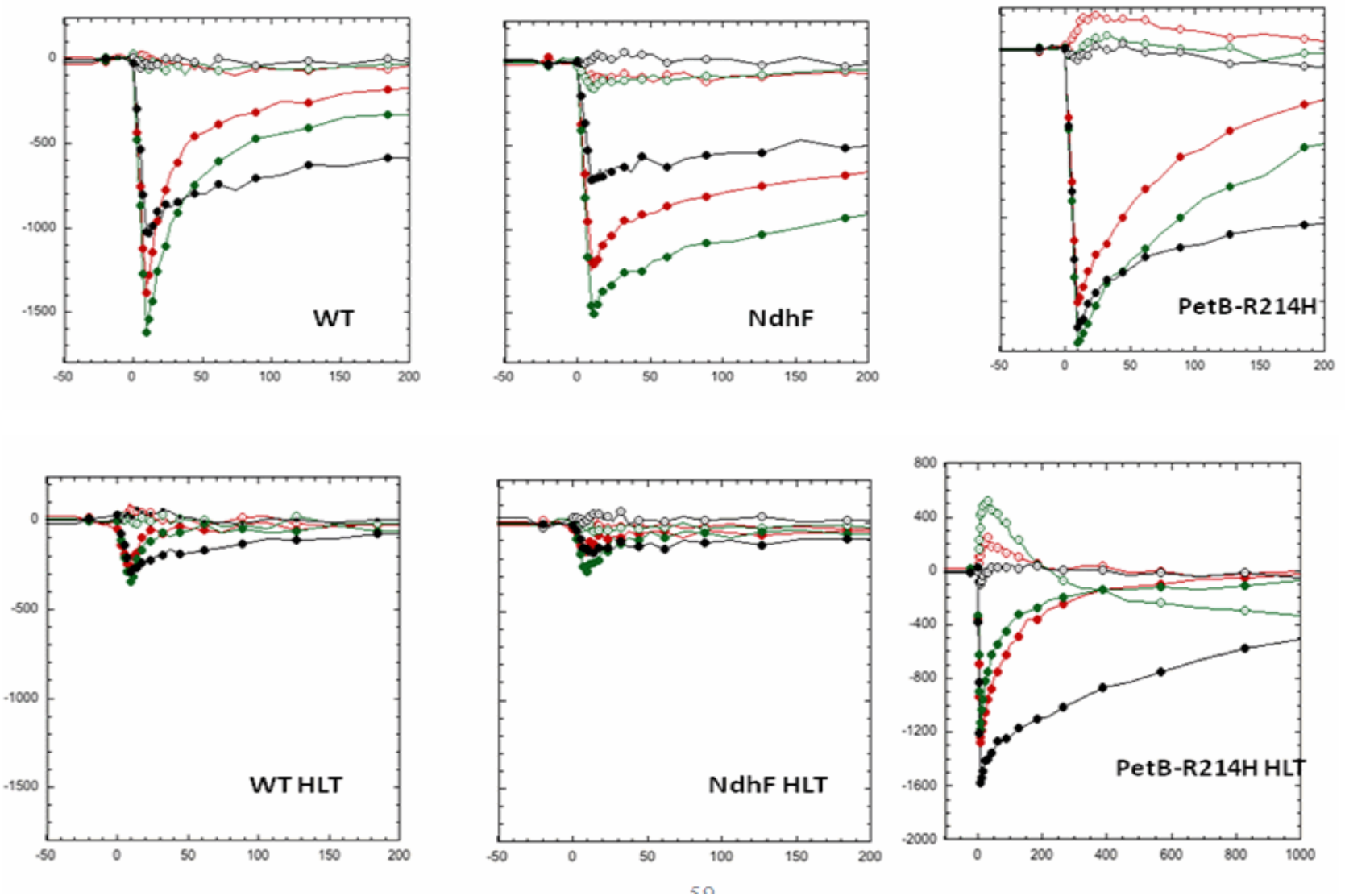

Figure 9: 9 ms Cyt *bf* kinetics with and without DCMU and DBMIB in WT, NdhF and PetBR214H cultures grown under optimal and high light conditions Upper panel consists of optimal light grown cultures; lower panel consists of high light grown cultures. The x-axes denote time in milliseconds (ms) and y-axes denote relative absorbance (ΔI/I). Open circles: b hemes at 563 nm; closed circles: Cyt f/c6 at 554 nm; red traces: untreated samples; green circles: DCMU-treated samples; black traces: DCMU+DBMIB treated samples.Green actinic light (~530 nm) was used at 300 µmol m^{-2} s^{-1}. Final concentrations of DCMU and DBMIB were 10 µM.

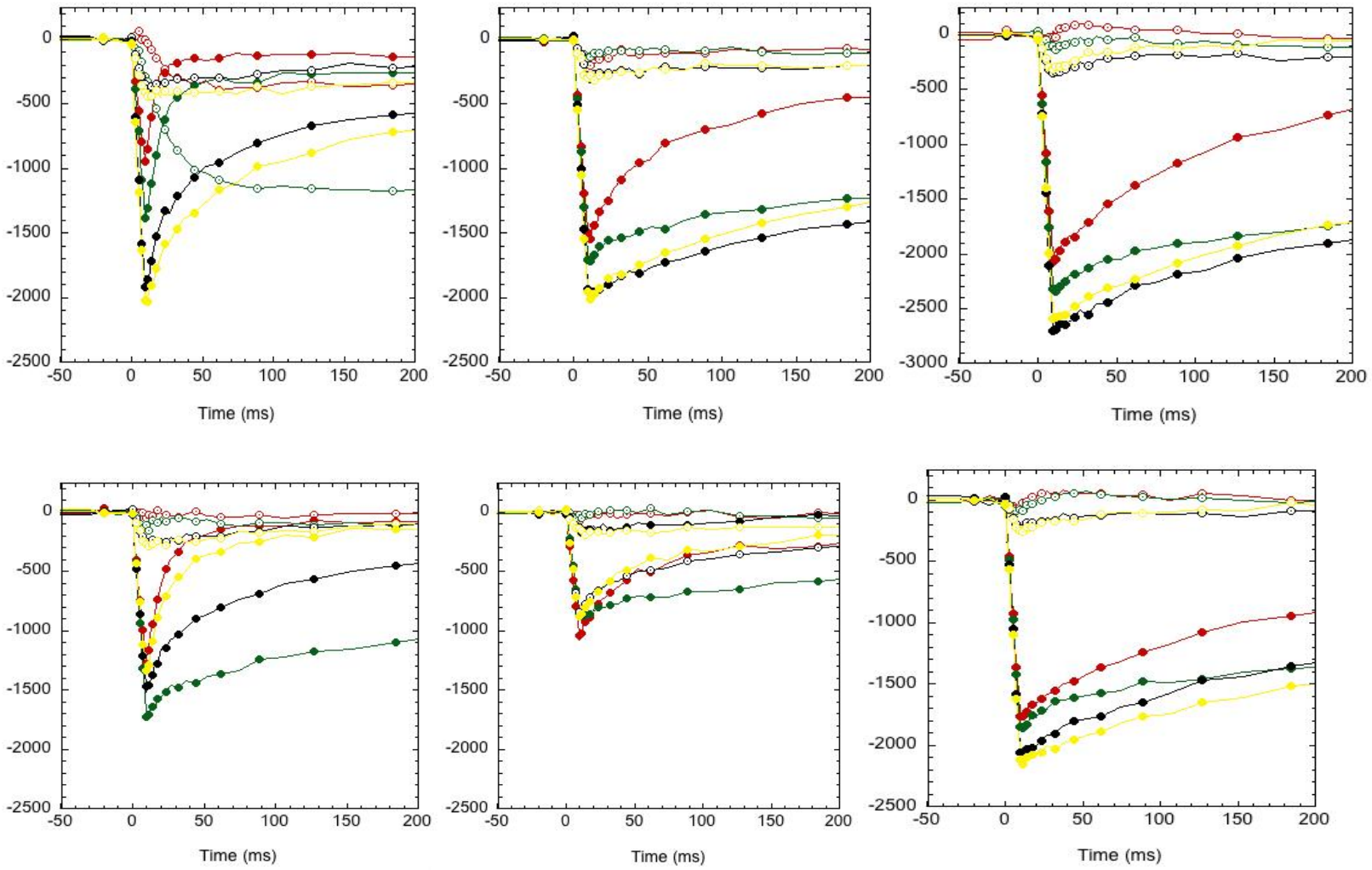

Figure 10: 9 ms Cyt *bf* kinetics with and without DBMIB and 4,1HQ in WT, NdhF and PetB-R214H cultures grown under optimal and high light conditions Upper panel consists of optimal light grown cultures; lower panel consists of high light grown cultures. The x-axes denote time in milliseconds (ms) and y-axes denote relative absorbance (ΔI/I). Open circles: *b* hemes at 563 nm; closed circles: Cyt *f*/c_6 at 554 nm; red traces: untreated samples; green circles: DBMIB-treated samples; black traces: 10 μM 4-1HQ treated samples; yellow traces: 20 μM 4-1HQ treated samples. Green actinic light (~530 nm) was used at 300 μmol m^{-2} s^{-1}. Final concentration of DBMIB was 10 μM and 4-1HQ was 10 μM and 20 μM.

REFERENCES

Albertsson P. 2001. A quantitative model of the domain structure of the photosynthetic membrane. *Trends Plant Sci* 6: 349–358

Allen J.F., Bennett J., Steinback K.E., and Arntzen C.J. 1981. Chloroplast Protein Phosphorylation Couples Plastoquinone Redox State to Distribution of Excitation Energy Between Photosystems. *NATURE*. 291: 25-29.

Allen J.F. 2002. Photosynthesis of ATP-Electrons, Proton Pumps, Rotors, and Poise. *Cell*. 110: 273-76.

AllenJ.F. 2003. Cyclic, Pseudocyclic and Non-Cyclic Photophosphorylation: New Links in the Chain, *Trends Plant sci*. 8: 15-19.

Allen J.F. 2004. Cytochrome b_6f Structure for Signaling and Vectorial Metabolism. *Trends Plant Sci*. 9: 130–37.

Alric J., Lavergne, and Rappaport F. 2010. Redox and ATP Control of Photosynthetic Cyclic Electron Flow in *Chlamydomonas reinhardtii* (I) Aerobic Conditions. *Biochim Biophys Acta*. 1797: 44-51.

Aluru M.R. and Rodermel S.R. 2004. Control of Chloroplast Redox by the IMMUTANS Terminal Oxidase. *Physiologia Plantarum*. 120: 4-11.

Arnon D.I. and Chain R.K. 1975. Regulation of Ferredoxin-Catalyzed Photosynthetic Phosphorylations. *Proc. Natl. Acad. Sci*. USA, 72(12): 4961-65.

Asada K. 1999. The Water-Water Cycle in Chloroplasts: Scavenging of Active Oxygens and Dissipation of Excess Photons. *Annu Rev Plant Physiol Plant Mol Biol*. 50: 601-39

Asada K. 2000. The water-water cycle as alternative photon and electron sinks. *Philos Trans R Soc*. 355(1402): 1419–1431.

Barth P., Lagoutte B., and Sétif P. 1998. Ferredoxin Reduction by Photosystem I from *Synechocystis* sp. PCC 6803: Toward an Understanding of the Respective Roles of Subunits *PsaD* and *PsaE* in Ferredoxin Binding. *Biochemistry*. 37:16233-41.

Baymann F., Rappaport F., Joliot P., and Kallas T. 2001. Rapid Electron Transfer to Photosystem I and Unusual Spectral Features of Cytochrome c_6 in *Synechococcus* sp. PCC 7002 in Vivo. *Biochemistry*. 40: 10570-77.

Bennoun P. 1982. Evidence for a Respiratory Chain in the Chloroplast. *Proct Natl Acad Sci* USA. 79: 4352-56.

Blankenship R.E. (2002). *Molecular Mechanisms of Photosynthesis*. Blackwell Science Limited, Oxford, UK.

Bonaventura C. and Myers J. 1969. Fluorescence and Oxygen Evolution from *Chlorella pyrenoidosa*. *Biochim. Biophys. Acta*. 189: 366-83.

Burnap R.L., Troyan T., and Sherman L. 1993. The Highly Abundant Chlorophyll Protein of Iron-Deficient *Synechococcus* sp. PCC 7942 (CP43′) is Encoded by *isiA* Gene. *Plant Physiol*. 103: 893-902.

Canaani O., Schuster G., and Ohad I. 1989. Photoinhibition in *Chlamydomonas reinhardtii*: Effect on State Transition, Intersystem Energy Distribution, and Photosystem I Cyclic Electron Flow. *Photosynth. Res*. 20: 129-46.

Carr M., Friedrichs M.A., Aita M.N., Antoine D., Arrigo K.R., Asunama I., Aumont O., and……Yamanaka Y. (2006). A comparison of global estimates of marine primary production from ocean color. *Deep-Sea Research II*. 53: 741-770.

Cardol P., Alric J., Girard-Bascou J., Franck F., Wollman F.A., and Finazzi G. 2009. Impaired Respiration Discloses the Physiological Significance of State Transitions in *Chlamydomonas*. *Proc Natl Acad Sci* USA 106: 15979–84.

Carpentier R., LaRue B., and LeBlanc R.M. 1984. Photoacoustic Spectroscopy of *Anacystis nidulans*. III. Detection of Photosynthetic Activities. *Arch Biochem Biophys*. 228: 534-43.

Casano L.M., Zapata J.M., Martin M., and Sabater B. 2000. Chlororespiration and Poising of Cyclic Electron Transport. Plastoquinone as Electron Transporter Between Thylakoid NADH Dehydrogenase and Peroxidase. *Journal of Biological Chemistry*. 275: 942-48.

Casano L.M., Martin M., and Sabater B. 2001. Hydrogen Peroxide Mediates the Induction of Chloroplastic *Ndh* Complex Under Photooxidative Stress in Barley. *Plant physiol.* 125: 1450-58.

Catala R., Sabater B., and Guera A. 1997. Expression of the Plastid *ndhF* Gene Product in Photosynthetic and Non-Photosynthetic Tissues of Developing Barley Seedlings. *Plant Cell Physiol*. 38:1382-88.

Cooley J.W., Howitt C., and Vermaas W. 2001. SuccinateDehydrogenase and Other Respiratory Pathways in Thylakoid Membranes of *Synechocystis* sp. Strain PCC 6803: Capacity Comparisons and Physiological Function. *J. Bacteriol*. 183(14): 4251-58.

Cramer W.A., Furbacher P.N., Szczepaniak A., and Tae G-S. 1991. Electron Transport Between Photosystem I and Photosystem II. *Curr Top Bioenerg*. 16: 179-222.

DeRuyter Y.S. and Fromme P. (2008). (Chapter 9) Molecular structure of the photosynthetic apparatus. In *The cyanobacteria: Molecular biology, Genomics and Evolution*. (Herrero A and Flores E Eds.). 217-269. Caister Academic Press, Nolfolk, UK.

Dong C., Tang A., Zhao J., Mullineaux C.W., Shen G. and Bryant D.A. 2009. ApcD is necessary for efficient energy transfer from phycobilisomes to photosystem I

and helps to prevent photoinhibition in the cyanobacterium *Synechococcus* sp. PCC 7002. *Biochim Biophys Acta.* 1787: 1122–1128.

El Bissati K., Delphin E., Murata N., Etienne A.L., and Kirilovsky D. 2000. Photosystem II Fluorescence Quenching in the Cyanobacterium *Synechocystis* PCC 6803: Involvement of Two Different Mechanisms. *Biochim. Biophys. Acta.* 1457: 229-42.

Endo T., Shikanai T., Takabayashi A., Asada K., Mi H., and Sato F. 1999. The Role of Chloroplastic NADH Dehydrogenase in Photoprotection. *FEBS Letters.* 457: 5-8.

Finazzi G., Rappaport F., Furia A., Fleischmann M., Rochaix J.D., Zito F., and Forti G. 2002. Involvement of the State Transitions in the Switch Between Linear and Cyclic Electron Flow in *Chlamydomonas reinhardtii*. *EMBO rep.* 3(3): 280-85.

Fork D.C. and Herbert S.K. 1993. Electron Transport and Photophosphorylation by Photosystem I in Vivo in Plants and Cyanobacteria. *Photosynthesis Research.* 36: 149-68.

Goedheer J.C. 1963. A Co-operation of Two Pigment Systems and Respiration in Photosynthetic Luminiscence. *Biochim Biophys Acta.* 66: 61-71

Golbeck J.H. 1992b. Spectroscopic Characterization of Wild-Type and Genetically Modified Photosystem I. In N Murata, ed, Research in Photosynthesis, Vol I. Kluwer Academic Publishers, Dordrecht, The Netherlands, pp 487-96.

Golding A.J, Finazzi G., and Johnson G.N. 2004. Reduction of the Thylakoid Electron Transport Chain by Stromal Reductants-Evidence for Activation of Cyclic Electron Transport Upon Dark Adaptation or Under Drought. *Planta*. 220: 356-63.

Gombos Z., Wada H., Murata N. 1992. Unsaturation of Fatty Acids in Membrane Lipids Enhances Tolerance of the Cyanobacterium *Synechocystis* PCC 6803 to Low-Temperature Photoinhibition. *Proc. Natl. Acad. Sci*. USA. 89: 9959-63.

Gombos Z., Wada H., and Murata N. 1994. The Recovery of Photosynthesis from Low-Temperature Photoinhibition is Accelerated by the Unsaturation of Membrane Lipids: A Mechanism of Chilling Tolerance. *Proc. Natl. Acad. Sci*. USA. 91: 8787-91

Hagemann M., Jeanjean R., Fulda S., Havaux M., Joset F., and Erdmann N. 1999. Flavodoxin Accumulation Contributes to Enhanced Cyclic Electron Flow Around Photosystem I in Salt-Stressed Cells of *Synechocystis* sp. Strain PCC 6803. *Physiol Planta*. 105: 670-78.

Harbinson J. and Foyer C.H. 1991. Relationships Between the Efficiencies of Photosystem-I and Photosystem-II and Stromal Redox State in CO_2-free air-Evidence for Cyclic Electron Flow in Vivo. *Plant Physiol*. 97: 41-49.

Havaux M., Greppin H., and Strasser R. 1991. Functioning of Photosystems I and II in Pea Leaves Exposed to Heat Stress in the Presence and Absence of Light. *Planta.* 186: 88-98.

Havaux M., Guedeney G., Hagemann M., Yeremenko N., Matthjis H., and Jeanjean R. 2005. The Chlorophyll-Binding Protein IsiA is Inducible by High Light and Protects Cyanobacterium *Synechocystis* PCC 6803 from Photooxidative Stress. *FEBS Lett.* 579: 2289-93.

Heber U. and Walker D. 1992. Concerning a Dual Function of Coupled Cyclic Electron Transport in Leaves. *Plant physiol.* 100: 1621-26.

Heber U. 2002. Irrungen, Wirrungen? The Mehler Reaction in Relation to Cyclic Electron Transport in C3 Plants. *Photosynth. Res.* 73: 223-31.

Heimann S., Ponamarev M., Cramer W. Movement of the Rieske iron-sulfur protein in the p-side bulk aqueous phase: effect of luminal viscosity on redox reactions of the cytochrome b_6f complex. *Biochemistry.* 2000. 39: 2692-2699.

Herbert S.K., Fork D.C., and Malkin S. 1990. Photoacoustic Measure in Vivo of Energy Storage by Cyclic Electron Flow in Algae and Higher Plants. *Plant physiol.* 94: 926-34.

Herbert S.K., Samson G., Fork D.C., and Lauenbach D.E. 1992. Characterization of Damage to Photosystem I and II in a Cyanobacterium Lacking Detectable Superoxide Dismutase Activity. *Proc. Natl. Acad. Sci.* USA. 89: 8716-20.

Herbert S.K., Martin R.E., and Fork D.C. 1995. Light Adaptation of Cyclic Electron Transport Through Photosystem I in the Cyanobacterium *Synechococcus* sp. PCC 7942. *Photosynth. Res.* 46: 277-85.

Herman C. and D'Ari R. 1998. Proteolysis and Chaperones: The Destruction/Reconstruction Dilemma. *Curr Opin Microbiol*. 1: 204–09.

Hibino T., Lee B.H., Rai A.K., Ishikawa H., Kojima H., Tawada M., Shimoyama H., and Takabe T. 1996. Salt Enhances Photosystem I Content and Cyclic Electron Flow via NAD(P)H Dehydrogenase in the Halotolerant Cyanobacterium *Aphanothece halophytica*. *Plant physiol.* 23: 321-30.

Hihara Y., Sonoike K., and Ikeuchi M. 1998. A Novel Gene, *pmgA*, Specifically Regulates Photosystem Stoichiometry in the Cyanobacterium *Synechocystis* Species PCC 6803 in Response to High Light. *Plant Physiol*. 117: 1205-16.

Horn D. M. 2005. Superoxide In the Cytochrome bf Complex of Photosynthesis. *Master's Thesis, University of Wisconsin-Oshkosh.*

Horton P. and Black M.T. 1981. Light-dependent Quenching of Chlorophyll Fluorescence in Pea Chloroplasts Induced by Adenosine 5'- triphosphate. *Biochim. Biophys. Acta*. 635: 53-62.

Howitt C.A., Cooley J.W., Wiskich J.T., and Vermaas W.F. 2001. A strain of *Synechocystis* sp. PCC 6803 Without Photosynthetic Oxygen Evolution and

Respiratory Oxygen Consumption: Implications for the Study of Cyclic Photosynthetic Electron Transport. *Planta*. 214: 46-56.

Huang C., Yuan X., Zhao J., and Bryant D.A. 2003. Kinetic Analyses of State Transitions of the Cyanobacterium *Synechococcus* sp. PCC 7002 ant its Mutant Strains Impaired in Electron Transport. *Biochim. Biophys. Acta*. 1607: 121-30.

Ivanov B., Kobayashi Y., Bukhov N.K., and Heber U. 1998. Photosystem I-dependent Cyclic Electron Flow in Intact Spinach Chloroplasts: Occurrence, Dependence on Redox Conditions and Electron Acceptors and Inhibition by Antimycin A. *Photosynth. Res*. 57: 61-70.

Ivanov A.G., Park Y.I., Miskiewicz E., Raven J.A., Huner N.P.A, and Öquist G. 2000. Iron Stress Restricts Photosynthetic Intersystem Electron Transport in *Synechococcus* sp. PCC 7942. *FEBS Letters*. 485: 173-77.

Iwai M., Takizawa K., Tokutsu R., Okamuro A., Takahashi Y., and Minagawa J. 2010. Isolation of the Elusive Supercomplex that Drives Cyclic Electron Flow in Photosynthesis. *NATURE*. 464: 1210-14.

Jeanjean R., Matthijs H.C.P, Onana B., Havaux M., and Joset F. 1993. Exposure of the Cyanobacterium *Synechocystis* PCC 6803 to Salt Stress Induces Concerted Changes in Respiration and Photosynthesis. *Plant Cell Physiol*. 34: 1073-79.

Joët T., Cournac L., Peltier G., and Havaux M. 2002. Cyclic Electron Flow Around Photosystem I in C3 Plants. In Vivo Control by the Redox State of Chloroplasts

and Involvement of the NADH-Dehydrogenase Complex. *Plant physiol.* 128: 760-69.

Joliot P. and Joliot A. 2002. Cyclic electron transfer in plant leaf. *Proc Natl Acad Sci* USA 99: 10209–10214.

Joliot P. and Joliot A. 2005. Quantification of cyclic and linear flows in plants. *Proc Natl Acad Sci* USA 102: 4913–18.

Jordan P., Fromme P., Witt H.T., Klukas O., Saenger W., and Kraub N. 2001. Three dimensional structure of cyanobacterial photosystem I as 2.5 Å resolution. Nature. 411: 909-917.

Joset F., Jeanjean R., and Hagemann M. 1996. Dynamics of the Response of Cyanobacteria to Salt-Stress: Deciphering the Molecular Events. *Plant physiol.* 96: 738-44.

Joshua S. and Mullineaux C.W. 2004. Phycobilisome Diffusion is Required for Light-State Transitions in Cyanobacteria. *Plant Physiol*. 135: 2112.

Kallas T. 1994 The cytochrome b_6f complex. The Molecular Biology of Cyanobacteria. Kluwer Acedemic Publishers. Netherlands. (ed) Bryant DA.259-317

Kallas T. 2012. Cytochrome *b6f* Complex at the Heart of Energy Transduction and Redox Signaling. J.J. Eaton-Rye, B.C. Tripathy and T.D. Sharkey (eds.),

Photosynthesis: Plastid Biology, Energy Conversion and Carbon Assimilation, Advances in Photosynthesis and Respiration 34, pp. 501–560

Kelly M.J.S, Poole R.K., Yates M.G., and Kenedy C. 1990. Cloning and Mutagenesis of Genes Encoding the Cytochrome *bd* Terminal Oxidase Complex in *Azotobacter vinelandii*: Mutants Deficient in the Cytochrome *d* Complex are Unable to Fix Nitrogen in Air. *J. Bacteriol*. 172: 6010-19.

Keren N. and Ohad I. 1998. State Transition and Photoinhibition In: Rochaix J-D, Goldschmidt-Clermont M and Merchant S (eds) The Molecular Biology of Chloroplasts and Mitochondria in *Chlamydomonas*, Advances in Photosynthesis, Vol 7, pp 569–96. Kluwer Academic Publishers, Dordrecht.

Kuntz M. 2004. Plastid Terminal Oxidase and its Biological Significance. *Planta*. 199: 276-81.

Kurisu G., Zhang H., Smith J.L., Cramer W.A. 2003. Structure of the cytochrome b_6f complex of oxygenic photosynthesis: Tuning the cavity. Science. 302: 1009-1014.

Kyle D.J., Ohad I., and Arntzen C.J. 1984. Membrane Protein Damage and Repair: Selective Loss of a Quinone-Protein Function in Chloroplast Membranes. *Proc. Natl. Acad. Sci*. USA 81: 4070-74.

Lambert D.H. and Stevens S.E. 1986. Photoheterotrophic Growth of *Agmenellum quadruplicatum* PR-6. *J. Bacteriol*. 165:654-56.

Laudenbach D. and Strauss N. 1988. Characterization of a Cyanobacterial Iron Stress-Induced Gene Similar to *psbC*. *J. Bacteriol*. 170: 5018-26.

Lemaire C., Wollman F.A., and Bennoun P. 1988. Restoration of Phototrophic Growth in a Mutant of *Chlamydomonas reinhardtii* in Which the Chloroplast *atpB* Gene of the ATP Synthase has a Deletion: An Example of Mitochondria-Dependent Photosynthesis, *Proc. Natl. Acad. Sci*. U.S.A. 85: 1344-48.

Livingston A.K., Cruz J.A., Kohzuma K., Dhingra A., and Cramer D.M. 2010. An *Arabidopsis* Mutant with High Cyclic Electron Flow Around Photosystem I (hcef) Involving NADH Dehydrogenase Complex. *Plant Cell*. 22: 221-33.

Makino A., Miyake C., and Yokota A. 2002. Physiological Functions of the Water-Water Cycle (Mehler Reaction) and the Cyclic Electron Flow Around PSI in Rice Leaves. *Plant Cell Physiol* 43(9):1017-26.

Martin M., Casano L.M., and Sabater B. 1996. Identification of the Product of *ndh* A Gene as a Thylakoid Protein Synthesized in Response to Photooxidative Treatment. *Plant Cell Physiol*. 37: 293-98.

Maxwell P.C. and Biggins J. 1976. Role of Cyclic Electron Transport in Photosynthesis as Measured by the Turnover of P700 in Vivo. *Biochemistry*. 15: 3975-81.

McConnell M.D., Koop R., Vasil´ev S., and Bruce D. 2002. Regulation of the Distribution of Chlorophyll and Phycobilin-absorbed Excitation Energy in

Cyanobacteria. A Structure-based Model for the Light State Transition. *Plant Physiol*. 130: 1201-12.

McFadden G.I. 2001. Primary and secondary endosymbiosis and the origin of plastids. *Journal of Phycology*. 37: 951-959.

Mehler A.H. 1951. Studies on reactions of illuminated chloroplasts. I. Mechanism of the reduction of oxygen and other Hill reagents. Arch Biochem 33: 65–77

Melkozernov A.N., Barber J., and Blankenship. 2006. Light Harvesting in Photosystem I Supercomplexes. Biochemistry. 45(2): 331-45.

Mi H., Endo T., Schreiber U. 1992a. Donation of Electrons from Cytosolic Components to the Intersystem Chain in the Cyanobacterium *Synechococcus* sp. PCC 7002 as Determined by Reduction of $P700^{+}$. *Plant Cell Physiol*. 33- 1099-1105.

Muller F. 2000. The nature and mechanism of superoxide production by the electron transport chain: its relevance to aging. *J Amer Aging Assoc*. 23: 227-253.

Munekage Y., Hashimoto M., Miyake C., Tomizawa K., Endo T., Tasaka M., and Shikanai T. 2004. Cyclic Electron Flow Around Photosystem I is Essential for Photosynthesis. *NATURE*. 429: 579-82.

Murakami A., Kim S.J., and Fujita Y. 1997. Changes in Photosystem Stoichiometry in Response to Environmental Conditions for Cell Growth Observed with the Cyanophyte *Synechocystis* PCC 6714. *Plant Cell Physiol*. 38: 392-97.

Nandha B., Finazzi G., Joliot P., Hald S., and Johnson G.N. 2007. The Role of PGR5 in Redox Poising of Photosynthetic Electron Transport. *Biochim Biophys Acta*. 1767: 1252-59.

Navarro J.A., Duran R.V., De la Rosa M.A., and Hervas M. 2005. Respiratory Cytochrome *c* Oxidase can be Efficiently Reduced by the Photosynthetic Redox Proteins Cytochrome c_6 and Plastocyanin in Cyanobacteria. *FEBS Letters*. 579: 3565-68.

Nelson M.E., Finazzi G., Wang Q.J., Middleton-Zarka K.A., Whitmarsh J., and Kallas T. 2005. Cytochrome b_6 Arginine 214 of *Synechococcus* sp. PCC 7002, A Key Residue for Quinone-Reductase Site Function and Turnover of the Cytochrome *bf* Complex. *J Biol Chem* 280: 10395–402.

Niyogi K.K. 1999. Photoprotection revisited: Genetic and molecular approaches. *Annu Rev Plant Physiol Plant Mol Biol* 50: 333–359.

Nomura C.T., Sakamoto T., and Bryant D.A. (2006). Roles for Heme-Copper Oxidases in Extreme High-Light and Oxidative Stress Response in the Cyanobacterium *Synechococcus* sp. PCC 7002. *Arch Microbiol*. 185: 471-79.

Ogawa T. and Mi H. 2007. Cyanobacterial NADPH Dehydrogenase Complexes. *Photosynth. Res*. 93: 69-77.

Olson J.M. 2006. Photosynthesis in the archean era. *Photosynth. Res*. 88 (2): 109-117.

Ort D.R., Yocum C.F. 1996. Electron transfer and energy transduction in photosynthesis: an overview. Oxygenic Photosynthesis: The Light Reactions. 1-9.

Osmond C.B., Austin M.P., Berry J.A., Billings W.D., Boyer J.S., Dacey J.W.H, ---------- and Winner W.E. 1987. Stress Physiology and the Distribution of Plants. *Bioscience*. 37: 38-48.

Ouyang Y., Horn D., Grebe R., Guo L.W., Nelson M., Wang Q., Whitmarsh J., Finazzi G. and Kallas T. 2004. Mutational analysis of the cytochrome *bf* Rieske iron-sulfur protein and quinone-reductase (Qi) site. In: Van der Est A and Bruce D (eds) Photosynthesis: Fundamental Aspects to Global Perspectives, pp 434–426. Allen Press, Lawrence, Kansas

Peltier G. and Cournac L. 2002. Chlororespiration. *Annu. Rev. Plant Biol*. 53: 523-50.

Powles S.B. 1984. Photoinhibition of Photosynthesis Induced by Visible Light. *Annu Rev Plant Physiol*. 35: 15-44.

Quiles M.J. and Cuello J. 1998. Association of Ferredoxin NADP-oxidoreductase With the Chloroplastic Pyridine Nucleotide Dehydrogenase Complex in Barley Leaves. *Plant Physiol*. 117: 235-44.

Quiles M.J., Garcia A., and Cuello J. 2000. Separation by Blue-native PAGE and Identification of the Whole NAD(P)H Dehydrogenase Complex from Barley Stroma Thylakoids. *Plant Physiology and Biochemistry*. 38: 225-32.

Quiles M.J. and Lopez N.I. 2004. Photoinhibition of Photosystems I and II Induced by Exposure to High Light Intensity During Oat Plant Growth. Effects on the Chloroplast NADH Dehydrogenase Complex. *Plant Science*. 166: 815-23.

Quiles M.J. 2005. Regulation of the Expression of Chloroplast *ndh* Genes by Light Intensity Applied During Oat Plant Growth. *Plant Science*. 168: 1561-69.

Quiles M.J. 2006. Stimulation of Chlororespiration by Heat and High Light Intensity in Oat Plants. *Plant, Cell and Environment*. 29: 1463-70.

Roelofs T.A., Liang W., Latimer M.J., Cinco R.M., Rompel A., Andrews J.C.,---------- and Klein M.P. 1995. "Oxidation States of the Manganese Cluster During the Flash-Induced S-State Cycle of the Photosynthetic Oxygen-Evolving Complex". *Proc. Natl. Acad. Sci*. USA. 93: 3335-40

Rousseau F., Sétif P., and Lagoutte B. 1993. Evidence for the Involvement of *PsaE* Subunit in the Reduction of Ferredoxin by Photosystem I. *EMBO J*. 12: 1755-65.

Rumeau D., Becuwe-Linka N., Beyly A., Louwagie M., Garin J., and Pelteir G. 2005. New Subunits NDH-M-N, and –O, Encoded by Nuclear Genes, are Essential for Plastid *Ndh* Complex Functioning in Higher Plants. *Plant Cell*. 17: 219-32.

Sacksteder C.A. and Kramer D.M. 2000. Dark-interval Relaxation Kinetics (DIRK) of Absorbance Changes as a Quantitative Probe of Steady-State Electron Transfer. *Photosynth Res*. 66: 145-58.

Sakamoto T., Bryant D.A. 1998. Growth at Low Temperature Causes Nitrogen Limitation in the Cyanobacterium *Synechococcus* sp. PCC 7002. *Arch Microbiol*. 169: 10-19.

Satoh K. and Fork D.C. 1983. The Relationship Between State II to State I Transitions and Cyclic Electron Flow Around Photosystem I. *Photosynth Res*. 4: 245-56.

Sazanov. LA, Burrows PA, and Nixon PJ. 1998b. The Plastid *ndh* Genes Code for an NADH-Specific Dehydrogenase: Isolation of a Complex I Analogue From Pea Thylakoid Membranes. *Proc. Natl. Acad. Sci*. USA. 95: 1319-24.

Scheibe. R. 1987. NADP+-Malate Dehydrogenase in C3-Plants: Regulation and Role of a Light-Activated Enzyme. *Physiol. Plant*. 71: 393-400.

Scheibe. R. 1990. Light/Dark Modulation: Regulation of Chloroplast Metabolism in a New Light. *Bot Acta*. 103: 327-34

Schluchter W.M., Zhao J., and Bryant D.A. 1993. Isolation and Characterization of An Interposon Mutant. *J. Bacteriol*. 175: 3343-52.

Schneider D., Berry S., Rich P., Seidler A., and Rögner M. 2001. A Regulatory Role of the PetM Subunit in a Cyanobacterial Cytochrome b_6f Complex. *J Biol Chem*. 276: 16780–85.

Schreiber U., Endo T., Mi H., and Asada K. 1995. Quenching Analysis of Chlorophyll Fluorescence by the Saturation Pulse Method: Particular Aspects

Relating to the Study of Eukaryotic Algae and Cyanobacteria. *Plant Cell Physiol*. 36: 873-82.

Schubert H., Matthijs H.C.P, and Mur L.R. 1995. In Vivo Assay of P700 Redox Changes in the Cyanobacterium *Fremyella diplosiphon* and The Role of Cytochrome *c* Oxidase in Regulation of Photosynthetic Electron Transfer. *Photosynthetica.* 31: 517-27.

Shikanai T. 2007. Cyclic Electron Transport Around Photosystem I: Genetic Approaches. *Annu. Rev. Plant Biol*. 58: 199-217.

Somerville C. 1995. Direct Tests of the Role of Membrane Lipid Composition in Low-Temperature-Induced Photoinhibition and Chilling Sensitivity in Plants and Cyanobacteria. *Proc. Natl. Acad. Sci*. USA. 92:6215-18.

Sonoike K., Hatanaka H., and Katoh S. 1993. Small Subunits of Photosystem I Reaction Center Complexes from *Synechococcus elongatus*. II. The *psaE* Gene Product Has a Role to Promote Interaction Between the Terminal Electron Acceptor and Ferredoxin. *Biochim. Biophys. Acta*. 1141: 52-57.

Stroebel D., Choquet Y., Popot J., Picot D. An atypical haem in the cytochrome b6f complex. Nature. 2003. 426: 413-418.

Strotmann H. and Weber N. 1993. On the Function of *PsaE* in Chloroplast Photosystem I. *Biochim Biophys Acta.* 1143(2): 204-10.

Sültemeyer D, Biehler K., and Fock H.P. 1993. Evidence for Contribution of Pseudocyclic Photophosphorylation to the Energy Requirement of the Mechanism for Concentrating Inorganic Carbon in Chlamydomonas. *Planta*. 189: 235-42.

Sültemeyer D., Price G.D., Bryant D.A., and Badger M.R. 1997. *PsaE*- and *NdhF*-Mediated Electron Transport Affect Bicarbonate Transport Rather Than Carbon Dioxide Uptake in the Cyanobacterium *Synechococcus* sp. PCC 7002. *Planta*. 201: 36-42.

Tanaka Y., Katada S., Ishikawa H., OgawaT. and Tanaka, T. 1997. Electron Flow From NAD(P)H Dehydrogenase to Photosystem I is Required for Adaptation to Salt Shock in the Cyanobacterium *Synechocystis* sp. PCC 6803. *Plant Cell Physiol*. 38: 1311-18.

Tasaka Y., Gombos Z., Nishiyama Y., Mohanty P., Ohba T., Ohki K., and Murata N. 1996. Targeted Mutagenesis of Acyl-Lipid Desaturases in *Synechocystis*: Evidence for the Roles of Polyunsaturated Membrane Lipids in Growth, Respiration and Photosynthesis. *EMBO J*. 15: 6416-25.

Teicher H.B., Moller B.L., and Scheller H.V. 2000. Photoinhibition of Photosystem I in Field-Grown Barley (*Hordeum Vulgare L.*): Induction, Recovery and Acclimation. *Photosynth. Res*. 64: 53-61.

Thomas D.J., Thomas J., Youderian P.A., and Herbert S.K. 2001. Photoinhibition and Light-Induced Cyclic Electron Transport in *ndhB*- and *psaE*- Mutants of *Synechocystis* sp. PCC 6803. *Plant Cell Physiol* 42(8): 803-12.

Van Baalen C. 1961. Studies on Marine Blue-Green Algae. Kitchawan Research Laboratory of the Brooklyn Botanic Garden, R.F. D.r, Ossining , N.Y. 129-39.

Vener A.V., Ohad I., and Andersson B. 1998. Protein Phosphorylation and Redox Sensing in Chloroplast Thylakoids. *Curr. Opin. Plant Biol*. 1: 217-23.

Volkmer T., Schneider D., Bernat G., Kirchhoff H., Wenk S.O., and Rögner M. 2007. Ssr2998 of *Synechocystis* sp. PCC 6803 is Involved in Regulation of Cyanobacterial Electron Transport and Associated With The Cytochrome b_6f Complex. *J Biol Chem*. 282: 3730–37.

Wada H., Gombos Z., Sakamoto T., and Murata N. 1992. Genetic Manipulation of the Extent of Desaturation of Fatty Acids in Membrane Lipids in the Cyanobacterium *Synechocystis* PCC 6803. *Plant Cell Physiol*. 33:535-40.

White D. 2000.The physiology and biochemistry of prokaryotes. Oxford University Press. New York.

Whitmarsh J. and Govindjee. Photosynthesis. Encyclopedia of Applied Biophysics. VCH Publishers Inc. 1995. p 513-532.

Wilson A., Ajlani G., Verbavatz J.M., Vass I., Kerfeld C.A., and Kirilovsky D. 2006. A Soluble Carotenoid Protein Involved in Phycobilisomes-Related Energy Dissipation in Cyanobacteria. *Plant Cell*. 18:992-1007.

Winkler H.H. and Neuhaus H.E. 1999. Non-Mitochondrial ATP Transport. *Trends Biochem*. Sci. 24: 64-68.

Wollman F.A. 2001. State Transitions Reveal the Dynamics and Flexibility of the Photosynthetic Apparatus. *EMBO J.* 20: 3623-30.

Yan J., Dashdorj N., Baniulis D., Yamashita E., Savikhin S., and Cramer W.A. 2008. On the Structural Role of the Aromatic Residue Environment of the Chlorophyll *a* in the Cytochrome b_6f Complex. *Biochemistry.* 47: 3654-3661.

Yousef N., Pistorius E.K., and Michel K.P. 2003. Comparative Analysis of *idiA* and *isiA* Transcription Under Iron Starvation and Oxidative Stress in *Synechococcus elongatus* PCC 7942 Wild-type and Selected Mutants. *Arch Microbiol.* 180: 471-83.

Yu L., Zhao J., Mühlenoff U., Bryant D.A and Golbeck J.H. 1993. *PsaE* is Required For in Vivo Cyclic Electron Flow Around Photosystem I in the Cyanobacterium *Synechococcus* sp. PCC 7002. *Plant Physiol.* 103: 171-80.